Uncovering miRNA regulatory mechanisms through functional assessment of miRNA-centered complexes during *C. elegans* development

by

Shilpa Hebbar

B.E., SJ College of Engineering, India 2011
M.Sc., Manipal University, India 2015

AN ABSTRACT OF A DISSERTATION

submitted in partial fulfillment of the requirements for the degree

DOCTOR OF PHILOSOPHY

Division of Biology
College of Arts and Sciences

KANSAS STATE UNIVERSITY
Manhattan, Kansas

2022

Abstract

Normal developmental and physiological processes depend on precise regulation of gene expression. miRNAs are a class of small non-coding RNAs that post-transcriptionally regulate gene expression by inducing gene silencing through translational inhibition and mRNA target destabilization. Currently, there is a lack of understanding of how miRNA biogenesis and activity is regulated under different developmental contexts or how they integrate with other regulatory signals. Using *C. elegans* as a model, we sought to address this gap in our knowledge by identifying components of miRNA-centered complexes and characterizing the molecular mechanisms through which they interact with miRNAs to regulate gene expression. miRNA pulldowns followed by mass spectrometric analysis of precipitated complexes identified 211 protein interactors of let-7, miR-58, and miR-2 miRNAs. To determine which of these interactors are functionally important for miRNA activity, we performed an RNAi screen of genes encoding a subset of miRNA complex components. Depletion of 26 of the 40 tested genes modified the miRNA mutant phenotypes in one or more functional assays, suggesting they play a role in miRNA-mediated gene regulation. Among the miRNA interactors found to be functionally important for miRNA activity were RNA binding proteins, splicing, and translational regulators suggesting a potential interplay between gene regulatory processes.

We sought to further characterize one candidate identified through our functional proteomics approach, HRPA-1. *hrpa-1* depletion enhanced developmental phenotypes of miRNA mutants, disrupted miRNA levels, and affected global gene expression profiles, consistent with an HRPA-1 role in gene expression regulation. Among the genes differentially expressed in *hrpa-1* depleted animals was *R06C1.4*, a homolog of yeast cleavage and polyadenylation factor complex (CFI) component. Depletion of *R06C1.4* partially recapitulated

the enhancement effects on miRNA mutant developmental phenotypes observed with *hrpa-1* loss. Thus, we identified a potential role for *R06C1.4* in mediating developmental gene expression downstream of *hrpa-1.* We propose several models describing potential mechanisms through which HRPA-1 may coordinate with miRNAs to regulate gene expression. Overall, this work identified novel factors that functionally support miRNA gene regulatory activity, discovering possible modes through which one such factor (HRPA-1) coordinates with miRNAs. In addition, this work generated avenues for future mechanistic investigations aimed at characterizing the dynamic nature of post-transcriptional gene regulation.

Uncovering miRNA regulatory mechanisms through functional assessment of miRNA-centered complexes during *C. elegans* development

by

Shilpa Hebbar

B.E., SJ College of Engineering, India 2011
M.Sc., Manipal University, India 2015

A DISSERTATION

submitted in partial fulfillment of the requirements for the degree

DOCTOR OF PHILOSOPHY

Division of Biology
College of Arts and Sciences

KANSAS STATE UNIVERSITY
Manhattan, Kansas

2022

Approved by:

Major Professor
Anna Zinovyeva

Copyright

Abstract

Normal developmental and physiological processes depend on precise regulation of gene expression. miRNAs are a class of small non-coding RNAs that post-transcriptionally regulate gene expression by inducing gene silencing through translational inhibition and mRNA target destabilization. Currently, there is a lack of understanding of how miRNA biogenesis and activity is regulated under different developmental contexts or how they integrate with other regulatory signals. Using *C. elegans* as a model, we sought to address this gap in our knowledge by identifying components of miRNA-centered complexes and characterizing the molecular mechanisms through which they interact with miRNAs to regulate gene expression. miRNA pulldowns followed by mass spectrometric analysis of precipitated complexes identified 211 protein interactors of let-7, miR-58, and miR-2 miRNAs. To determine which of these interactors are functionally important for miRNA activity, we performed an RNAi screen of genes encoding a subset of miRNA complex components. Depletion of 26 of the 40 tested genes modified the miRNA mutant phenotypes in one or more functional assays, suggesting they play a role in miRNA-mediated gene regulation. Among the miRNA interactors found to be functionally important for miRNA activity were RNA binding proteins, splicing and translational regulators suggesting a potential interplay between gene regulatory processes.

We sought to further characterize one candidate identified through our functional proteomics approach, HRPA-1. *hrpa-1* depletion enhanced developmental phenotypes of miRNA mutants, disrupted miRNA levels, and affected global gene expression profiles, consistent with HRPA-1 role in gene expression regulation. Among the genes differentially expressed in *hrpa-1* depleted animals was *R06C1.4*, a homolog of yeast cleavage and polyadenylation factor complex (CFI) component. Depletion of *R06C1.4* partially recapitulated

the enhancement effects on miRNA mutant developmental phenotypes observed with *hrpa-1* loss. Thus, we identified a potential role for *R06C1.4* in mediating developmental gene expression downstream of *hrpa-1.* We propose several models describing potential mechanisms through which HRPA-1 may coordinate with miRNAs to regulate gene expression. Overall, this work identified novel factors that functionally support miRNA gene regulatory activity, discovering possible modes through which one such factor (HRPA-1) coordinates with miRNAs. In addition, this work generated avenues for future mechanistic investigations aimed at characterizing the dynamic nature of post-transcriptional gene regulation.

Table of Contents

List of Figures

List of Tables

Acknowledgements

It is with the deepest sense of eternal gratitude and affection that I acknowledge the support, kindness, motivation and guidance of my advisor, Dr. Anna Zinovyeva. Your constant encouragement helped me push my limits. Very grateful for the scientific training I received from you in the exciting RNA biology field. I have learnt a great deal from you and have grown as a researcher!

I would also like to acknowledge the support from my thesis committee Dr. Michael Veeman, Dr. Erika Geisbrecht, and Dr. Michael Herman during these past 6 years as I navigated my time in graduate school. Special thanks to past and current members of the Zinovyeva lab for making it a fun lab space to work and for their constant support and feedback. So grateful to have been a part of the brilliant *C. elegans* community, who in addition to conducting cool science, are a group of scientists that host the most fun conference!

I'm struggling to find the right words to express my gratitude towards my parents, Raghavendra Hebbar and Vijayalaxmi Hebbar. I couldn't have come this far without their unconditional love, support and belief in me. To my loving sister Sneha, and my brother-in-law Abhiram, thank you for making it easier for me to dream about coming to USA and help make it a reality. To my friend, companion, and loving husband, Pramod, thank you for being my rock-solid support system and inspiring me to do my best every day. To Nirupama, my best friend, thank you for being there for me always!

Dedication

I'd like to dedicate my work to my parents who never had the opportunity to fulfil their dreams and sacrificed everything to ensure that I get to fulfill mine! Appa and Amma, though you never had even a fraction of the same opportunities, encouragement, and support in your time, you went above and beyond to support my journey. Eternally grateful and proud to be your daughter!

Chapter 1 - Introduction

miRNAs are potent gene regulatory molecules

Spatiotemporal regulation of gene expression is critical for developmental and physiological processes. The outcomes of gene expression programs are orchestrated by multiple regulatory processes occurring on many levels that are dictated by diverse cis elements and trans-acting factors. Regulation can occur at the level of transcription through chromatin remodeling, and transcription factor binding, co-transcriptionally (splicing, capping, and polyadenylation), post-transcriptionally (splicing, mRNA turnover), translationally and post-translationally through protein modifications and localization (Fig 1.1).

One level of posttranscriptional gene regulation is exerted by a class of small non-coding RNAs called the microRNAs (miRNAs). miRNAs associate with proteins to assemble the miRNA induced silencing complexes (miRISCs), which repress gene expression by targeting mRNA transcripts for translational inhibition and degradation. Mature miRISC comprises an Argonaute and a GW182 protein, with additional effector proteins recruited to the target site to mediate gene silencing (Fig 1.2). Gene target specificity is primarily dictated by the seed region of miRNAs, which spans positions 2-8 (Brennecke *et al*. 2005) and miRNAs with identical seed sequence are grouped into families (Lim *et al.* 2003). Non-canonical sites can also confer targeting specificities (Agarwal *et al.* 2015) (Fig 1.2). miRNAs are predicted to target over 60% of human protein coding genes, with functional roles identified in several developmental and cellular processes (Friedman *et al.* 2009; Hogg and Harries, 2014).

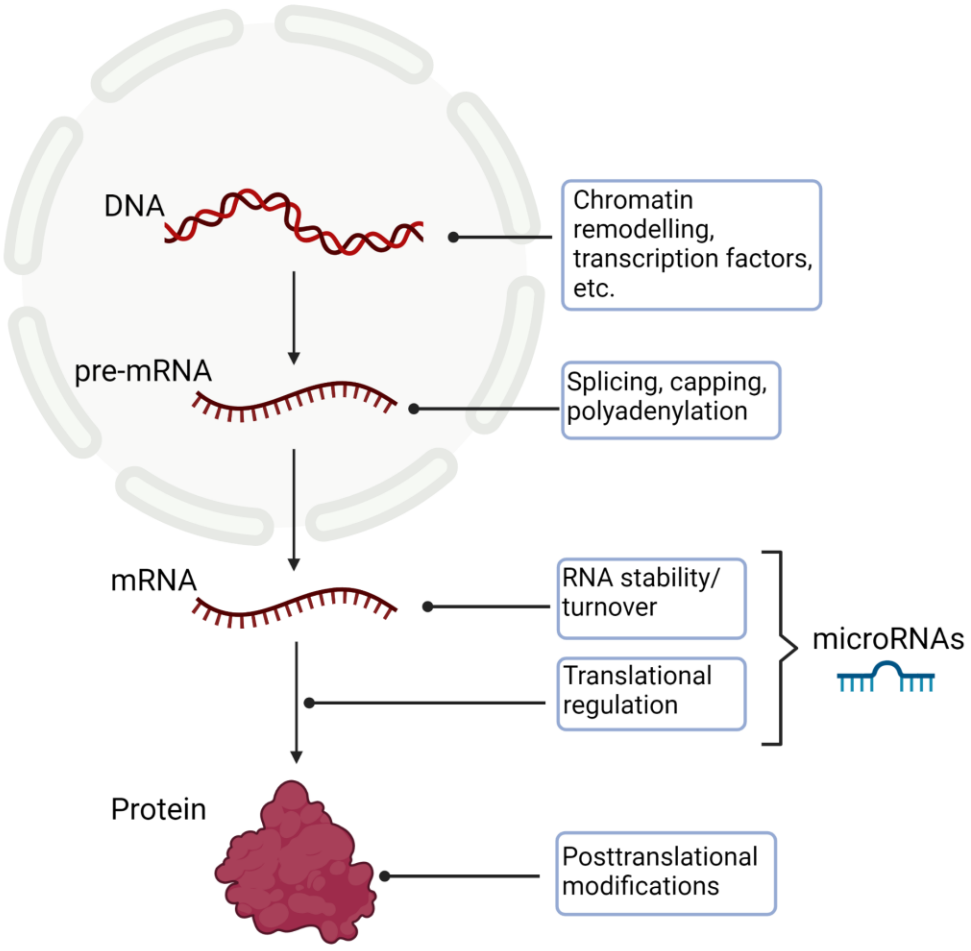

Figure 1.1 Gene expression is regulated through multi-layered mechanisms.
Pre-mRNA generated through highly regulated transcription is processed and exported out into cytoplasm. Post transcriptional regulation by miRNAs impacts both mRNA levels and protein translation. Final layer of regulation occurs post translationally. Schematic was made using BioRender (biorender.com).

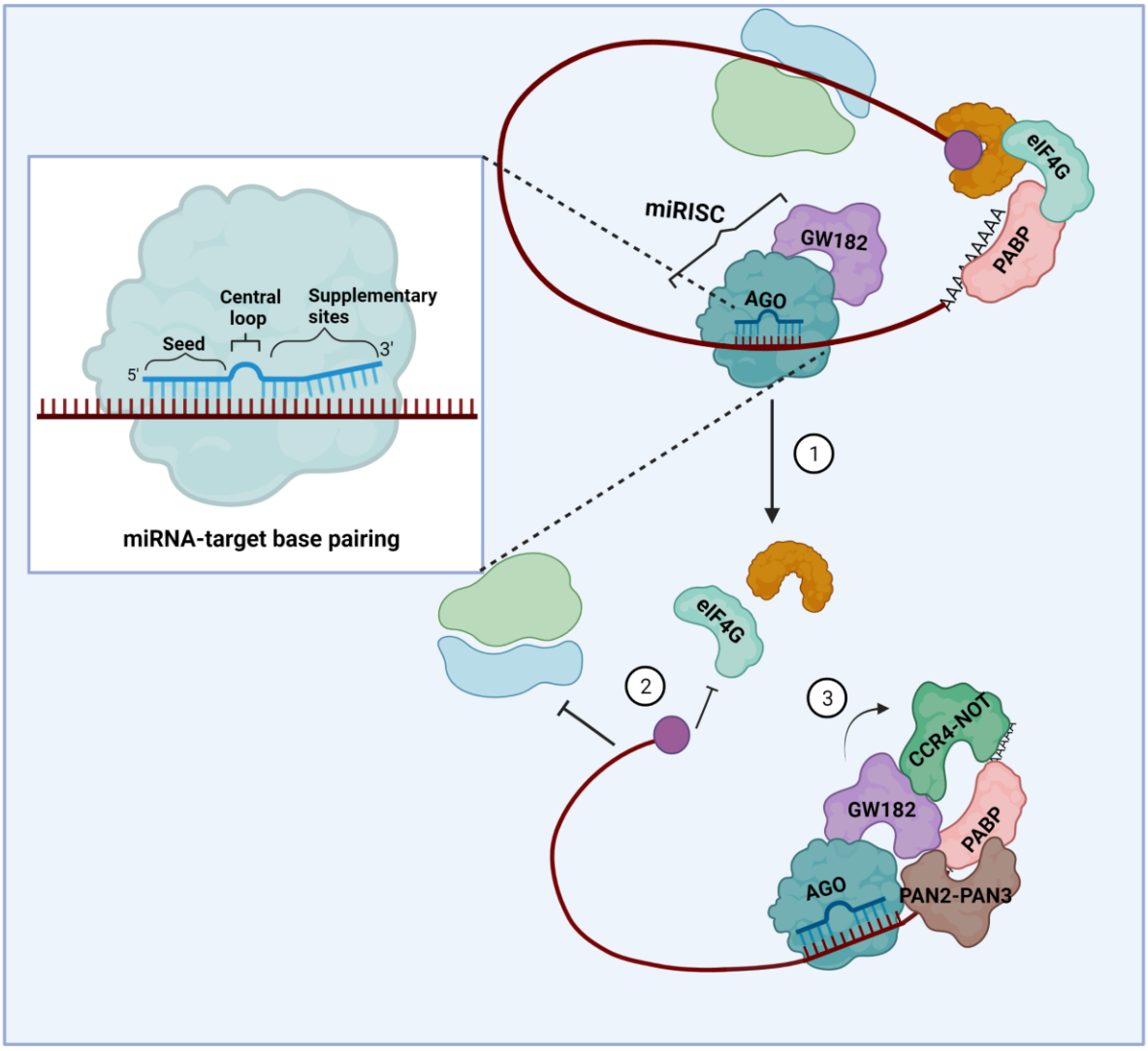

Figure 1.2 miRNA-mediated post-transcriptional gene regulation.

(1) miRNAs direct miRISC to target sites using partial base pair complementarity. Inset shows the canonical (seed region) and non-canonical (central and supplementary region) base pairing sites. miRNA-target binding triggers gene silencing through (2) translational inhibition and (3) mRNA destabilization by recruiting effector proteins. Schematic was made using BioRender (biorender.com).

Functional role of miRNAs in developmental processes

The broad functional roles of miRNAs in regulating developmental and physiological processes can be attributed to their dual gene regulatory role which shapes both the transcriptome, and the protein expression outputs. miRNAs have been implicated in early embryonic and post-embryonic developmental processes (reviewed by Ambros and Ruvkun, 2018; Alberti and Cochella, 2017; DeVeale *et al.* 2021). For example, early embryogenesis is associated with significant changes to the transcriptome landscape which involves clearing of maternal mRNAs (Yartseva and Giraldez, 2015). In zebrafish, flies and Xenopus, miRNAs are critical for such maternal clearance (Giraldez *et al.* 2006; Lund *et al.* 2009; Bushati *et al.* 2008). At the onset of zygotic genome activation in zebrafish, *mir-430* is highly expressed and represses several hundred targets including maternal mRNAs (Giraldez *et al.* 2006). Similarly, miR-309 and miR-427 have also been demonstrated to massively repress maternal mRNA targets in *Xenopus* and *Drosophila,* respectively, and failure to downregulate maternal gene expression results in reduced survival and delayed development (Lund *et al.* 2009; Bushati *et al.* 2008).

During postembryonic development, miRNAs have been reported to regulate cell fate specification and developmental timing. lin-4, the first miRNA to be discovered, is a crucial component of the heterochronic pathway in *C. elegans* that regulates the timing of developmental decisions (Lee *et al.* 1993; Wightman and Ruvkun, 1993). The heterochronic pathway also includes let-7 family miRNAs that govern larval stage-specific cell fate specification of hypodermal cell lineages (Reinhart *et al.* 2000; Abbott *et al.* 2005). In mammals, miRNAs also make up the heterochronic pathway facilitating axial patterning and the timely onset of neurogenesis (Mallo and Alonso, 2013; Yekta *et al.* 2004). Genetic analysis in *C. elegans* and other species have revealed critical functions of miRNAs in several other developmental processes

including growth, longevity, and behavior (reviewed in Ambros and Ruvkun, 2018; DeVeale *et al.* 2021).

miRNAs also regulate physiological processes and maintenance of homeostasis in response to environmental perturbations. For example, miR-128 targets ion channels and neurotransmitter transporters and loss of this miRNA activity leads to fatal epilepsy (Tan *et al*. 2013). In mouse, miR-429 coordinates a hormone surge essential for regulating female fertility (Hasuwa *et al*. 2013). miRNAs that confer robustness in response to environmental perturbations have also been identified in several species (Li *et al.* 2009; Burke *et al.* 2015; Kasper *et al.* 2017). While most miRNAs described above are expressed broadly in multiple tissues leading to easily observable phenotypes upon their disruption, some miRNAs are expressed and function at a tissue or cell-specific level (Alberti and Cochella, 2017). Thus, their depletion may not cause disruption at the whole organism level hindering their functional identification. Hence, efforts remain focused on developing tools for assessing tissue-specific functions of miRNAs. Genetic models such as *C. elegans* have been useful in revealing complexities of miRNA functions at tissue specific levels (for an example, see Johnston and Hobert, 2003).

miRNA biogenesis and processing

miRNAs are transcribed from their diverse genomic locations by RNA Pol II to form primary miRNAs that are capped and polyadenylated and harbor hairpins (Fig 1.3) (Lee *et al.* 2004; Cai *et al.* 2004). Genes encoding miRNAs can reside within the exons or introns of protein coding genes, lncRNA genes or be intergenic (Kim and Kim, 2007; Rodriguez *et al.* 2004). miRNAs can be transcribed as independent units or generated as a part of host gene transcription. miRNAs can comprise one hairpin (single miRNA) or multiple hairpins (clustered miRNAs).

Primary miRNAs are capped at their 5' ends and polyadenylated at their 3' ends (Fig 1.3) (Cai *et al.* 2004). The heterotrimeric microprocessor complex consisting of one DROSHA and two DGCR8 proteins processes primary miRNAs to generate precursor miRNAs (Beezhold *et al.* 2010; Li *et al*. 2020; Creugny *et al.* 2018). While Drosha recognizes the dsRNA-ssRNA junction in the base of the stem, DGCR8 ensures accurate cleavage (Nguyen *et al.* 2015). The resulting precursor miRNA, typically 60-120nt long harboring a stem loop structure with the 3' 2-nucleotide overhang is then bound by Exportin to be exported into the cytoplasm (Yi *et al.* 2003). The RNase III enzyme, Dicer, then processes the pre-miRNA by acting as a molecular ruler and cleaving the precursor at a specific sequence length to release the loop, generating the miRNA duplex (Bernstein *et al.* 2001). This duplex loads into the Argonaute protein as a part of the miRNA loading complex (miRLC) (McRae *et al.* 2008). Argonaute unwinds the duplex and strategically retains one of the miRNA strands as the guide strand and releases the passenger strand for degradation (Michlewksi and Cáceres, 2019). The mature miRNA then guides AGO to target sites for gene silencing (Fig 1.3).

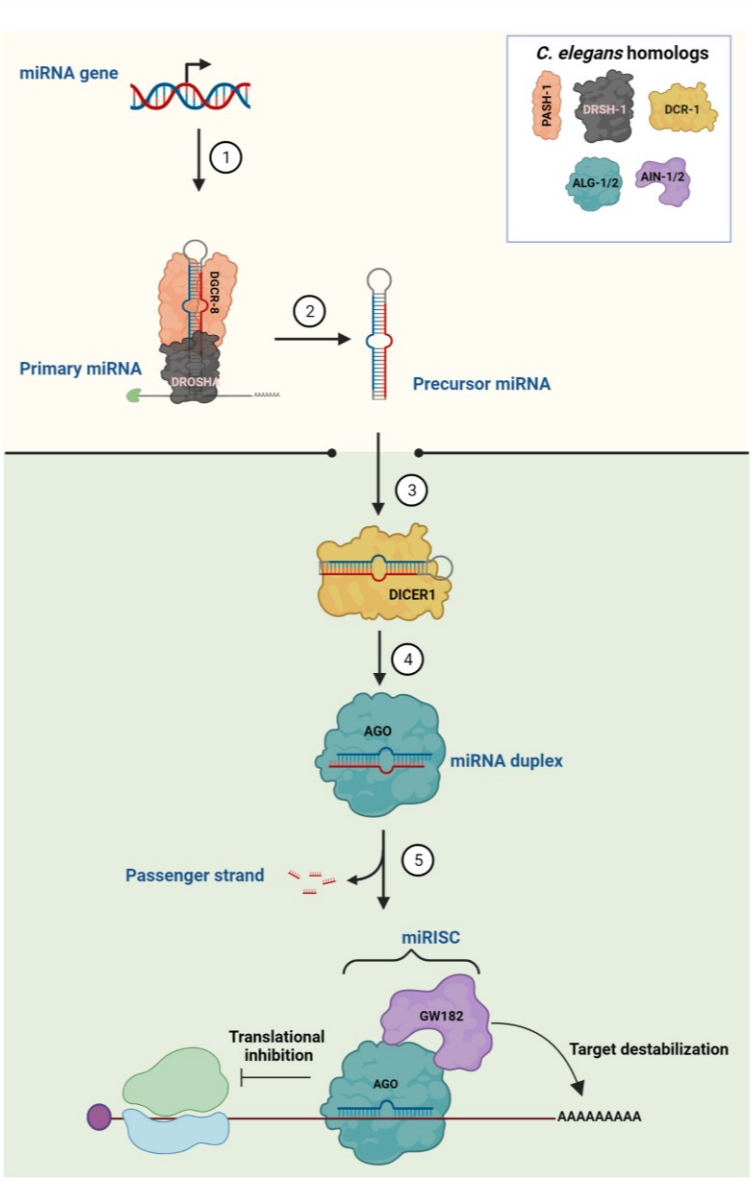

Figure 1.3 A schematic of miRNA biogenesis pathway.

Biogenesis entails (1) miRNA transcription by RNA pol II as primary miRNAs. (2) Primary miRNAs are bound and processed by the microprocessor complex to generate precursor miRNAs. (3) Precursors are exported to the cytoplasm where (4) Dicer cleaves it to generate miRNA duplex which is loaded into Argonaute. (5) Argonaute selectively retains one strand of the duplex (guide), discards the other strand (passenger). miRNAs guide miRISCs to target sites to bring about target repression. Schematic was made using BioRender (biorender.com).

Molecular basis of target recognition

miRNAs guide the miRISC to target mRNAs via sequence complementarity between miRNAs and their targets. miRNA seed region spans positions 2-8 which recognizes partial complementary sites within the 3' UTR region of target mRNAs (Bartel, 2009). While the most efficient canonical site is the 8-mer (matching 2-8 seed position), lesser efficient 7-mer and 6-mer base pairing between miRNAs and their targets are also observed (Agarwal *et al.* 2015) (Fig 1.2). In addition to the seed region, base pairing also occurs at the non-canonical sites such as the central sites (position 11-12) and the 3' end sites (Agarwal *et al.* 2015). While the relevance and target repression efficiencies of these non-canonical sites require further exploration, studies suggest in some cases they lead to specificity of target binding (Duan *et al.* 2022; Broughton *et al.* 2016; Wahlquist *et al.* 2014; Brennecke *et al.* 2005; Grimson *et al.* 2007). A high resolution, protein-RNA interaction detection technique entailing crosslinking and immunoprecipitation (iCLIP) of Ago-bound RNA in *C. elegans* revealed that although base pairing with the targets occurs predominantly at the seed, base pairing at the 3' ends of miRNAs determine target-binding specificities to individual members within miRNA families (Broughton *et al.* 2016). In some cases, extensive 3' end pairing can compensate for imperfect seed pairing (Chi *et al.* 2012; Doench and Sharp, 2004). Further, a massive parallel reporter assay approach demonstrated that the target repression efficiency is dependent on the number of target sites as well as the relative positions of these miRNA and other trans-factor binding sites (Cotrell *et al.* 2018). The extent and nature of base pairing as well as their target site overlap with other trans-factors such as RNA binding proteins can influence gene silencing efficiencies by miRNAs emphasizing the need to assess factors that interplay with miRNAs at the target sites.

Many modes of miRNA mediated gene silencing

mRNAs targeted by miRNAs are subjected to gene silencing by mechanisms including translational inhibition, decapping, deadenylation and decay (Djuranovic *et al.* 2012; Mathonnet *et al.* 2007). Core miRISC components, Argonaute and GW182 recruit effector complexes including the CCR-NOT, PAN2-PAN3 deadenylase complexes, and mRNA decapping factors to the target site that mediate gene silencing through distinct mechanisms (Fig 1.2) (Braun *et al*. 2011; Fabian *et al.* 2011). GW182 binds to the poly(A)-tail binding protein PABP and disrupts its interaction with the cap binding protein eIF4G thereby triggering events that lead to translational inhibition (Derry *et al.* 2006; Smith *et al.* 2014). Studies also suggest that miRISC binding disassociates PABP from poly-A sites, especially when CCR4-NOT and PAN2-PAN3 deadenylase complexes are recruited which initiate deadenylation and subsequent mRNA decay (Zekri *et al.* 2013; Chekulaeva *et al.* 2011; Fabian *et al.* 2011). Thus, PABP is suggested as a key link connecting the two modes of miRNA mediated target repression (Duchaine and Fabian, 2019).

Translational inhibition is facilitated by disassociation of cap binding proteins which inhibits translation at the initiation step (Fig 1.2) (Zekri *et al.* 2013; Rissland *et al.* 2017; Moretti *et al.* 2012). CCR4-NOT binding leads to recruitment of decapping enhancers and translation repressors including 4E-T, 4EHP, GIGYF2 among others. Other effectors proteins have also been reported to mediate gene silencing by miRNAs (Duchaine and Fabian, 2019). Several reports suggest translation inhibition is a consequence of deadenylation as the latter leads to target destabilization which impacts translation efficiency. Contrary to that, deadenylation independent translation inhibition is also reported to occur and the underlying mechanism is not well established (Cooke *et al.* 2010; Braun *et al.* 2011; Fukaya and Tomari, 2012; Jannot *et al.* 2016; Dallaire *et al.* 2018). Also unclear is the chronological and molecular sequence of different gene

silencing events and their relative contribution towards target repression. While translation inhibition is a reversible process, mRNA decay is irreversible, and "choosing" the target suppression mode is a critical process in regulating the gene expression.

Several attempts have been made to clarify the relative timeline of gene silencing events by miRNAs in different systems. One study concurrently measured target transcript levels and translation efficiencies for predicted targets following depletion of select miRNAs in different mammalian cells. This study reported that mRNA decay is the predominant gene silencing event regardless of the context (Eichhorn *et al.* 2014). In addition, this study corroborated previous findings that translation repression precedes mRNA decay, and mRNA destabilization dominates over time (Guo *et al.* 2010; Djuranovic *et al.* 2012; Bazzini *et al.* 2012; Larsson and Nadon, 2013). Another study developed reporters to track RISC binding, translation repression, and mRNA decay through single molecule imaging. Simultaneous tracking of cytoplasmic mRNAs through smFISH, single molecule-based imaging of nascent peptide (SINAP) technique and AGO-based detection of RISC revealed that translation repression precedes target decay (Kobayashi and Singer, 2022). Future work is necessary to assess the effects of deadenylation on translational inhibition and vice versa.

On the other hand, a meta-analysis of studies conducted in miRNA mutant mice including a total of 159 target genes of 77 miRNAs revealed that 48% of the targets are regulated by translational inhibition only, 29% by mRNA decay and 23% by both decay and translational inhibition (Jin and Xiao, 2015). A few other studies have also reported translational inhibition of targets in the absence of mRNA decay (Fukaya and Tomari, 2012; Jafarnejad *et al.* 2018; Jannot *et al.* 2016, Dallaire *et al.* 2018). The variations in outcomes of these studies could be due to inherent limitations of their respective approaches. For instance, high throughput approach-based

assessment of bulk molecules in cell culture systems often fail to reveal the nuances of specific extrinsic and intrinsic factors that influence the outcomes of miRNA targeting (Kobayashi and Singer, 2022). In addition, transgenic induction of miRNA targeting in cell lines may not accurately reflect the dynamics of gene silencing events in response to developmental cues *in vivo*. Despite their limitations, the collective efforts at uncovering the mechanism underlying miRNA mediated gene regulation have revealed that the ultimate outcome of miRNA targeting is heavily influenced by several extrinsic (miRISC composition) and intrinsic factors (cis elements in target 3' UTR) (reviewed in Naeli *et al.* 2022).

Heterogeneity in miRISC composition and miRNA interactions and their impact on outcomes of miRNA-mediated gene silencing

miRISC composition and interactions are more dynamic than previously perceived and emerging evidence point towards this heterogeneity to be the source of variations in miRNA activity (Fig 1.4). The dynamicity may first arise from heterogeneity of core miRISC components as well as differences in their interactions (Fig 1.4A, B). There are multiple Argonautes in both mammalian and non-mammalian species. Human and mammalian Argonautes (AGO 1-4) have been all reported to function in the miRNA pathway while sharing about 75% of the miRNAs they associate with. While they all have overlapping functions, a few reports suggest discreet roles for each AGO when bound to specific miRNAs under distinct conditions (Hu *et al.* 2012; Miyazaki *et al.* 2016; Adiliaghdam *et al.* 2010). In *C. elegans*, the two Argonautes that predominantly function in the miRNA pathway, ALG-1 and ALG-2, show some degree of uniqueness in their miRNA repertoire, perhaps owing to subtle differences in their spatiotemporal expression patterns (Brown *et al.* 2017; Brosnan *et al.* 2021). Apart from ALG-1 and ALG-2, other Argonautes such as ALG-

5, associate with a small fraction of miRNAs (Fig 1.4A) (Brown *et al.* 2017). In addition, ALG-1 and ALG-2 were identified to have opposing roles on aging, potentially stemming from differences in miRNA loading and distinct effects on protein coding gene expression profiles (Aalto *et al.* 2018). Spatiotemporal dissections of miRISC composition in *C. elegans* also revealed differential association of AIN-1 with miRNAs in germline and somatic tissues (Fig 1.4B) (Jannot *et al*. 2016, Dallaire *et al.* 2018). GW182 homologs AIN-1 and AIN-2 were not a part of miRISC in the germline or in the embryos (Jannot *et al.* 2016, Dallaire *et al.* 2018). In the germline, miRISC-targeted mRNA transcripts were sequestered to the perinuclear region (Fig 1.4B). An integral P-granule component GLH-1 was found to be required for such sequestration, which in turn precluded the mRNA transcript from translation initiation and decay (Dallaire *et al.* 2018). This mode of target repression is likely adopted when translation is required to quickly resume at a later stage of development.

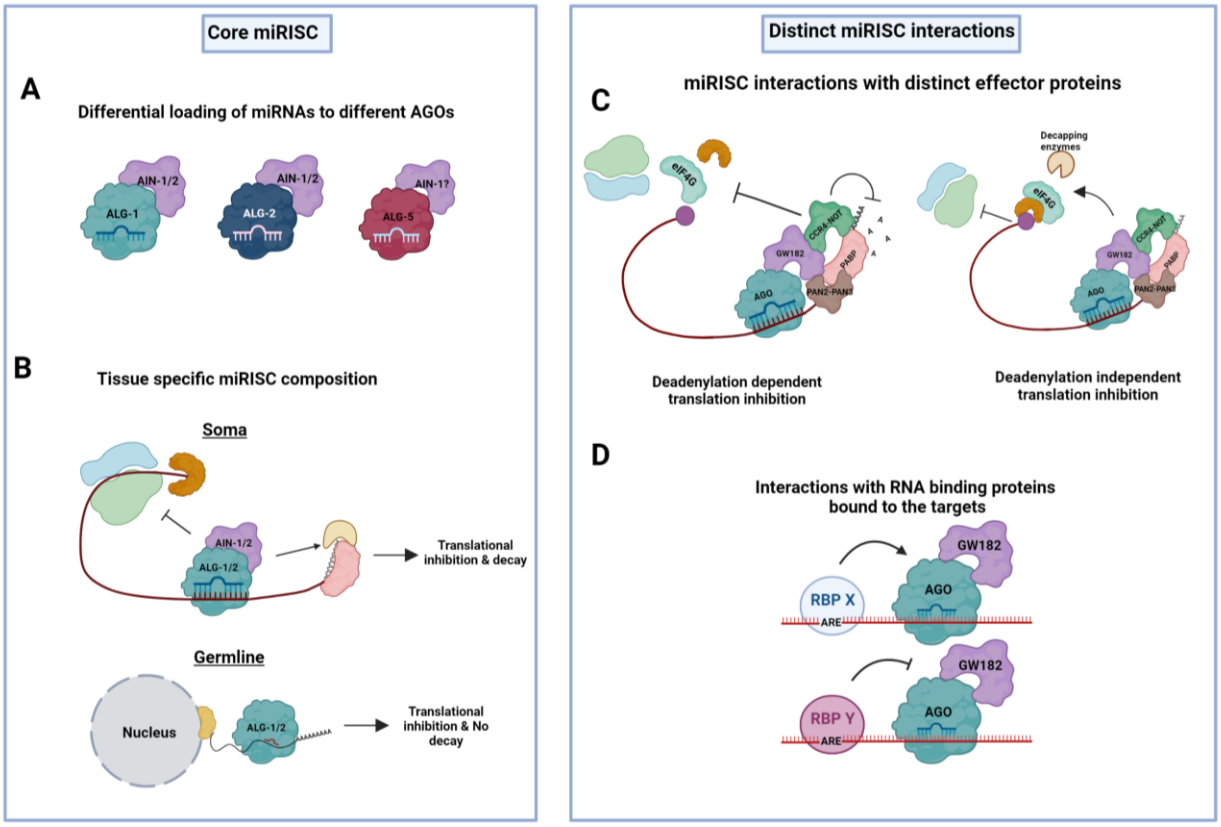

Figure 1.4 Heterogeneity in miRISC composition and interactions.

A) Different AGOs can have both distinct and overlapping miRNA binding preferences. Shown here are prominent miRNA binding Argonautes in *C. elegans*. (B) In *C. elegans* germline, GW182 homolog AIN-1 does not associate with miRISC unlike in somatic tissues which impacts outcomes of miRNA activity. (C) Heterogeneity in miRISC interactions with effector proteins has been reported to affect the mode of gene silencing. (D) RNA binding proteins that bind to different cis elements within mRNA 3' UTR can either promote or inhibit miRISC activity. Schematic was made using BioRender (biorender.com).

In addition to distinct core miRISC composition, distinct effector protein recruitment has been previously reported to result in variation in gene silencing modes by miRNAs (Fig 1.4C) (Duchaine and Fabian, 2019; Naeli *et al.* 2022). The dynamic nature of miRISC interactions could also be the result of differential subcellular localization of miRNAs. It is possible that different locations might facilitate distinct miRISC interactions ultimately dictating the mode of gene regulation. For instance, some miRNAs localize to the rough ER where bulk of the translation occurs, thus making it an ideal site for miRNA mediated translational repression for miRNA targets (Bharman and Bhattacharya, 2015; Wu *et al.* 2013). Other sites such as the cytoplasmic P-bodies, the endosomal trafficking organelles such as Golgi network and vesicles are also reported as sites of miRISC activity. miRNAs are also found in the mitochondria where they regulate gene expression using both conventional and unconventional modes. Mito-miR-181c represses translation of mtCOX1 (Das *et al.* 2014), while mito-miR-1 stimulates translation of COX1 and other genes that enable muscle differentiation. Interestingly, different studies have reported that mitochondrial miRISCs are composed of Ago2 but lack GW182 (Zhang *et al.* 2014; Jagannathan *et al.* 2015). However, the mechanism of gene regulation in mitochondria in the absence of GW182 is not known (Larriba *et al.* 2018; Duarte *et al.* 2014). Similarly, miRNAs localized to the nucleus or nucleolus have also been suggested to perform unconventional gene regulatory functions such as transcriptional regulation and splicing (Carissimi *et al.* 2015; Leucci *et al.* 2013; Nishi *et al*. 2013). AGOs in the nucleus have been reported to interact with chromatin modifiers suggesting that distinct miRISC functions are dictated by distinct interactions.

Another source of variation in miRNA activity is the intrinsic sequence features of mRNA targets, bound by an assortment of trans-acting RNA binding proteins. Cis elements such as AU-rich elements (AREs) can both promote or inhibit gene silencing by miRNAs depending on the

context such as their relative position as well as the trans-acting factors that bind to them (Cotrell *et al.* 2018). In addition, relative positions of miRNA binding sites and AREs within 3' UTRs have also been demonstrated to result in target destabilization and translation repressions of varied efficiencies (Cotrell *et al.* 2018). A systematic analysis of binding sites of 150 human RBPs and their effects on miRNA targeting efficiencies uncovered that the majority of RBPs enhance miRNA targeting (Kim *et al.* 2021). However, there is likely diversity among the functional contributions of RBPs on miRNA activity, one that is dependent on miRNA/RBP/target "pairing". In addition to coordinating with miRNAs at their target sites to modulate miRNA activity, RBPs have also been identified to influence other aspects of the miRNA lifecycle including biogenesis and stability (as reviewed in Hao *et al.* 2017; Treiber *et al.* 2019). Thus, a given RBP can influence miRNA-mediated gene regulation through multiple mechanisms, adding an additional layer of complexity to post-transcriptional gene regulation. Our understanding of miRNA-mediated gene regulation will be greatly enhanced by characterizing individual miRNA-RBP coordination during different developmental contexts.

Overall, a comprehensive understanding of the heterogeneity of protein complexes associated with miRNAs in various contexts has the potential to reveal the dynamic nature of miRNA mediated gene silencing and uncover the wide range of functions miRNAs perform during development. In this dissertation, I aimed to fill this gap in our understanding of miRNA biology, particularly with respect to regulation of miRNA activity by heterogenous association between the miRISC and auxiliary proteins. In Chapter 2, I describe a miRNA-centered functional proteomics approach employed to capture miRNA auxiliary factors. In addition, I determined the context-dependent functional role of the newly identified miRNA complex components, with several RNA binding proteins identified to functionally support developmental functions of distinct miRNAs.

Heterogenous nuclear ribonucleoprotein family

Among the various RNA binding proteins that extensively regulate RNA metabolism are one of the largest families of highly abundant proteins called the Heterogenous nuclear ribonucleoproteins (hnRNPs). This family constitutes approximately 25 proteins that form complexes with newly transcribed RNAs in the nucleus to process them into mature RNAs (Dreyfuss *et al.* 1993; Beyer *et al.* 1977; Pinol-Roma *et al.* 1988). The HnRNP family of proteins are conserved across humans, flies, *C. elegans* among other species. 14 members of this family have been identified in *Drosophila* while 13 hnRNPs have been identified in *C. elegans* (Piccolo *et al.* 2018; Busch and Hertel. 2012). Of the approximately 25 proteins in the family, six members that make up the hnRNPA/B subgroup (A1, A2B1, A3, and A0) are considered the core proteins (Fig 1.5) (Mayeda *et al.* 1994; Dreyfuss *et al.* 1993).

hnRNPA/B subgroup members harbor two-three RNA Recognition Motif (RRM) RNA binding domains and intrinsically disordered domains (Prion-like domain) containing Glycine or Proline rich regions (Fig 1.5) (Geuens *et al*. 2016; Dangli *et al.* 1996). HnRNPs also harbor canonical and non-canonical nuclear localization and nucleo-cytoplasmic shuttling signals. All the human hnRNPs are known to shuttle between nucleus and cytoplasm as a result of these localization signals (Harrison and Shorter, 2017; Kim *et al.* 2013; Mears and Rice, 1996; Wu *et al.* 2018). The RNA binding domains of these proteins allow them to sequence specifically bind to different classes of RNA, while the intrinsic disordered domains drive extensive protein-protein interactions (Hans *et al*. 2010). Some hnRNPs have also been reported to form liquid-liquid phase separations (Ritsch *et al.* 2022; Ryan *et al.* 2021).

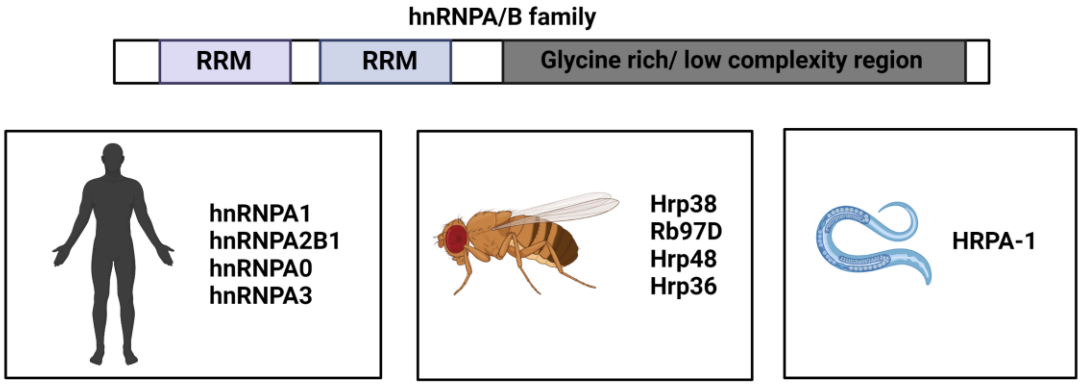

Figure 1.5 hnRNPA/B family proteins in humans, flies, and *C. elegans*.

(A) A schematic of the most common protein domains harbored by hnRNPA/B family proteins across different species. RRM RNA Recognition Motif. Schematic was made using BioRender (biorender.com).

Co-transcriptional and posttranscriptional gene regulatory functions of hnRNPA/B proteins.

hnRNPA/B and splicing

Regulation of splicing is a conserved functional role of hnRNP family proteins with both mammalian and non-mammalian orthologues implicated in either constitutive or alternative splicing (Piccolo *et al.* 2014; Sun *et al.* 2020; Bruun *et al.* 2016; Heintz *et al.* 2017; Barberan-Soler *et al.* 2011). The subgroups within the family hnRNPA/B and hnRNPF/H are mostly considered splicing silencers as they antagonize the effects of splicing enhancers such as the SR proteins (Zhu *et al.* 2001). Both RRM domains and unstructured C-terminal domains (Glycine-rich, Proline-rich) of these proteins play a role in modulating splicing outcomes (Jean-Philippe *et al.* 2013). While the RRM domains facilitate binding to specific cis elements in the exon and intron, the Prion like domains recruit accessory proteins that inhibit spliceosome complex assembly (Jean-Philippe *et al.* 2013).

The hnRNPA/B subfamily of proteins bind to cis- elements such as Intronic Splicing Silencers (ISS), Exonic Splicing Silencer (ESS) or Exonic Splicing Enhancers (ESE) and regulate splicing through diverse mechanisms (Zhu *et al.* 2001). HnRNPs antagonize the splicing effects of the serine/arginine-rich (SR) family of splicing activators (Caceres *et al.* 1994). For instance, SR proteins bind to ESEs and promote exon inclusion in the mature mRNA. hnRNPA1 bound to ESSs downstream of or overlapping with ESEs can displace SR proteins by recruiting additional hnRNPA1 proteins and inhibiting the assembly of the core spliceosome complex (Caceres *et al.* 1994). This eventually prevents the exon from being included in the mature mRNA (Cartegni and Krainer, 2002; Venables *et al.* 2005). Binding of hnRNPA1 to ISSs in introns or branch points also has similar effects, ultimately preventing the splicing of the downstream exon (Guo *et al.* 2013;

Tange *et al.* 2001). Despite extensive research, the transcriptome-wide splicing targets of the hnRNPA/B family is not well characterized. The *C. elegans* homolog, HRPA-1 has also been reported to regulate splicing, with alternative splicing of 11 transcripts being affected by loss of this protein (Barberan-Soler *et al.* 2011). The implications of HRPA-1-mediated alternative splicing on developmental programs and the underlying mechanism has not been studied in detail. *Drosophila* hnRNPA/B homologs were also reported to play a role in splicing regulation (Borah *et al.* 2009; Venables *et al*. 2012).

hnRNPA/B and miRNAs

The RNA binding ability of hnRNPA/B proteins is not just restricted to pre-mRNAs. hnRNPA1 has been identified to bind pri-miRNAs in the nucleus (Fig 1.6) (Guil and Ca´ceres, 2007, Michlewski and Ca´ceres, 2010, Kooshapaur *et al*. 2018). CLIP experiments first revealed hnRNPA1 to bind to pri-miR-18a (Guil and Ca´ceres, 2007). miR-18a is transcribed as a part of a miR-17-92 cluster consisting of six individual miRNAs (Guil and Ca´ceres, 2007). hnRNPA1 was identified to specifically bind the terminal loop of pri-miR-18a and induce conformational changes making the stem structure readily accessible for microprocessor binding, thus promoting pri-miR-18a processing (Kooshapaur *et al.* 2018). hnRNPA1 was not found to bind to or regulate the processing of any other miRNAs in that cluster, suggesting a sequence and context dependent association between hnRNPA1 and miR-18a (Fig 1.6A) (Kooshapaur *et al.* 2018). Interestingly, pri-miR-18a terminal loop is highly conserved among the vertebrates and conservation of terminal loops has been suggested as an indication of their potential role in miRNA processing (Michlewski *et al.* 2008). One of the other miRNAs with a conserved terminal loop is pri-let-7a and RNA chromatography followed by Mass-spectrometric analysis revealed hnRNPA1 binding to the pri-

let-7 terminal loop (Michlewski *et al.* 2008). The hnRNPA1 binding site on pri-let-7 coincided with that of KSRP (K-homology Splicing Regularory Protein) highlighting a possible competition among these proteins for occupancy of pri-let-7 terminal loop (Fig 1.6B) (Michlewski *et al.* 2008). Interestingly, hnRNPA1 binds pri-let-7 and blocks microprocessor complex binding thereby negatively regulating let-7 miRNA (Fig 1.6C) (Michlewski and Ca´ceres, 2010). Despite acting at the level of primary miRNA processing, hnRNPA1 appears to affect miR-18 and let-7 differently. In hepatic stellate cells, depleting hnRNPA1 led to reduced miR-18 levels and upregulation of several predicted targets which promoted fibrotic signaling (Koo *et al.* 2016). Whether the target upregulation was due to disruption of miR-18 regulation of its targets and how such a disruption affects developmental processes *in vivo* remains to be investigated.

hnRNPA2B1, another member within the hnRNPA/B subgroup, has also been previously implicated in miRNA processing. m6A modification on nuclear transcripts affects their localization and stability (Fig 1.7A) (Pajares *et al.* 2021). In addition to the messenger RNAs, nuclear primary miRNA transcripts have also been shown to undergo m6A modification (Alarco´n *et al.* 2015). hnRNPA2B1 was identified as a reader of m6A modification of both primary miRNA and pre-mRNA transcripts (Alarco´n *et al.* 2015). hnRNPA2B1 recruits the microprocessor complex to m6A methylated primary miRNA transcripts thereby promoting their processing. hnRNPA2B1 also acts as an effector protein that facilitates miRNA targeting by rearranging RNA secondary structure within the target 3' UTR (Fig 1.7B) (Yin *et al.* 2021). For instance, CDK6 mRNA harbors binding sites for each hnRNPA2B1 and miR-506, which when unoccupied form a stem-loop structure owing to their complementarity. This prevents miR-506 from accessing its binding site. Binding of hnRNPA2B1 unwinds the stem structure exposing the miRNA binding site, thus promoting miRNA targeting (Yin *et al*. 2021).

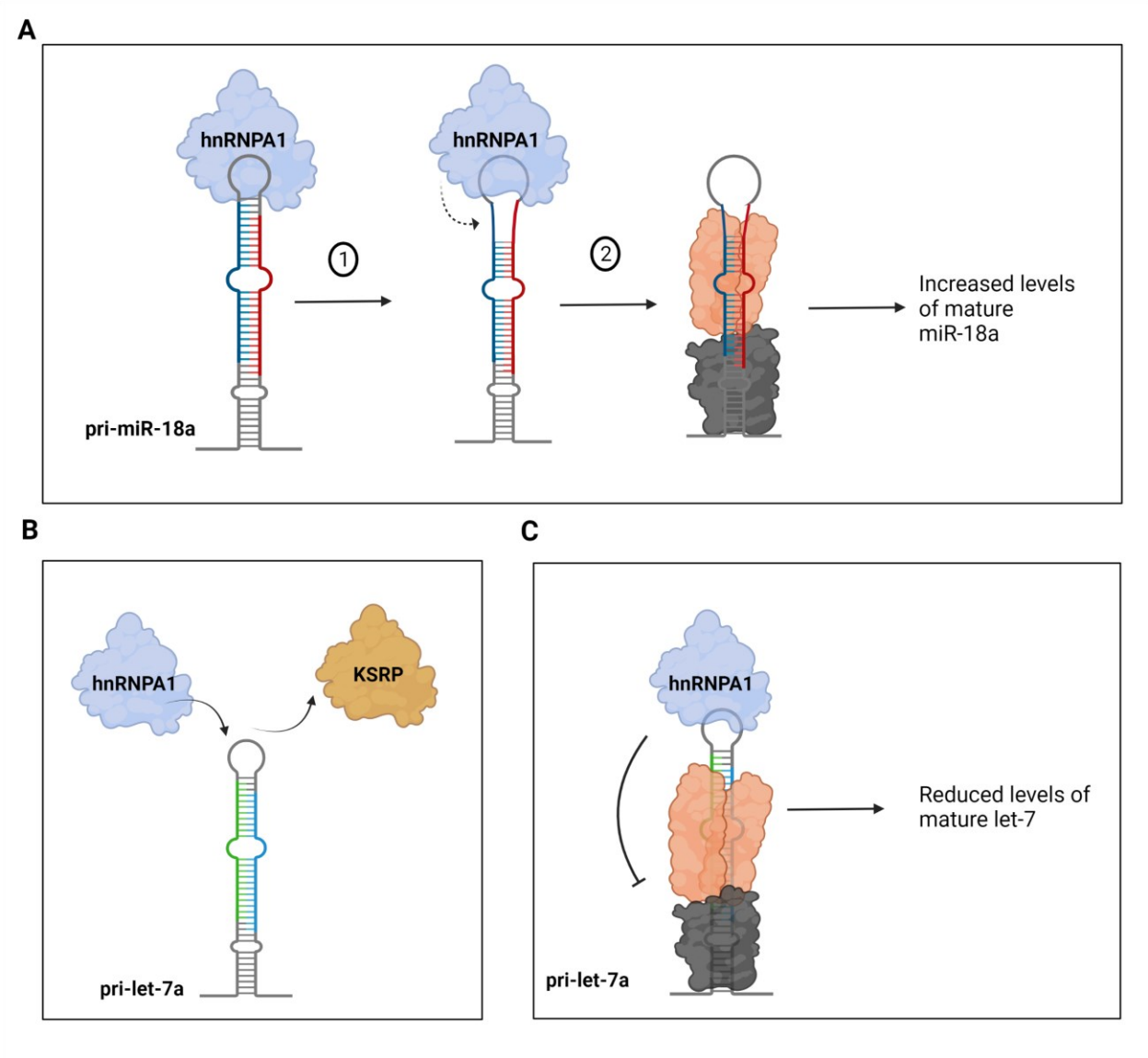

Figure 1.6 hnRNPA1 regulates primary miRNA processing leading to different outcomes. A) hnRNPA1 regulates pri-miR-18a processing by (1) binding to terminal loop to (2) induce conformational change which is believed to promote processing my microprocessor complex and increased levels of mature miR-18a. (B) hnRNPA1 competes with KSRP to bind to terminal loop of pri-let-7a. (C) Association of hnRNPA1 with pri-let-7a inhibits processing by the microprocessor complex, thus decreasing the levels of mature let-7. Schematic was made using BioRender (biorender.com).

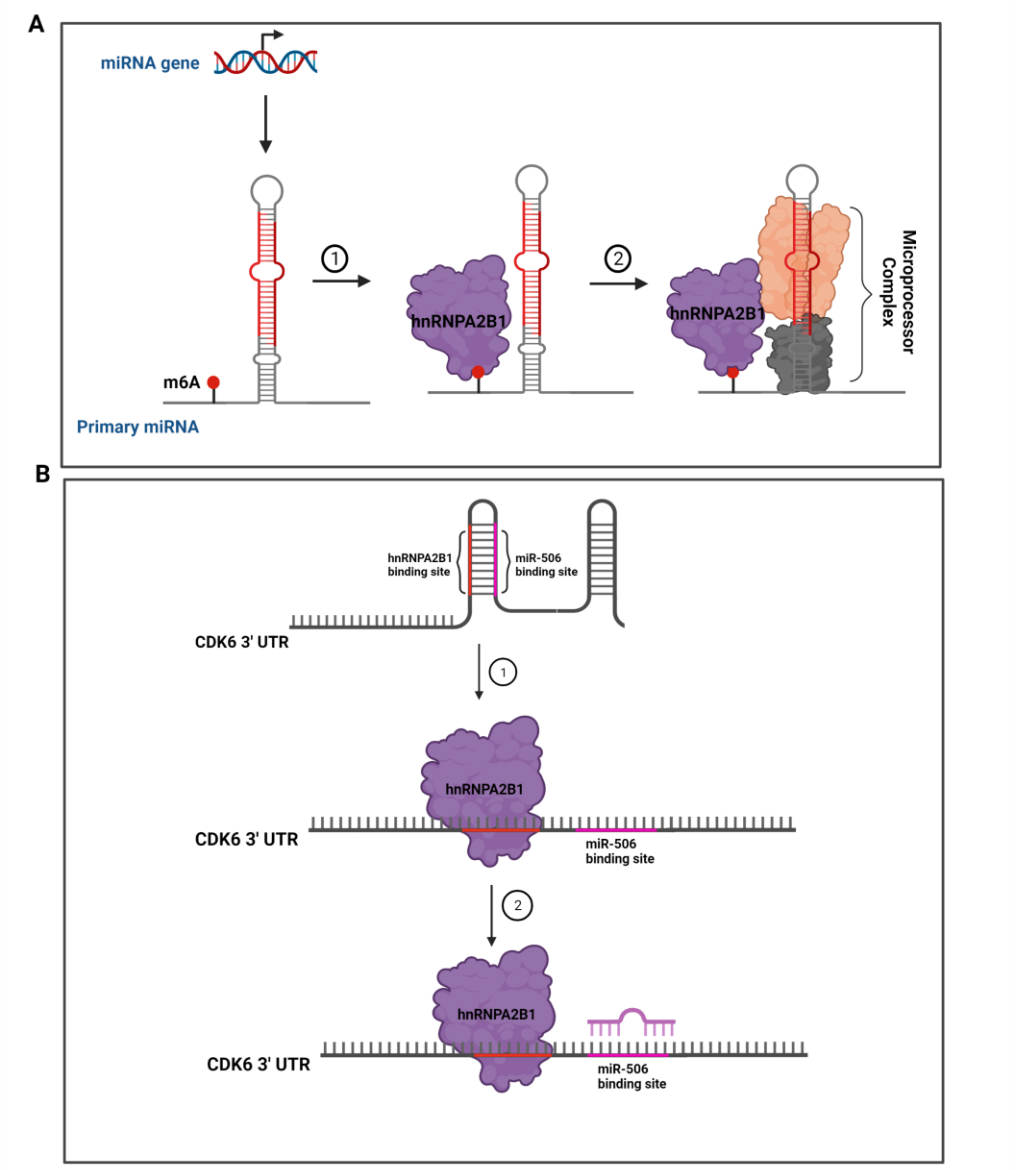

Figure 1.7 Distinct mechanisms through which hnRNPA2B1 regulates miRNA mediated gene regulation.

(A) hnRNPA2B1 binds to m6A modified sites within primary miRNAs (1) and recruits microprocessor complex (2). (B) hnRNPA2B1 also impacts miRNA activity by binding to targets (1) and promoting the accessibility to miRNA/miRISC (2). Schematic was made using BioRender (biorender.com).

Through their gene regulatory functions, hnRNPA/B proteins could be playing critical roles in several developmental and physiological processes. The fact that dysregulation of hnRNPA/B proteins have been implicated in several diseases supports this view (reviewed in Liu and Shi, 2020). Although investigations in tissue culture systems have been very valuable in revealing the structural and biochemical basis of gene regulation by hnRNPA/B proteins, we understand very little about the effects of these events on developmental processes *in vivo*. In addition, changes in miRNA levels observed in gene knockouts or overexpression studies in tissue cultures may not always accurately reflect their impacts on developmental processes. By contrast, functional investigations *in vivo* in genetic models can assess the effects of perturbations of specific gene regulatory functions on developmental processes. For instance, investigation of an hnRNP homolog, HRPK-1, in our lab revealed the complexity of consequences of coordination between this protein and miRNAs (Li *et al.* 2019). The effects of loss of *hrpk-1* on miRNA levels did not always correlate with the effects on developmental processes, suggesting a complex molecular relationship. Thus, to comprehensively understand the functions of hnRNPA/B proteins in gene regulation and developmental processes, we need to use genetic and molecular approaches in model systems. The availability of miRNA sensitized backgrounds and conservation of hnRNPA/B protein between humans and *C. elegans* make them a great model to study these gene regulatory processes. In Chapter 3, I describe functional characterizations of an hnRNPA/B homolog, HRPA-1, identified as a physical interactor of miRNA complexes (Chapter 2) and demonstrate a previously unknown HRPA-1 role in regulation of gene expression by distinct, developmentally important, miRNAs.

References

Aalto, A. P. et al. Opposing roles of microRNA Argonautes during Caenorhabditis elegans aging. Plos Genet 14, e1007379 (2018).

Abbott, A. L. *et al.* The let-7 MicroRNA Family Members mir-48, mir-84, and mir-241 Function Together to Regulate Developmental Timing in Caenorhabditis elegans. *Dev Cell* 9, 403–414 (2005).

Agarwal, V., Bell, G. W., Nam, J.-W. & Bartel, D. P. Predicting effective microRNA target sites in mammalian mRNAs. *Elife* 4, e05005 (2015).

Alarcón, C. R. *et al.* HNRNPA2B1 Is a Mediator of m6A-Dependent Nuclear RNA Processing Events. *Cell* 162, 1299–1308 (2015).

Ambros, V. & Ruvkun, G. Recent Molecular Genetic Explorations of *Caenorhabditis elegans* MicroRNAs. *Genetics* 209, 651–673 (2017).

Barberan-Soler, S., Medina, P., Estella, J., Williams, J. & Zahler, A. M. Co-regulation of alternative splicing by diverse splicing factors in Caenorhabditis elegans. *Nucleic Acids Res* 39, 666–674 (2011).

Barman, B. & Bhattacharyya, S. N. mRNA Targeting to Endoplasmic Reticulum Precedes Ago Protein Interaction and MicroRNA (miRNA)-mediated Translation Repression in Mammalian Cells*. *J Biological Chem* 290, 24650–24656 (2015).

Bartel, D. P. MicroRNAs: Target Recognition and Regulatory Functions. *Cell* 136, 215–233 (2009).

Bazzini, A. A., Lee, M. T. & Giraldez, A. J. Ribosome Profiling Shows That miR-430 Reduces Translation Before Causing mRNA Decay in Zebrafish. *Science* 336, 233–237 (2012).

Beezhold, K. J., Castranova, V. & Chen, F. Microprocessor of microRNAs: regulation and potential for therapeutic intervention. *Mol Cancer* 9, 134–134 (2010).

Bernstein, E., Caudy, A. A., Hammond, S. M. & Hannon, G. J. Role for a bidentate ribonuclease in the initiation step of RNA interference. *Nature* 409, 363–366 (2001).

Beyer, A. L., Christensen, M. E., Walker, B. W., & LeStourgeon, W. M. Identification and characterization of the packaging proteins of core 40S hnRNP particles. *Cell* 11, 127-138 (1977).

Borah, S., Wong, A. C. & Steitz, J. A. Drosophila hnRNP A1 homologs Hrp36/Hrp38 enhance U2-type versus U12-type splicing to regulate alternative splicing of the prospero twintron. *Proc National Acad Sci* 106, 2577–2582 (2009).

Braun, J. E., Huntzinger, E., Fauser, M. & Izaurralde, E. GW182 Proteins Directly Recruit Cytoplasmic Deadenylase Complexes to miRNA Targets. *Mol Cell* 44, 120–133 (2011).

Brennecke, J., Stark, A., Russell, R. B. & Cohen, S. M. Principles of MicroRNA–Target Recognition. *Plos Biol* 3, e85 (2005).

Brosnan, C. A., Palmer, A. J. & Zuryn, S. Cell-type-specific profiling of loaded miRNAs from *Caenorhabditis elegans* reveals spatial and temporal flexibility in Argonaute loading. *Nat Commun* 12, 2194 (2021).

Broughton, J. P., Lovci, M. T., Huang, J. L., Yeo, G. W. & Pasquinelli, A. E. Pairing beyond the Seed Supports MicroRNA Targeting Specificity. *Mol Cell* 64, 320–333 (2016).

Brown, K. C., Svendsen, J. M., Tucci, R. M., Montgomery, B. E. & Montgomery, T. A. ALG-5 is a miRNA-associated Argonaute required for proper developmental timing in the Caenorhabditis elegans germline. *Nucleic Acids Res* 45, 9093–9107 (2017).

Bruun, G. H. *et al.* Global identification of hnRNP A1 binding sites for SSO-based splicing modulation. *Bmc Biol* 14, 54 (2016).

Burke, S. L., Hammell, M. & Ambros, V. Robust Distal Tip Cell Pathfinding in the Face of Temperature Stress Is Ensured by Two Conserved microRNAS in Caenorhabditis elegans. *Genetics* 200, 1201–1218 (2015).

Bushati, N., Stark, A., Brennecke, J. & Cohen, S. M. Temporal Reciprocity of miRNAs and Their Targets during the Maternal-to-Zygotic Transition in Drosophila. *Curr Biol* 18, 501–506 (2008).

Cáceres, J. F., Stamm, S., Helfman, D. M., & Krainer, A. R. Regulation of alternative splicing in vivo by overexpression of antagonistic splicing factors. *Science* 265, 1706-1709 (1994).

CAI, X., HAGEDORN, C. H. & CULLEN, B. R. Human microRNAs are processed from capped, polyadenylated transcripts that can also function as mRNAs. *Rna* 10, 1957–1966 (2004).

Carissimi, C. *et al.* ARGONAUTE2 cooperates with SWI/SNF complex to determine nucleosome occupancy at human Transcription Start Sites. *Nucleic Acids Res* 43, 1498–1512 (2015).

Chekulaeva, M., Mathys, H., Zipprich, J. T., Attig, J., Colic, M., Parker, R., & Filipowicz, W. miRNA repression involves GW182-mediated recruitment of CCR4–NOT through conserved W-containing motifs. *Nature structural & molecular biology* 18, 1218-1226 (2011).

Chi, S. W., Hannon, G. J. & Darnell, R. B. An alternative mode of microRNA target recognition. *Nat Struct Mol Biol* 19, 321–327 (2012).

Cooke, A., Prigge, A. & Wickens, M. Translational Repression by Deadenylases*. *J Biol Chem* 285, 28506–28513 (2010).

Cottrell, K. A., Chaudhari, H. G., Cohen, B. A. & Djuranovic, S. PTRE-seq reveals mechanism and interactions of RNA binding proteins and miRNAs. *Nat Commun* 9, 301 (2018).

Creugny, A., Fender, A. & Pfeffer, S. Regulation of primary microRNA processing. *Febs Lett* 592, 1980–1996 (2018).

Dallaire, A., Frédérick, P.-M. & Simard, M. J. Somatic and Germline MicroRNAs Form Distinct Silencing Complexes to Regulate Their Target mRNAs Differently. *Dev Cell* 47, 239-247.e4 (2018).

Dangli, A., Plomaritoglou, A., Boutou, E., Vassiliadou, N., Moutsopoulos, H. M., & Guialis, A. Recognition of subsets of the mammalian A/B-type core heterogeneous nuclear

ribonucleoprotein polypeptides by novel autoantibodies. *Biochemical Journal* 320, 761-767 (1996).

Das, S. *et al.* miR-181c Regulates the Mitochondrial Genome, Bioenergetics, and Propensity for Heart Failure In Vivo. *Plos One* 9, e96820 (2014).

Derry, M. C., Yanagiya, A., Martineau, Y. & Sonenberg, N. Regulation of Poly(A)-binding Protein through PABP-interacting Proteins. *Cold Spring Harb Sym* 71, 537–543 (2006).

DeVeale, B., Swindlehurst-Chan, J. & Blelloch, R. The roles of microRNAs in mouse development. *Nat Rev Genet* 22, 307–323 (2021).

Djuranovic, S., Nahvi, A. & Green, R. miRNA-Mediated Gene Silencing by Translational Repression Followed by mRNA Deadenylation and Decay. *Science* 336, 237–240 (2012).

Doench, J. G. & Sharp, P. A. Specificity of microRNA target selection in translational repression. *Gene Dev* 18, 504–511 (2004).

Dreyfuss, G., Matunis, M. J., Pi ol-Roma, S., & Burd, C. G. hnRNP proteins and the biogenesis of mRNA. *Annu rev biochem,* 62, 289-289 (1993).

Duan, Y., Veksler-Lublinsky, I. & Ambros, V. Critical contribution of 3′ non-seed base pairing to the in vivo function of the evolutionarily conserved let-7a microRNA. *Cell Reports* 39, 110745–110745 (2022).

Duchaine, T. F. & Fabian, M. R. Mechanistic Insights into MicroRNA-Mediated Gene Silencing. *Csh Perspect Biol* 11, a032771 (2019).

Eichhorn, S. W. *et al.* mRNA Destabilization Is the Dominant Effect of Mammalian MicroRNAs by the Time Substantial Repression Ensues. *Mol Cell* 56, 104–115 (2014).

Fabian, M. R. *et al.* miRNA-mediated deadenylation is orchestrated by GW182 through two conserved motifs that interact with CCR4–NOT. *Nat Struct Mol Biol* 18, 1211–1217 (2011).

Friedman, R. C., Farh, K. K.-H., Burge, C. B. & Bartel, D. P. Most mammalian mRNAs are conserved targets of microRNAs. *Genome Res* 19, 92–105 (2009).

Fukaya, T. & Tomari, Y. MicroRNAs Mediate Gene Silencing via Multiple Different Pathways in Drosophila. *Mol Cell* 48, 825–836 (2012).

Geuens, T., Bouhy, D., & Timmerman, V. The hnRNP family: insights into their role in health and disease. Human genetics, 135, 851-867 (2016).

Giraldez, A. J., Mishima, Y., Rihel, J., Grocock, R. J., Van Dongen, S., Inoue, K., ... & Schier, A. F. Zebrafish MiR-430 promotes deadenylation and clearance of maternal mRNAs. *Science* 312, 75-79 (2006).

Grimson, A. *et al.* MicroRNA Targeting Specificity in Mammals: Determinants beyond Seed Pairing. *Mol Cell* 27, 91–105 (2007).

Guil, S. & Cáceres, J. F. The multifunctional RNA-binding protein hnRNP A1 is required for processing of miR-18a. *Nat Struct Mol Biol* 14, 591–596 (2007).

Guo, H., Ingolia, N. T., Weissman, J. S. & Bartel, D. P. Mammalian microRNAs predominantly act to decrease target mRNA levels. *Nature* 466, 835–840 (2010).

Guo, R. *et al.* HnRNP A1/A2 and SF2/ASF Regulate Alternative Splicing of Interferon Regulatory Factor-3 and Affect Immunomodulatory Functions in Human Non-Small Cell Lung Cancer Cells. *Plos One* 8, e62729 (2013).

Han, S. P. *et al.* Functional implications of the emergence of alternative splicing in hnRNP A/B transcripts. *Rna* 16, 1760–1768 (2010).

Han, S. P., Tang, Y. H., & Smith, R. Functional diversity of the hnRNPs: past, present and perspectives. *Biochemical Journal* 430, 379-392 (2010).

Harrison, A. F. & Shorter, J. RNA-binding proteins with prion-like domains in health and disease. *Biochem J* 474, 1417–1438 (2017).

Hasuwa, H., Ueda, J., Ikawa, M., & Okabe, M. miR-200b and miR-429 function in mouse ovulation and are essential for female fertility. *Science*, 341, 71-73(2013).

Heintz, C. *et al.* Splicing Factor 1 Modulates Dietary Restriction and TORC1 Pathway Longevity in *C. elegans*. *Nature* 541, 102–106 (2017).

Hogg, D. R., & Harries, L. W. Human genetic variation and its effect on miRNA biogenesis, activity and function. *Biochemical Society Transactions* 42, 1184-1189(2014).

Jafarnejad, S. M. *et al.* Translational control of ERK signaling through miRNA/4EHP-directed silencing. *Elife* 7, e35034 (2018).

Jagannathan, R. *et al.* Translational Regulation of the Mitochondrial Genome Following Redistribution of Mitochondrial MicroRNA in the Diabetic Heart. *Circulation Cardiovasc Genetics* 8, 785–802 (2018).

Jean-Philippe, J., Paz, S. & Caputi, M. hnRNP A1: The Swiss Army Knife of Gene Expression. *Int J Mol Sci* 14, 18999–19024 (2013).

Jin, H. Y. & Xiao, C. MicroRNA Mechanisms of Action: What have We Learned from Mice? *Frontiers Genetics* 6, 328 (2015).

Johnston, R. J. & Hobert, O. A microRNA controlling left/right neuronal asymmetry in Caenorhabditis elegans. *Nature* 426, 845–849 (2003).

Jovanovic, M., & Hengartner, M. O. miRNAs and apoptosis: RNAs to die for. *Oncogene* 25, 6176-6187(2006).

Kasper, D. M. *et al.* MicroRNAs Establish Uniform Traits during the Architecture of Vertebrate Embryos. *Dev Cell* 40, 552-565.e5 (2017).

Kim, H. J. *et al.* Prion-like domain mutations in hnRNPs cause multisystem proteinopathy and ALS. *Nature* 495, 467–473 (2013).

Kim, S. *et al.* The regulatory impact of RNA-binding proteins on microRNA targeting. *Nat Commun* 12, 5057 (2021).

Kim, Y. & Kim, V. N. Processing of intronic microRNAs. *Embo J* 26, 775–783 (2007).

Kobayashi, H. & Singer, R. H. Single-molecule imaging of microRNA-mediated gene silencing in cells. *Nat Commun* 13, 1435 (2022).

Koo, J. H., Lee, H. J., Kim, W., & Kim, S. G. Endoplasmic reticulum stress in hepatic stellate cells promotes liver fibrosis via PERK-mediated degradation of HNRNPA1 and up-regulation of SMAD2. *Gastroenterology* 150, 181-193 (2016).

Kooshapur, H. *et al.* Structural basis for terminal loop recognition and stimulation of pri-miRNA-18a processing by hnRNP A1. *Nat Commun* 9, 2479 (2018).

Larriba, E., Rial, E. & Mazo, J. del. The landscape of mitochondrial small non-coding RNAs in the PGCs of male mice, spermatogonia, gametes and in zygotes. *Bmc Genomics* 19, 634 (2018).

Larsson, O. & Nadon, R. Re-analysis of genome wide data on mammalian microRNA-mediated suppression of gene expression. *Transl* 1, e24557 (2013).

Lee, R. C., Feinbaum, R. L. & Ambros, V. The *C. elegans* heterochronic gene lin-4 encodes small RNAs with antisense complementarity to lin-14. *Cell* 75, 843–854 (1993).

Lee, Y. *et al.* MicroRNA genes are transcribed by RNA polymerase II. *Embo J* 23, 4051–4060 (2004).

Leucci, E. *et al.* microRNA-9 targets the long non-coding RNA MALAT1 for degradation in the nucleus. *Sci Rep-uk* 3, 2535 (2013).

Li, S., Nguyen, T. D., Nguyen, T. L. & Nguyen, T. A. Mismatched and wobble base pairs govern primary microRNA processing by human Microprocessor. *Nat Commun* 11, 1926 (2020).

Lim, L. P. *et al.* The microRNAs of Caenorhabditis elegans. *Gene Dev* 17, 991–1008 (2003).

Lima, S. A. *et al.* Short Poly(A) Tails are a Conserved Feature of Highly Expressed Genes. *Nat Struct Mol Biol* 24, 1057–1063 (2017).

Lund, E., Liu, M., Hartley, R. S., Sheets, M. D. & Dahlberg, J. E. Deadenylation of maternal mRNAs mediated by miR-427 in Xenopus laevis embryos. *Rna* 15, 2351–2363 (2009).

MacRae, I. J., Ma, E., Zhou, M., Robinson, C. V. & Doudna, J. A. In vitro reconstitution of the human RISC-loading complex. *Proc National Acad Sci* 105, 512–517 (2008).

Mallo, M. & Alonso, C. R. The regulation of Hox gene expression during animal development. *Development* 140, 3951–3963 (2013).

Mathonnet, G., Fabian, M. R., Svitkin, Y. V., Parsyan, A., Huck, L., Murata, T., ... & Sonenberg, N. MicroRNA inhibition of translation initiation in vitro by targeting the cap-binding complex eIF4F. *Science* 317, 1764-1767 (2007).

Mears, W. E. & Rice, S. A. The RGG box motif of the herpes simplex virus ICP27 protein mediates an RNA-binding activity and determines in vivo methylation. *J Virol* 70, 7445–7453 (1996).

Michlewski, G. & Cáceres, J. F. Antagonistic role of hnRNP A1 and KSRP in the regulation of let-7a biogenesis. *Nat Struct Mol Biol* 17, 1011–1018 (2010).

Michlewski, G. & Cáceres, J. F. Post-transcriptional control of miRNA biogenesis. *Rna* 25, 1–16 (2019).

Moretti, F., Kaiser, C., Zdanowicz-Specht, A. & Hentze, M. W. PABP and the poly(A) tail augment microRNA repression by facilitated miRISC binding. *Nat Struct Mol Biol* 19, 603–608 (2012).

Naeli, P., Winter, T., Hackett, A. P., Alboushi, L. & Jafarnejad, S. M. The intricate balance between microRNA-induced mRNA decay and translational repression. *Febs J* (2022) doi:10.1111/febs.16422.

Nguyen, T. A. *et al.* Functional Anatomy of the Human Microprocessor. *Cell* 161, 1374–1387 (2015).

Nishi, K., Nishi, A., Nagasawa, T. & Ui-Tei, K. Human TNRC6A is an Argonaute-navigator protein for microRNA-mediated gene silencing in the nucleus. *Rna* 19, 17–35 (2013).

Pajares, M. J., Palanca-Ballester, C., Urtasun, R., Alemany-Cosme, E., Lahoz, A., & Sandoval, J. (2021). Methods for analysis of specific DNA methylation status. *Methods*, *187*, 3-12.

Piñol-Roma, S., Choi, Y. D., Matunis, M. J. & Dreyfuss, G. Immunopurification of heterogeneous nuclear ribonucleoprotein particles reveals an assortment of RNA-binding proteins. *Gene Dev* 2, 215–227 (1988).

Radhakrishnan, A. *et al.* The DEAD-Box Protein Dhh1p Couples mRNA Decay and Translation by Monitoring Codon Optimality. *Cell* 167, 122-132.e9 (2016).

Reinhart, B. J. *et al.* The 21-nucleotide let-7 RNA regulates developmental timing in Caenorhabditis elegans. *Nature* 403, 901–906 (2000).

Rissland, O. S. *et al.* The influence of microRNAs and poly(A) tail length on endogenous mRNA–protein complexes. *Genome Biol* 18, 211 (2017).

Ritsch, I. *et al.* Phase separation of hnRNP A1 upon specific RNA-binding observed by magnetic resonance. *Biorxiv* 2022.03.21.485092 (2022) doi:10.1101/2022.03.21.485092.

Ritsch, I., Lehmann, E., Emmanouilidis, L., Yulikov, M., Allain, F., & Jeschke, G. (2022). Phase separation of hnRNP A1 upon specific RNA-binding observed by magnetic resonance. *bioRxiv*.

Rodriguez, A., Griffiths-Jones, S., Ashurst, J. L. & Bradley, A. Identification of Mammalian microRNA Host Genes and Transcription Units. *Genome Res* 14, 1902–1910 (2004).

Ryan, V. H. *et al.* Tyrosine phosphorylation regulates hnRNPA2 granule protein partitioning and reduces neurodegeneration. *Embo J* 40, e105001 (2021).

Shao, W., Bi, X., Pan, Y., Gao, B., Wu, J., Yin, Y., ... & Shen, X. Phase separation of RNA-binding protein promotes polymerase binding and transcription. *Nature Chemical Biology* 18, 70-80 (2022).

Smith, R. W. P., Blee, T. K. P. & Gray, N. K. Poly(A)-binding proteins are required for diverse biological processes in metazoans. *Biochem Soc T* 42, 1229–1237 (2014).

Subtelny, A. O., Eichhorn, S. W., Chen, G. R., Sive, H. & Bartel, D. P. Poly(A)-tail profiling reveals an embryonic switch in translational control. *Nature* 508, 66–71 (2014).

Sun, G. *et al.* HnRNP A1 - mediated alternative splicing of CCDC50 contributes to cancer progression of clear cell renal cell carcinoma via ZNF395. *J Exp Clin Canc Res* 39, 116 (2020).

Tan, C. L. *et al.* MicroRNA-128 Governs Neuronal Excitability and Motor Behavior in Mice. *Science* 342, 1254–1258 (2013).

Tange, T. Ø., Damgaard, C. K., Guth, S., Valcárcel, J., & Kjems, J. The hnRNP A1 protein regulates HIV-1 tat splicing via a novel intron silencer element. *The EMBO journal* 20, 5748-5758 (2001).

Treiber, T., Treiber, N. & Meister, G. Regulation of microRNA biogenesis and its crosstalk with other cellular pathways. *Nat Rev Mol Cell Bio* 20, 5–20 (2019).

Hao, J., Duan, F.-F. & Wang, Y. MicroRNAs and RNA binding protein regulators of microRNAs in the control of pluripotency and reprogramming. *Curr Opin Genet Dev* 46, 95–103 (2017).

Venables, J. P., Tazi, J. & Juge, F. Regulated functional alternative splicing in Drosophila. *Nucleic Acids Res* 40, 1–10 (2012).

Wahlquist, C. *et al.* Inhibition of miR-25 Improves Cardiac Contractility in the Failing Heart. *Nature* 508, 531–535 (2014).

Wightman, B., Ha, I. & Ruvkun, G. Posttranscriptional regulation of the heterochronic gene lin-14 by lin-4 mediates temporal pattern formation in C. elegans. *Cell* 75, 855–862 (1993).

Wu, Y. *et al.* Function of HNRNPC in breast cancer cells by controlling the dsRNA-induced interferon response. *Embo J* 37, e99017 (2018).

Xiang, K. & Bartel, D. P. The molecular basis of coupling between poly(A)-tail length and translational efficiency. Elife 10, e66493 (2021).

Yartseva, V. & Giraldez, A. J. Chapter Six The Maternal-to-Zygotic Transition During Vertebrate Development A Model for Reprogramming. *Curr Top Dev Biol* 113, 191–232 (2015).

Yekta, S., Shih, I. H., & Bartel, D. P. MicroRNA-directed cleavage of HOXB8 mRNA. *Science* 304, 594-596 (2004).

Yi, R., Qin, Y., Macara, I. G. & Cullen, B. R. Exportin-5 mediates the nuclear export of pre-microRNAs and short hairpin RNAs. *Gene Dev* 17, 3011–3016 (2003).

Yin, M. *et al.* HNRNPA2B1 as a trigger of RNA switch modulates the miRNA-mediated regulation of CDK6. *Iscience* 24, 103345 (2021).

Zekri, L., Kuzuoğlu-Öztürk, D. & Izaurralde, E. GW182 proteins cause PABP dissociation from silenced miRNA targets in the absence of deadenylation. *Embo J* 32, 1052–1065 (2013).

Zhang, X. *et al.* MicroRNA Directly Enhances Mitochondrial Translation during Muscle Differentiation. *Cell* 158, 607–619 (2014).

Zhu, J., Mayeda, A. & Krainer, A. R. Exon Identity Established through Differential Antagonism between Exonic Splicing Silencer-Bound hnRNP A1 and Enhancer-Bound SR Proteins. *Mol Cell* 8, 1351–1361 (2001).

Chapter 2 - Functional identification of microRNA-centered complexes in *C. elegans*.

This chapter is published as-

Hebbar, S. *et al.* Functional identification of microRNA-centered complexes in *C. elegans*. *Sci Rep-uk* 12, 7133 (2022).

2.1 Abstract

microRNAs (miRNAs) are crucial for normal development and physiology. To identify factors that might coordinate with miRNAs to regulate gene expression, we used 2′O-methylated oligonucleotides to precipitate *Caenorhabditis elegans* let-7, miR-58, and miR-2 miRNAs and the associated proteins. A total of 211 proteins were identified through mass-spectrometry analysis of miRNA co-precipitates, which included previously identified interactors of key miRNA pathway components. Gene ontology analysis of the identified interactors revealed an enrichment for RNA binding proteins, suggesting that we captured proteins that may be involved in mRNA lifecycle. To determine which miRNA interactors are important for miRNA activity, we used RNAi to deplete putative miRNA co-factors in animals with compromised miRNA activity and looked for alterations of the miRNA mutant phenotypes. Depletion of 25 of 39 tested genes modified the miRNA mutant phenotypes in three sensitized backgrounds. Modulators of miRNA phenotypes ranged from RNA binding proteins RBD-1 and CEY-1 to metabolic factors such as DLST-1 and ECH-5, among others. The observed functional interactions suggest widespread coordination of these proteins with miRNAs to ultimately regulate gene expression. This study provides a foundation for future investigations aimed at deciphering the molecular mechanisms of miRNA-mediated gene regulation.

2.2 Introduction

Developmental and physiological processes require precise spatio-temporal regulation of gene expression. One post-transcriptional gene regulatory mechanism is directed by a class of small non-coding RNAs called microRNAs (miRNAs). miRNAs regulate a wide range of developmental and cellular processes, with dysregulated miRNA activity prevalent in diseases (as

reviewed by Ma *et al*. 2019; Ebrahimi *et al*. 2020). To exert their regulatory roles, miRNAs are loaded into Argonaute (AGO) proteins to form a miRNA Induced Silencing Complex (miRISC), which ultimately associates with an effector protein GW182. miRISC binding to the target mRNA via partial sequence complementarity between a miRNA and 3′ UTR of mRNA triggers a series of gene silencing mechanisms including translation inhibition, decapping, and mRNA decay (Bagga *et al.* 2005; Mayya *et al.* 2021).

miRNAs are produced by a complex biogenesis process which involves enzymatic processing of miRNA intermediates in the nucleus and cytoplasm. Primary miRNAs are first cleaved by the Microprocessor complex (Drosha and DGCR8) to form pre-miRNAs (Lee *et al*. 2003; Han *et al*. 2006). After export from nucleus into cytoplasm, pre-miRNAs are further processed by Dicer to generate a miRNA duplex (Hutvágner *et al*. 2001; MacRae *et al*. 2007). The miRNA duplex bound by Argonaute is then unwound, with the guide miRNA strand retained to form the mature miRISC, and the passenger strand released and degraded (Kwak *et al*. 2012; Meijer *et al*. 2014). Each of the steps in miRNA biogenesis process can be regulated by RNA binding and other auxiliary factors thereby modulating the final gene-regulatory impact of miRNAs. These factors could bind miRNA intermediates or miRISC protein components to affect miRNA activity. For example, several RNA binding proteins including RBFOX3 and HnRNP A1 have been identified to bind to the hairpin structures of primary miRNAs and modulate their processing (Kim *et al*. 2014; Guil & Cáceres, 2007). Other proteins, such as NHL-2 and CGH-1, associate with ALG-1 and AIN-1 to promote mRNA targeting (Hammell *et al.* 2009). RNA binding proteins Staufen (Ren *et al*. 2016) and HuR (Srikantan *et al*. 2012; Kundu *et al.* 2012) indirectly affect miRNA-mediated gene silencing by competing for binding of the 3′UTRs of target mRNAs. Characterizing miRISC-associated protein complexes followed by functional analyses

and mechanistic studies has high potential to identify additional mechanisms by which miRNA activity may be regulated.

Identifying proteins that associate with Argonaute proteins or miRNAs has been a productive approach to begin to unravel the mechanisms by which aspects of miRNA biogenesis and activity are regulated (Landthaler *et al*. 2008; Frohn *et al.* 2012; Zinovyeva *et al*. 2015; Wu *et al*. 2017). In human cells, investigation of proteomic profiles of AGO complexes led to identification of common protein interactors of all four AGO proteins, which included heat shock proteins, helicases, and components of translational machinery (Landthaler *et al*. 2008). Some proteins identified in this study, including Hsc70/Hsp90 chaperone machinery, were later characterized for their roles in RISC loading of small RNA duplexes (Iwasaki *et al*. 2010). In mice, exploration of Dicer dependent and independent interactions of Ago2 (Frohn *et al*. 2012) identified proteins that participate in miRISC-mediated decapping (Nishihara *et al*. 2013), among other mechanisms. However, while proteomic approaches have characterized miRNA-associated complexes, it has been challenging to identify which of these co-factors are functionally important for miRNA activity, especially in tissue culture. In contrast, functional assays that quantitatively assess miRNA activity are available in model organisms such as *C. elegans.*

To identify miRNA/miRISC auxiliary cofactors important for miRNA gene regulatory activity, we took a functional proteomics approach. Specifically, we used 2′O-methylated biotinylated oligonucleotides to pull down three miRNAs of interest (let-7, miR-58, and miR-2) and subjected the associated protein complexes to proteomic analysis. Comparative analysis of miRNA pulldown and ALG-1 immunoprecipitation precipitates (Zinovyeva *et al.* 2015) identified high confidence interactors common to all four datasets. In addition, we identified a unique set of interactors in each miRNA pulldown dataset. To assess whether the co-precipitated proteins are

functionally important for miRNA activity, we performed RNAi knockdown of genes encoding for the putative physical interactors in multiple miRNA sensitized genetic backgrounds. Of the 39 interactors tested, depletion of 25 factors modified miRNA reduction of function phenotypes in one or more assays. Overall, we demonstrate that capturing physical interactors of miRNA machinery followed by *in vivo* functional assays is an efficient approach to identify novel players in miRNA-mediated gene regulation. While further mechanistic characterizations are necessary to determine the extent of the physical and functional interactions, this study identifies a functional requirement for a subset of potential ALG-1 and miRNA co-factors.

2.3 Materials and Methods

C. elegans maintenance, strains, and RNAi

All *C. elegans* strains were maintained on NGM and fed with *E. coli* OP50. Strains were maintained at 20°C unless otherwise noted. RNAi knockdown was performed by feeding as previously described (Kamath *et al*. 2003).

The following strains were used in this study: N2 (wild type), MT7626 *(let-7(n2853)),* HW1113 *[Pdpy-30::GFP(PEST)-H2B::lin-41 3' UTR (xeSi78); Pdpy-30::mCherry::H2B::artificial 3' UTR (xeSi36)]*, HW1114 *[Pdpy-30::GFP (PEST)-H2B::lin-41 3' UTR (xeSi78); Pdpy-30::mCherry::H2B::artificial 3' UTR (xeSi36), let-7(n2853)]*, VT1367 *(col-19::gfp (maIs105)),* VT1296 (*mir-48 mir-241(nDf51) col-19::gfp (maIs105)),* BW1932 *[hbl-1p::gfp::NLS::hbl-1 3' UTR (ctIS39)]* and UY458 (*mir-48 mir-241(nDf51); hbl-1p::gfp::NLS::hbl-1 3' UTR (ctIS39)]),* OH812 (*otIs114 [Plim-6-gfp + rol-6(su1006)]),* OH3646 (*lsy-6(ot150); otIs114 [Plim-6-gfp + rol-6(su1006)])*, PS3662 *(syIs63[cog-1*::*gfp + unc-119(+)])*, OH7310 *(otIs193 [cog-1p*::*lsy-6 + rol-6(su1006)] syIS63[cog-1*::*gfp + unc-119(+)]).*

2′O-Methyl oligo pulldowns and mass spec analysis

All experiments were performed on mixed-stage animals. Whole worm extracts and 2′O-methyl oligo pulldowns were performed as previously described (Li and Zinovyeva, 2020; Jannot *et al*. 2011). For mass spectrometry, each sample contained 20 mg of total protein. miRNA pulldowns were performed in two biological replicates using 2′O-methylated oligos with perfect complementation to miR-58, let-7, and miR-2, and scrambled oligo control (IDT). Sequences of the 2′O-methylated, biotinylated oligonucleotides are as follows: miR-58 oligo (5′-CAUCAUUGCCGUACUGAACGAUCUCAAGUC-3′), miR-2 oligo (5′-AUUCAGCACAUCAAAGCUGGCUGUGAUAUUCCA-3′), let-7 oligo (5′-UCUUCACUAUACAACCUACUACCUCAACCUU-3′), and scrambled oligo (5′-CAUCACGUACGCGGAAUACUUCGAAAUGUC-3′).

Mass spectrometric analysis of pulldown factors was performed as previously described (Zinovyeva *et al*. 2015). Briefly, DTASelect was used to filter the proteins identified by applying a criterion that required proteins to have at least two unique peptides with total spectral intensities greater or equal to four in both replicates (Tabb *et al.* 2002). To determine enrichment of protein association in a miRNA pulldown, the Normalized Spectral Abundance Factor (NSAF) values in miRNA pulldown were divided by that in control pulldown. NSAF value of zero in control was replaced by 1. Proteins with the pulldown/control ratio of ≥ 4 in all replicates were considered putative physical interactors.

GO term and network analysis

Gene ontology analysis was performed using Database for Annotation, Visualization, and Integrated Discovery (DAVID) (Huang *et al.* 2009). Factors that had a fold change ≥ 4 in both

replicates of the miRNA pulldowns were used for this analysis. For comparison, we included factors identified in at least two replicates of ALG-1 IP for GO term analysis (Zinovyeva *et al*. 2015). Protein domain information, domain enrichment analysis, and the associated statistics were retrieved using STRING (Snel *et al*. 2000). Enrichment for proteins harboring an RNA binding domain (RBD) among the proteins that passed our criteria was determined against a background set of *C. elegans* proteins that harbor the same RNA binding domain. Statistically significant enrichment was determined by applying Benjamini–Hochberg procedure on p-values to correct for multiple-testing. Network analysis was performed on the top 40 most enriched factors using STRING after excluding ribosomal proteins (Snel *et al*. 2000).

Functional assays

let-7(n2853) vulval bursting assay

Vulval bursting assay was performed as previously described (Parry *et al.* 2007). Briefly, *let-7(n2853)* and N2 worms were grown and maintained at 15°C. Embryos obtained through bleaching (Porta-de-la-Riva *et al*. 2012) were plated on RNAi plates and grown until L4 larval stage. L4 animals were shifted to new RNAi plates and scored as day 1 adults for vulval bursting using a Leica dissecting microscope. Total number of worms (n) scored for this assay across two to four independent RNAi experiments ranged from 45 to 330.

col-19::gfp expression and seam cell number assay

mir-48 mir-241(nDf51) col-19::gfp (maIs105) animals were transferred to RNAi plates as L3 stage larvae and their progeny were scored for heterochronic phenotypes for hypodermal *col-19::gfp* expression. Worms with seam-only reporter expression were classified as having “delayed

hypodermal *col-19::gfp* expression". Seam cell numbers were scored by counting the number of seam cells expressing *col-19::gfp* between pharynx and anus. For most candidates, the total number of worms scored (n) across two to four replicates ranged from 22 to 80. For genes whose knockdowns resulted in severe developmental defects such as *snr-4, snr-6, let-363,* and *rnp-7,* the (n) was either 18 or 19.

lsy-6(ot150) ASEL cell fate assay

lsy-6(ot150); plim-6::gfp and *plim-6::gfp* worms were transferred onto RNAi plates as embryos. Their progeny were scored as L4s for specification of ASEL cell fate based on *plim-6::gfp* reporter expression. Worms lacking the reporter expression in ASEL neurons were scored as cell fate defective. Across two to four replicates, a total of 90 to 286 worms were scored.

pdpy-30::gfp::lin-41 reporter assay

pdpy-30::GFP(PEST)-H2B::lin-41 3′ UTR (xeSi78); pdpy-30::m Cherry::H2B::artificial 3′ UTR (xeSi36) and *pdpy-30::GFP (PEST)-H2B::lin-41 3′ UTR (xeSi78); pdpy-30::mCherry::H2B::artificial 3′ UTR (xeSi36), let-7(n2853)* embryos obtained by bleaching were plated on RNAi plates and grown at 15°C. Reporter expression was measured in L4 stage animals by imaging the vulva at 63× magnification. To quantify expression levels in six vulval cells, ROIs were manually drawn and signal intensities within the ROI were measured using the Leica image analysis software. For each vulval cell, GFP signal intensity was divided by mCherry signal intensity and relative signal intensities were averaged across the six cells imaged in an individual animal. Representative images were equally adjusted after quantification to make the fluorescence more observable.

hbl-1p::gfp reporter assay

hbl-1p::gfp::NLS::hbl-1 3′ UTR (ctIS39) and *mir-48 mir-241(nDf51); hbl-1p::gfp::NLS::hbl-1 3′ UTR (ctIS39)* embryos were obtained by bleaching. Embryos were transferred to RNAi plates and animals were scored for *hbl-1p::gfp* expression in hypodermal cells at early to mid L3 stage. Animals were staged by time of development, and gonad size and shape.

Uterine *cog-1* reporter expression

cog-1::gfp and *pcog-1::lsy-6; cog-1::gfp* animals were transferred onto RNAi plates as embryos and their F1 progeny were scored at L4 stage for *cog-1::gfp* expression in the uterine cells. Worms expressing *cog-1::gfp* in both uterine cells and vulval cells were scored as wild type. Worms that lacked *cog-1::gfp* reporter expression in either of the two uterine cells were scored as abnormal.

Fluorescence microscopy, image capture and illustrations

Fluorescence equipped Zeiss Axioplan 2 or Leica DM6 upright microscopes were used for scoring phenotypes. Images were captured using the Leica DM6B camera and processed using the Leica Application Suite X (3.4.1.17822) software (https://www.leica-microsystems.com/products/microscope-software/p/leica-las-x-ls/). Illustrations in Figs. 1a and 6e–g were drawn using BioRender (biorender.com).

Statistical analysis

All statistics were done using GraphPad Prism (9.2.0 (332)) software. Statistical significance was determined using a one-way ANOVA test with predetermined comparisons.

Bonferroni correction was applied as a post hoc analysis. T-test was used to determine statistical significance of *pdpy-30::gfp::lin-41*, *hbl-1p::gfp,* and *cog-1::gfp* reporter assays.

2.4 Results

miRNA pulldowns (PDs) identify overlapping sets of putative physical interactors of miRNA-centered complexes

To identify factors that may regulate miRNA activity, we sought to determine the molecular composition of protein complexes associated with let-7*,* miR-58, and miR-2 miRNAs. *let-7* is highly conserved across all bilateral animals and is required for the larval to adult transition in *C. elegans* (Pasquinelli *et al*. 2000; Reinhart *et al*. 2000). miR-58 is a highly abundant miRNA that regulates lifespan and dauer formation (Jan *et al*. 2011), primarily by coordinating with the TGF-β pathway (de Lucas *et al*. 2015; Subasic *et al*. 2015). miR-2, a neuronal miRNA conserved among invertebrates (Marco *et al*. 2012), is necessary for proper neuromuscular junction function in *C. elegans* (O'Hern *et al*. 2017). We used biotinylated, 2′O-methylated oligonucleotides with perfect sequence complementarity to mature miRNA sequences to pulldown miRNAs of interest and characterized the precipitates using a shotgun proteomics approach (Fig. 2.1a) to identify proteins associated with miRNAs of interest compared to scrambled control (Fig. 2.1b–d, Table A.1). To identify high confidence interactors, we retained only the proteins that were ≥ fourfold enriched in miRNA pulldowns over the scrambled control, had a minimum NSAF value of 4, and were identified in all replicates. Overall, a total of 211 proteins passed the criteria we set (Fig. 2.1e), with 136 factors co-precipitating with let-7, 54 factors co-precipitating with miR-58, and 25 factors co-precipitating with miR-2 (Fig. 2.1e, Table A.1). Among the proteins enriched in miRNA co-precipitates were known miRISC components ALG-1 and ALG-2, the two major miRNA-

associated Argonautes in *C. elegans* (Grishok *et al*. 2001) and AIN-1 and AIN-2, GW182 homologs and miRISC effectors (Ding *et al*. 2005; Zhang *et al*. 2007) (Fig. 2.1b–f). In addition, DCR-1 nuclease, responsible for pre-miRNA processing, was detected in all pulldown experiments performed, but did not meet our stringent interaction criteria in the let-7 pulldown (Fig. 2.1e,f, Table A.1).

To determine the overlap between complexes precipitated by miRNA pulldowns and those previously found to associate with ALG-1 (Zinovyeva *et al*. 2015), we compared miRNA and ALG-1 co-precipitated factors (Fig. 2.1e, f, Table A.1). Eleven (8%) let-7 interactors, ten (18.5%) miR-58 interactors, and five (24%) miR-2 interactors were found to overlap with the ALG-1 co-immunoprecipitated dataset (Fig. 2.1e, Table 2.1). Overall, 41 proteins were present in at least two interaction datasets (Fig. 2.1e,f, Table 2.1), potentially representing general miRNA-associated co-factors. In addition, four proteins, HRPK-1, SMG-2, IMPH-1, and SUP-26, were present in 2 out of 3 pulldowns and the ALG-1 IP (Fig. 2.1e,f, Table 2.1). Their homologs were also found to co-immunoprecipitate with human and/or mouse Argonautes suggesting that they may have a conserved function in miRNA-mediated gene regulation (Landthaler *et al*. 2008; Frohn *et al*. 2012; Zinovyeva *et al*. 2015). In fact, we previously confirmed a physical HRPK-1 interaction with ALG-1 and reported *hrpk-1* to genetically interact with multiple miRNAs (Li *et al.* 2019). Five proteins were commonly captured in all the miRNA pulldowns (Fig. 2.1e,f, Table 2.1). Interestingly, one such protein was LET-363, an mTOR homolog (Long *et al*. 2002) (Fig. 2.1e,f, Table 2.1). Similarly, we observed overlaps between our miRNA co-precipitates and previously reported miRNA physical interactors (Wu *et al*. 2010; Dallarie *et al*. 2018) (Table A.2).

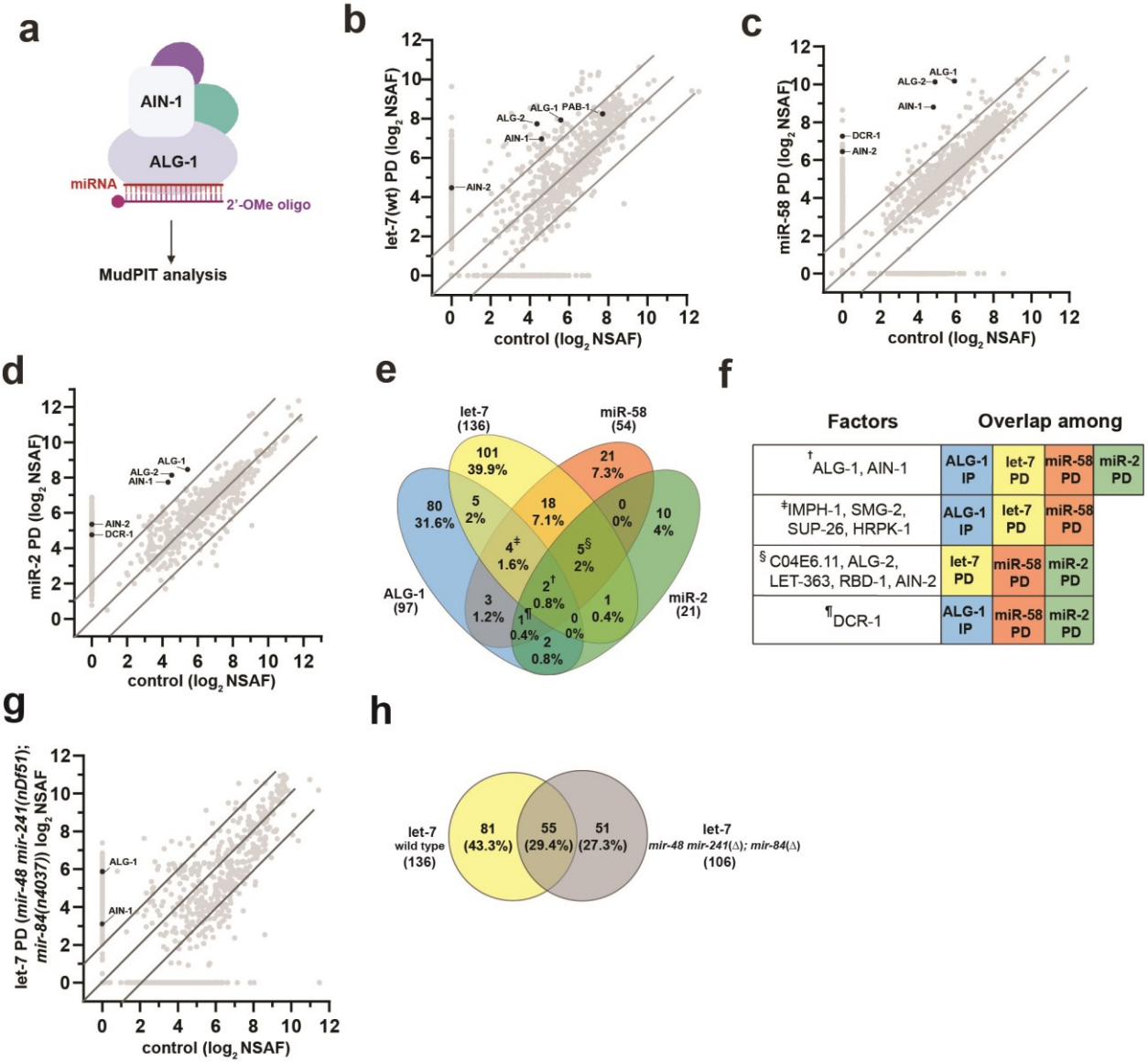

Figure 2.1 miRNA pulldowns (PDs) identify putative physical interactors of miRNA complexes.

(a) Protein complexes associated with miRNAs were isolated using 2′-OMe modified oligonucleotides complementary to the miRNA of interest and subjected to MudPIT mass spectrometry analysis (drawn using BioRender (biorender.com)). (b–d) Average Normalized Spectral Abundance Factor (NSAF) values of factors identified in pulldown experiments (Y-axis) are plotted against that of corresponding scrambled oligo controls (X-axis) for (b) let-7 PD, (c)

miR-58 PD and (d) miR-2 PDs. Highlighted in black are key miRISC components and components of miRNA biogenesis machinery. (e) Venn diagram showing the number of factors that passed a set of criteria to qualify as a putative interactor (for description of criteria, see "Methods"). Percentages shown here are percentage of total number of proteins (308) that passed the criteria in interaction datasets including ALG-1 (Zinovyeva et al. 2015). Proteins commonly co-precipitated with †ALG-1, let-7, miR-58, and miR-2, ǂALG-1 IP, let-7 PD, and miR-58 PD, §let-7 PD, miR-58 PD, miR-2 PD, and ¶ALG-1 IP, miR-58 PD, and miR-2 PD. (f) Factors commonly identified in two or more interaction datasets include core miRNA machinery components. Symbols in the left column correspond to overlapping protein populations in (e). Colored boxes show which IP or PD precipitated the proteins listed in the left column. (g) NSAF values of proteins identified in pulldowns with let-7 complementary oligonucleotide from *mir-48 mir-241(nDf51); mir-84(n4037)* mutant animals, plotted against NSAF of proteins identified in scrambled oligo control. (h) let-7 complementary oligonucleotide precipitates a partially overlapping set of factors from let-7-family miRNA deletion backgrounds.

		Average of NSAF ratios$_{pulldown/control}$ (spectral count)				
Sequence name	**Protein name**	**let-7**	**miR-58**	**miR-2**	**ALG-1**	**Description**
F48F7.1	ALG-1	6 (88)	19 (328)	8 (73)	573 (229)	Argonaute, miRISC component
C06G1.4	AIN-1	5 (25)	16 (83)	11 (28)	125 (122)	miRISC component (GW182 homolog)
C04E6.11	C04E6.11	6 (86)	5 (35)	5 (7)	NA	Unknown
T07D3.7	ALG-2	115 (70)	293 (292)	105 (47)	NA	Argonaute
B0261.2	LET-363	5 (8)	9 (8)	47 (24)	NA	*C. elegans* Mtor
T23F6.4	RBD-1	20 (124)	5 (55)	27 (28)	NA	rRNA processing
M88.5	IMPH-1	9 (310)	10 (237)	NA	23 (39)	KH domain, RNA binding protein
F26B1.2	HRPK-1	146 (19)	44 (4)	NA	8 (14)	KH domain, RNA binding protein
R10E4.2	SUP-26	139 (20.5)	43 (5)	NA	113 (29)	Translational regulation
Y48G8AL.6	SMG-2	6 (43)	45 (17)	NA	9 (4)	NMD protein
B0041.2	AIN-2	22 (6)	87 (83)	NA	NA	miRISC component
Y49E10.15	SNR-6	7 (41)	5 (19)	NA	NA	Small nuclear ribonucleoprotein
Y71F9B.4	SNR-7	8 (42)	260 (14)	NA	NA	Small nuclear ribonucleoprotein
W08E3.1	SNR-2	9 (48)	5 (19)	NA	NA	Small nuclear ribonucleoprotein
Y116A8C.42	SNR-1	10 (55)	4 (10)	NA	NA	Small nuclear ribonucleoprotein
C52E4.3	SNR-4	381 (31)	4 (13)	NA	NA	Small nuclear ribonucleoprotein
F43H9.3	F43H9.3	4 (23)	52 (8)	NA	NA	Predicted to enable nucleotidyltransferase activity
ZC373.2	ZC373.2	56 (5)	43 (5)	NA	NA	Unknown
W07E6.1	NSUN-1	12 (5)	67 (12)	NA	NA	Nop2 (NOP2)/SUN domain family member
Y38C9A.2	CGP-1	61 (22)	52 (8)	NA	NA	Predicted to enable GTPase activity
K10D2.3	CID-1	16 (53)	14 (6)	NA	NA	RNA 3' uridylation
W05F2.6	W05F2.6	139 (21)	114 (14)	NA	NA	Unknown
T01H10.8	LYST-1	41 (38)	15 (12)	NA	NA	Lysosomal trafficking regulator protein
K04G7.10	RNP-7	36 (14)	66 (5)	NA	NA	RNA binding protein
Y37H2A.1	Y37H2A.1	147 (25)	65 (8)	NA	NA	Predicted to enable hydrolase activity
F56B3.5	ECH-5	94 (20)	64 (12)	NA	NA	Enoyl-CoA Hydratase
F57H12.6	F57H12.6	166 (12)	4 (9)	NA	NA	Unknown
F42A6.7	HRPA-1	30 (5)	14 (4)	NA	NA	RNA binding protein
F25B5.7	NONO-1	84 (14)	100 (13)	NA	NA	Conserved nuclear protein
H20J04.8	MOG-2	161 (34)	NA	114 (6)	NA	Enables U2 snRNA binding activity
W02F12.5	DLST-1	88 (75)	NA	NA	18 (12)	DihydroLipoamide S-SuccinylTransferase
F33D11.10	F33D11.10	16 (7)	NA	NA	29 (4)	RNA helicase activity
ZC434.5	EARS-1	14 (9)	NA	NA	7 (4)	Glutamate-tRNA ligase activity
H05C05.1	H05C05.1	32 (9)	NA	NA	12 (4)	Predicted to enable RNA strand annealing activity
Y47D3B.10	DPY-18	NA	15 (9)	NA	23 (5)	Procollagen-proline 4-dioxygenase activity
K02F2.1	DPF-3	NA	58 (14)	NA	42 (15)	Serine-type peptidase
F52B5.3	F52B5.3	6 (40)	NA	NA	6 (4)	Predicted to enable ATP binding activity
F18H3.3	PAB-2	NA	20 (9)	NA	5 (69)	Poly-A-binding protein
K12H4.8	DCR-1	NA	153 (84)	27 (10)	6 (5)	Small RNA processor
F37C12.11	RPS-21	NA	NA	89 (4)	39 (33)	Ribosomal protein
Y71F9AL.9	Y71F9AL.9	NA	NA	45 (6)	37 (7)	Unknown

Table 2.1 Proteins that co-precipitated with two or more miRNAs or with ALG-1. The table shows the proteins that co-precipitated with either two or more miRNAs in our study and/or identified in previously reported ALG-1 IP (Zinovyeva *et al.* 2015).

Overlaps among our miRNA interaction datasets and AIN-1 and AIN-2 co-precipitates were also observed, further emphasizing that our approach captured potential miRISC interactors (Zhang *et al*. 2007; Dallarie *et al*. 2018) (Table A.2). Finally, candidates identified in genetic screens for miRNA and siRNA pathway genes also intersected with many of our miRNA co-precipitates (Parry *et al*. 2007; Kim *et al*. 2005; Zhou *et al*. 2008) (Table A.2). The observed overlaps among various groups of physical and genetic interactors support the idea that we are detecting real physical interactors of miRNA-centered complexes.

Due to a high level of sequence similarity amongst the *let-7* miRNA family members, the *let-7* complementary oligonucleotide precipitates other members of the miRNA family, albeit with reduced efficiency (Zinovyeva *et al*. 2014). To determine whether distinct populations of proteins might associate with *let-7* miRNA family members, we performed additional *let-7* pulldown experiments in *mir-48 mir-241(nDf51); mir-84(n4037)* mutant animals (Fig. 2.1g, Table A.1). 55 (29.4%) proteins were in common among both *let-7* pulldowns, suggesting that these factors may interact with let-7 itself (Fig. 2.1h). The 51 (27.3%) proteins that precipitated with the let-7-complementary oligonucleotide from the *mir-48 mir-241(nDf51); mir-84 (n4037)* animals may similarly represent let-7-interacting factors, having been enriched in the let-7 pulldown in the absence of miR-48, miR-241, and miR-84 (Fig. 2.1h). In contrast, 81 (43.3%) proteins were present only in wildtype background pulldowns (Fig. 2.1h), suggesting that these factors may normally associate with miR-48, miR-241 and miR-84 (Fig. 2.1h). While we cannot rule out an association with the remaining let-7 family miRNAs, miR-793–795, the low relative abundance of these miRNAs (Zinovyeva *et al*. 2015) suggests that miR-793–795 interactors are unlikely to represent significant fractions of the observed co-precipitates. Finally, some co-precipitates could represent non-specific interactions.

Ribonucleoprotein complex components are enriched among miRNA interactors

To understand what biological processes and functions are represented in the miRNA-precipitated complexes, we performed Gene Ontology (GO) analysis on putative miRNA interactors (Fig. 2.2a–d, Table A.3). Factors implicated in embryonic and larval developmental processes were commonly enriched in all interaction datasets (Fig. 2.2a–c; ALG-1 interactome analysis is shown in Fig. 2.2d for comparison (Zinovyeva *et al*. 2015), Table A.3). Selective enrichment for splicing associated factors was observed in let-7 and miR-58 PD datasets (Fig. 2.2a, c, Table A.3). Components of intracellular ribonucleoprotein complexes were consistently captured in all datasets (Fig. 2.2a–d and Zinovyeva *et al*. 2015). Enrichment for ribosomal components was observed only in let-7 and ALG-1 datasets (Fig. 2.2a,b,d and Zinovyeva *et al*. 2015). Unsurprisingly, the RNA/nucleic acid binding term was commonly overrepresented in all the datasets in the molecular function category (Fig. 2.2a–d and Zinovyeva *et al*. 2015). miR-2 interactors did not show an enrichment for any of the GO terms (Table A.3), potentially due to the low number of interactors captured in our pulldown and were therefore excluded from further analysis.

As RNA binding proteins (RBPs) were enriched in miRNA co-precipitates (Fig. 2.2a–d) and RBPs carry distinct domains critical for their RNA binding activity, we examined what RNA binding domains (RBDs) were present in proteins identified in our pulldowns and ALG-1 IP (Fig. 2.2e–h, Table A.3). At least 5 different RBDs were observed among RBPs in all the datasets. Notably, RBDs such as RNA Recognition Motif, KH, PAZ, and Nucleotide-binding alpha–beta plait domain superfamily were present in RBPs in one or more datasets (Fig. 2.2e–h, Table A.3). Overall, miRNA pulldowns captured factors that may play critical roles during the lifecycle of RNA.

To determine whether factors identified through our proteomics approach form a functional network, we performed network analysis using STRING (Snel *et al*. 2000) (Fig. 2.2i–l). STRING predicts candidate protein interactions by utilizing both known and predicted protein–protein interactions sourced from databases, text mining, experimental, and co-expression data (Snel *et al*. 2000). Top 40 enriched putative interactors in each dataset, minus the ribosomal proteins, were chosen for this analysis. Interestingly, we observed that in all the datasets proteins formed functional networks with a significant number of edges (p-value < 1.0e−16, as determined by STRING) (Fig. 2.2i–l), further supporting the idea that miRNA pulldown-captured proteins form functional complexes that may coordinate with miRNAs to regulate gene expression.

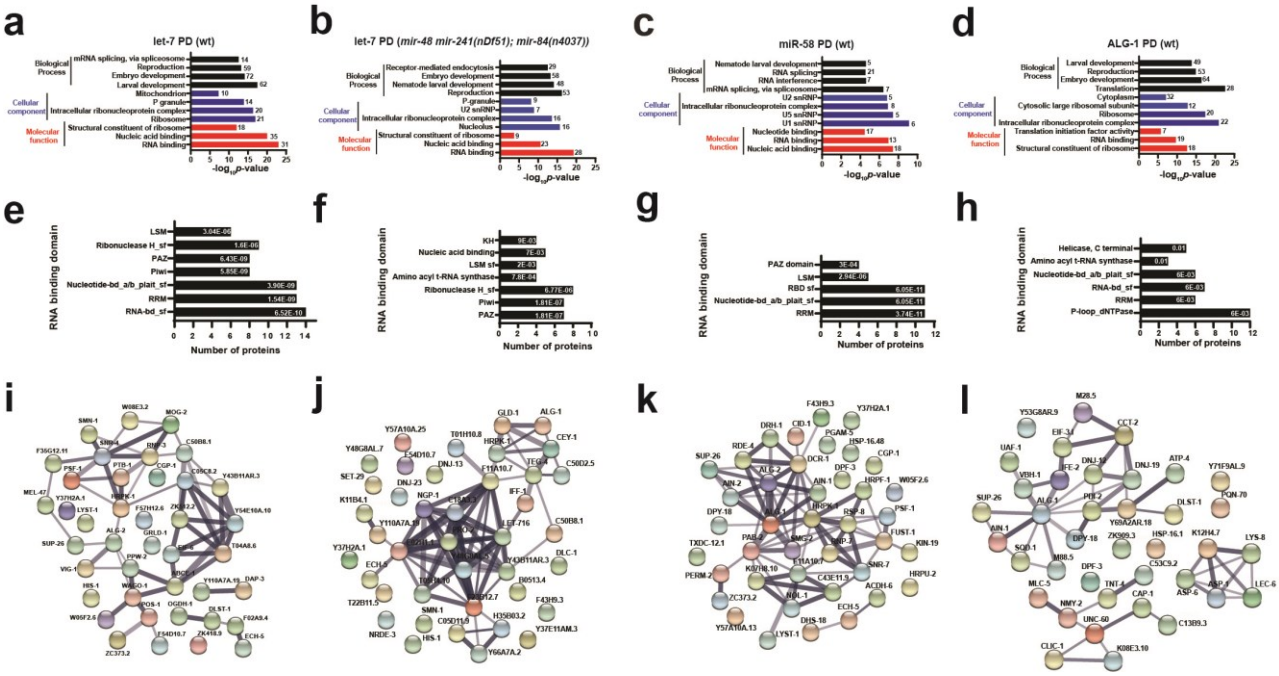

Figure 2.2 miRNA pulldowns identify components of translation machinery and mRNA processing factors, which may form a functional network.

(**a**–**d**) Terms identified through GO analysis for biological processes (top four), cellular components (top four) and molecular function categories (top three) among let-7 PDs in (**a**) wild type, (**b**) *mir-48 mir-241(nDf51); mir-84(n4037)* backgrounds, (**c**) miR-58 PD and (**d**) ALG-1 IP (Zinovyeva et al. 2015). Total number of proteins classified under each term shown adjacent to respective bars. (**e**–**h**) RNA binding domains identified in factors captured in let-7 PDs from (**e**) wild type, and (**f**) *mir-48 mir-241(nDf51); mir-84(n4037))* backgrounds, (**g**) miR-58 PD and (**h**) ALG-1 IP. The FDR adjusted p-values for enrichment of proteins harboring individual domains are shown within the respective bars. (**i**–**l**) The reproducibly enriched proteins form functional network. Network analysis was performed using STRING (Snel et al. 2000) on top 40 enriched interactors in (**i**) let-7 PD (wild type), (**j**) let-7 PD (*mir-48 mir-241(nDf51); mir-84(n4037*)) (**k**) miR-58 PD and (**l**) ALG-1 IP. Ribosomal proteins were excluded from this analysis. Thickness

of edges represents degree of confidence of functional linkages. The number of edges is significantly higher than expected, with a p-value < 1.0e−16.

Functional analysis of putative miRNA interactors

To identify which putative interactors might functionally coordinate with miRNAs to regulate gene expression, we took advantage of sensitized genetic backgrounds with reduced miRNA or miRNA family activity. These functional assays with quantifiable phenotypic outputs allow for assessment of a gene's role in miRNA-mediated gene repression. Our pulldown experiments targeted miRNAs with varied functions and spatio-temporal expression patterns. Some of the identified interactors of miRNA- or ALG-1-centered complexes could have broad functional requirements, while others could be specific to a particular tissue or a developmental time. We hypothesized that knockdown of generally-required factors in multiple sensitized miRNA backgrounds would modulate phenotypes in multiple functional assays. In contrast, spatio-temporal specificity of the putative interactors may limit their functional relevance to specific miRNAs and may not result in a phenotype in some, or all, of our assays. In addition, the miRNA-centered protein complex analyses potentially identified interactors that may positively or negatively modulate microRNA activity. Knockdown of these factors in sensitized genetic backgrounds may therefore result in an enhancement or a suppression of the phenotype associated with reduction of miRNA function.

For our functional assessment, we prioritized factors that were highly enriched in our pulldown and/or ALG-1 IP experiments and were captured in multiple datasets (Zinovyeva *et al*. 2015). We excluded ribosomal proteins and factors lacking RNAi clones. The 39 candidates assayed ranged from common interactors of miRNA(s) and ALG-1 (6), common miRNA interactors (6), ALG-1 interactors (16), and specific miRNA interactors [let-7 (10), and miR-58 (1)] (Table A.4). Among the ALG-1 interactors, we assayed genes encoding for six proteins

consistently identified in human and mouse AGO IP (referred to as conserved AGO interactors from hereon).

RNAi knockdown of genes of let-7 and ALG-1 interactors alters *let-7(n2853)* mutant phenotype

let-7 is essential for *C. elegans* development and promotes transition from the fourth larval stage (L4) to adulthood (Reinhart *et al*. 2000). Loss of *let-7* function results in vulval bursting and failure of seam cells to differentiate during the L4 to adult transition (Reinhart *et al*. 2000). *let-7(n2853)* is a temperature-sensitive reduction of function mutation that impairs regulation of let-7 targets, including *lin-41* (Vella *et al*. 2000). *let-7(n2853)* mutants have a partially penetrant vulval bursting phenotype at permissive temperature (15°C) (Reinhart *et al*. 2000) (Fig. 2.3a). To determine whether the identified let-7 and ALG-1 interactors are functionally important for let-7 miRNA activity, we used this well-established genetic background to assay the effects of gene knockdown on *let-7(n2853)* bursting phenotype. RNAi of six genes enhanced vulval bursting of *let-7(n2853)* mutant (Fig. 2.3b,c, Table A.4). One such gene (*pab-1)* enc0oded a conserved AGO interactor (Zinovyeva *et al*. 2015) (Fig. 2.3b, Table A.4) and five genes including *C04E6.11, ech-5*, and *rbd-1,* which code for let-7 interactors (Fig. 2.3c, Table A.4). RNAi of *cey-1* suppressed the bursting (Fig. 2.3c, Table A.4). Knockdown of *ifg-1* also mildly suppressed *let-7(n2853)* vulval bursting from 30 to 6% (Fig. 2.3b, Table A.4), although the suppression did not reach a statistically significant level (Anova p-value = 0.078). RNAi knockdown of these genes in the wild type background did not result in vulval bursting, suggesting that these genes do not play a central role in gene regulation, only revealing the function in the sensitized *let-7(n2853)* background (Fig. 2.3b,c). We cannot, however, rule out the possibility that RNAi knockdown in wild type background may have been ineffective. Overall, these findings support

our hypothesis that the identified let-7 physical interactors play a role in let-7-mediated gene repression.

Since dysregulation of *let-7* target gene *lin-41* in vulval-uterine system is sufficient to cause vulval rupturing (Ecsedi *et al*. 2015), we wanted to determine how depletion of putative physical and genetic *let-7* interactors affects *lin-41* expression in the relevant cells. To do this, we used an established *let-7-lin-41* reporter system (Ecsedi *et al*. 2015). We performed RNAi knockdown of genes that enhance (*ech-5*, *rbd-1*, *C04E6.11,* and *let-363*) and suppress (*cey-1*) *let-7(n2853)* vulval bursting in the background of two reporter strains: *pdpy-30::gfp::lin-41 3'UTR* and *pdpy-30::gfp::lin-41 3'UTR; let-7(n2853)* (Ecsedi *et al*. 2015). RNAi depletion of these genes did not alter *pdpy-30::gfp::lin-41 3'UTR* reporter levels in the wildtype background (Fig. 2.3d,e, Table A.5), suggesting that these genes do not have a major effect on *lin-41* levels on their own. However, in *let-7(n2853)* background at 15°C, knockdown of *ech-5* or *rbd-1* substantially increased *lin-41* levels, while *cey-1* depletion reduced *pdpy-30::gfp::lin-41 3'UTR* reporter levels in the vulval cells (Fig. 2.3d,e, Table A.5). RNAi of *let-363* led to a mild increase in the reporter levels in *let-7(n2853)* at 15°C, although the increase was not statistically significant (Fig. 2.3e, Table A.5). Interestingly, *let-363* depletion was previously reported to increase levels of let-7 target reporters *hbl-1p::gfp::hbl-1* in VNC and *col-10::gfp::lin-41 3'UTR* in hypodermal cells (Zhang & Zhang. 2013). These observations suggest that *ech-5, rbd-1, cey-1* and perhaps even *let-363* may be contributing to regulation of vulval bursting by modulating *let-7* miRNA activity.

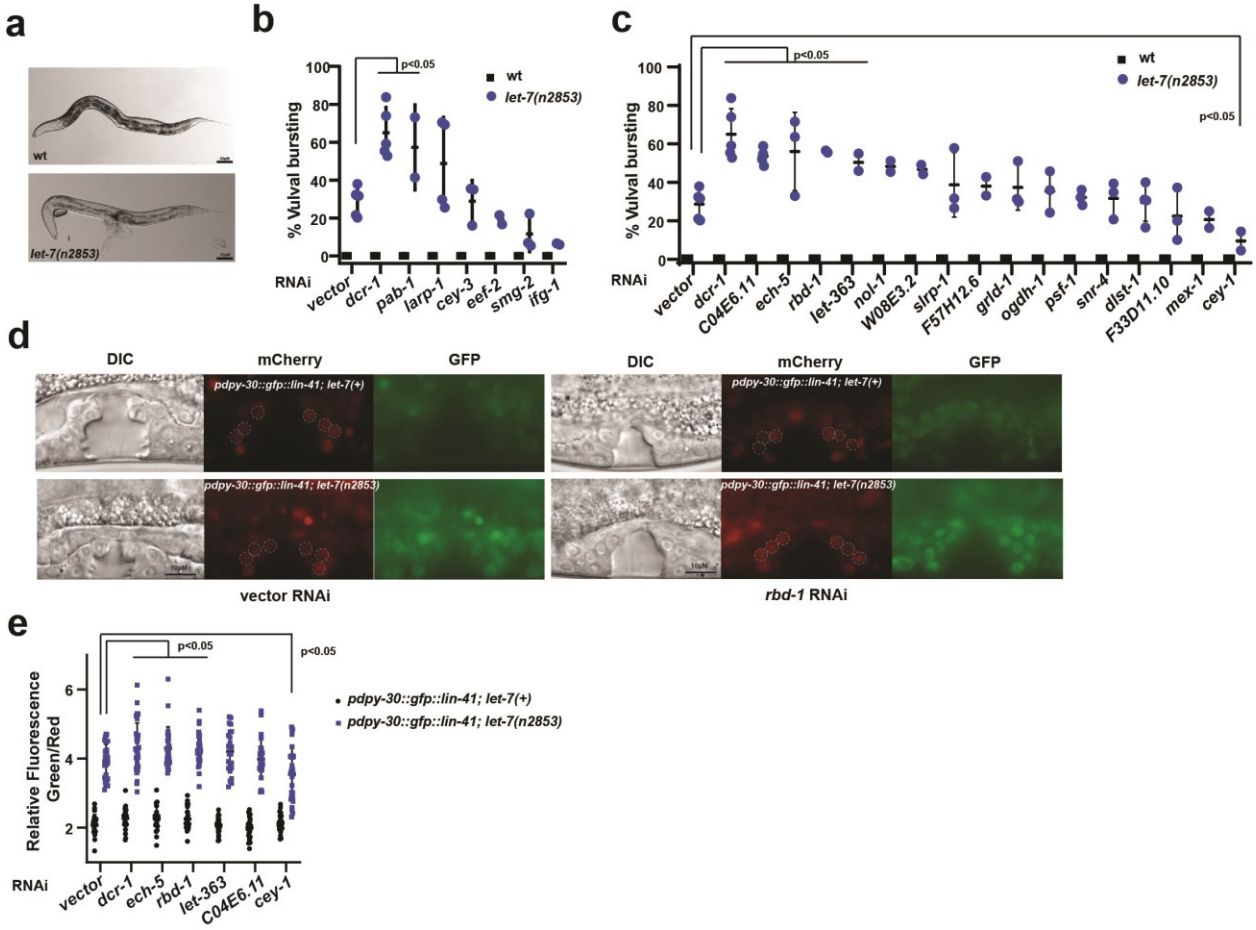

Figure 2.3 RNAi knockdown of genes encoding ALG-1 and let-7-associated factors genetically modifies *let-7(n2853)* vulval bursting phenotype.

(**a**) *let-7(n2853)* mutants show partially penetrant vulval bursting phenotype at 15 °C. RNAi of (**b**) genes of previously reported conserved interactors of AGO (Zinovyeva *et al.* 2015) and (**c**) let-7-precipitated factors in wild type and *let-7(n2853)* mutants. Each dot represents an independent RNAi experiment. Statistical significance was determined by one-way ANOVA with post hoc Bonferroni correction. (**d**) Effects of vector and *rbd-1* RNAi on *pdpy-30::gfp::lin-41* 3′UTR reporter expression in the vulval cells of wild type and *let-7(n2853)* L4 larvae. Compromised miRNA activity in *let-7(n2853)* background leads to de-repression of *pdpy-30::gfp::lin-41 3′ UTR* reporter expression levels (quantified in **e**). (**e**) RNAi of genes of modifiers of *let-*

7(n2853) vulval bursting phenotype affects *pdpy-30::gfp::lin-41 3'UTR* reporter expression levels in *let-7(n2853)* background. Each dot represents the relative intensity in an individual worm. Vulval precursor cells used for fluorescence quantification are highlighted with dashed circles. T-test was used to determine statistical significance. Vector = empty vector RNAi control.

RNAi knockdown of genes of let-7 and ALG-1 interactors alters *mir-48 mir-241(nDf51)* mutant phenotype

We next asked whether miRNA and ALG-1 interactors might functionally coordinate with other members of the *let-7* family of miRNAs. *let-7* family members *mir-48, mir-84* and *mir-241* specify developmental timing in *C. elegans*, regulating seam cell divisions and contributing to L2–L3 larval developmental transition (Abbott *et al*. 2005) (Fig. 2.4a). Deletion of all three miRNAs (*mir-48 mir-241(nDf51); mir-84(n4037)*) results in reiteration of L2 stage seam cell divisions, resulting in an increased number of seam cells and delayed terminal cell differentiation in young adults (Abbott *et al*. 2005) (Fig. 2.4a). Partial deletion (*mir-48 mir-241(nDf51)*) mutants display incompletely penetrant heterochronic phenotype which can be monitored using an adult stage marker, *col-19::gfp,* expressed in seam and hypodermal cells (Fig. 2.4b). RNAi of 11 genes enhanced the abnormal *col-19::gfp* expression in hypodermal cells (Fig. 2.4c,d, Table A.4), with five genes, *pab-1, dlst-1, C43E11.9, snr-4,* and *rbd-1*, enhancing the phenotype to > 50% (Fig. 2.4c,d Table A.4). This suggests that these potential miRNA interactors are required for regulation of developmental timing programs. We also examined the effects of gene knockdown on seam cell number. RNAi of three genes, *pqn-70, dlst-1*, and *cey-1*, increased the seam cell number of *mir-48 mir-241(nDf51)* mutants (Fig. 2.4f, Table A.4). RNAi of nine genes suppressed seam cell lineage defect, with knockdown of *let-363*, *rbd-1*, *snr-6,* and *snr-4,* restoring the seam cell number to an average of 13 or lower (Fig. 2.4e,f, Table A.4). We should note that while most genes were assayed across a minimum of two independent RNAi experiments, four genes (*snr-6*, *snr-4*, *let-363,* and *rnp-7)* were tested only once, as knockdown of these genes caused lethality, reduced brood size, and slowed growth. Depletion of some genes had varied effects on hypodermal *col-19::gfp* expression and seam cell lineage. Knockdown of *C43E11.9, pdi-*

2, and *Y71F9AL.9* modified *col-19::gfp* expression but not seam cell number, while knockdown of *pqn-70* and *C28H8.3* modified the seam cell number of *mir-48 mir-241(nDf51)* animals without affecting hypodermal *col-19::gfp* expression (Fig. 2.4d,f). This could perhaps be explained by distinct roles these genes may play during proliferative seam cell divisions and terminal hypodermal cell fate specification.

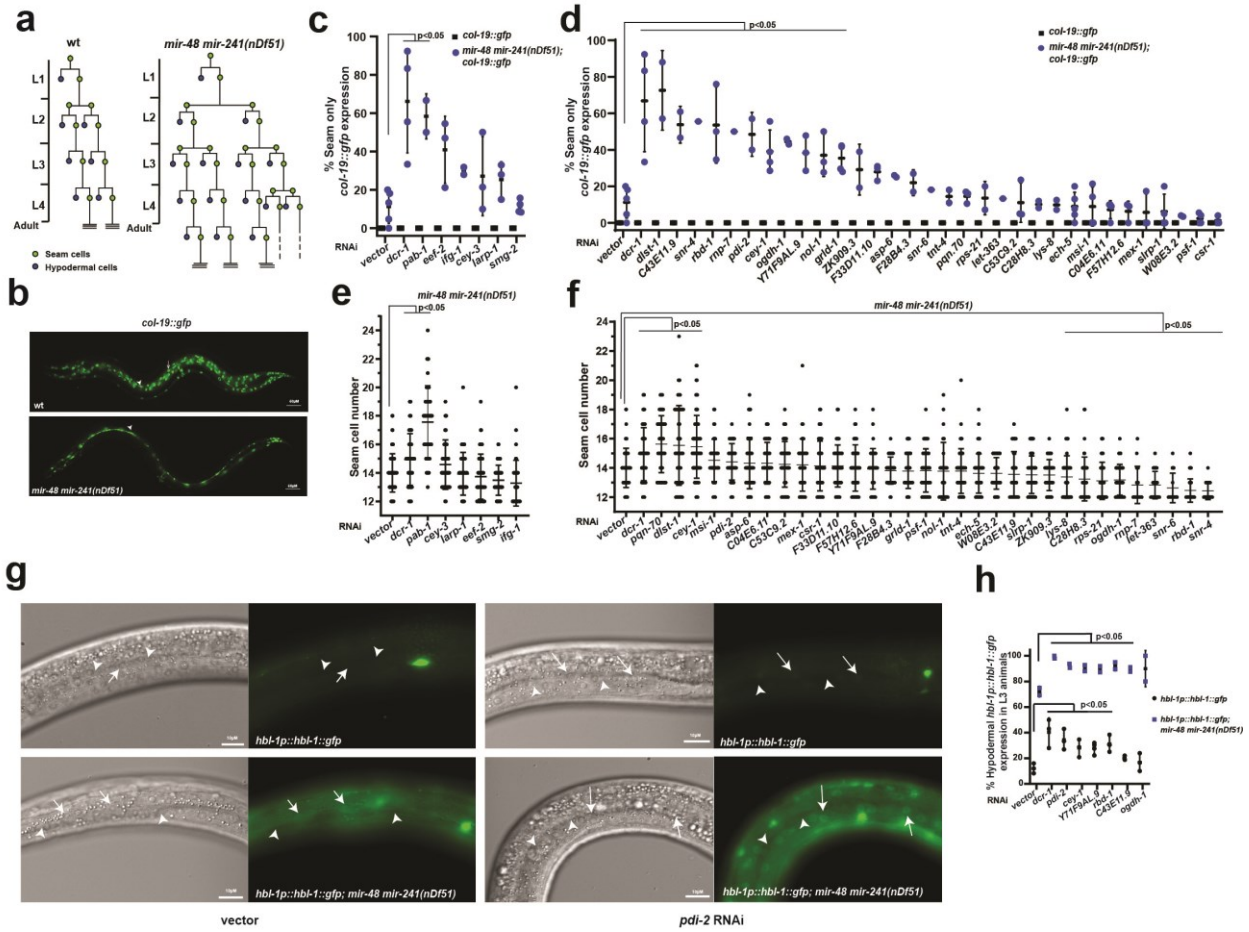

Figure 2.4 RNAi knockdown of genes encoding for putative ALG-1 and miRNA interactors modulates *mir-48 mir-241(nDf51)* seam cell lineage and hypodermal cell fate defects.

(a) A schematic representation of seam cell lineages of wild type and *mir-48 mir-241(nDf51)* mutant animals throughout *C. elegans* larval development. (**b**) Wild type young adult animals express adult cell fate marker, *col-19::gfp*, in seam and hypodermal cells, while *mir-48 mir-241(nDf51)* mutants show lack the *col-19::gfp* expression in the hypodermis as young adults some of the time (quantified in c). (**c**,**d**) Effects of RNAi knockdown of genes of (**c**) conserved AGO (Zinovyeva *et al.* 2015) and (**d**) other miRISC interactors on hypodermal *col-19::gfp* expression in wild type and *mir-48 mir-241(nDf51)* mutants. Each dot represents an independent RNAi experiment. (**e**,**f**) Effects of RNAi knockdown of genes of (**e**) conserved AGO

(Zinovyeva *et al.* 2015) and (**f**) other miRISC interactors on the seam cell number in *mir-48 mir-241(nDf51)* mutant young adults. Each dot represents seam cell number in an individual worm. Statistical significance was determined by One-way ANOVA with post hoc Bonferroni correction. (**g**) Expression of *hbl-1::gfp::hbl-1 3′ UTR* reporter in control and *pdi-2* RNAi in wild type and *mir-48 mir-241(nDf51)* L3 larvae. Arrows indicate hypodermal cells and arrowheads indicate seam cells. (**h**) RNAi of most genes that genetically modified heterochronic defects in *mir-48 mir-241(nDf51)* mutants significantly affected *hbl-1::gfp::hbl-1 3′ UTR* reporter expression in both wildtype and *mir-48 mir-241(nDf51)* backgrounds. Each dot represents an independent RNAi experiment. T-test was used to determine statistical significance. Vector = empty vector RNAi control.

Since *let-7* family miRNAs promote L3 cell fates by repressing *hbl-1* (Abbott *et al*. 2005), we sought to determine whether the genes that affect heterochronic phenotypes in *mir-48 mir-241*(*nDf51*) background do so by regulating *hbl-1*. We used the *hbl-1p::gfp::hbl-1 3'UTR* fusion construct as a reporter to assess the effects of gene knockdown on levels of HBL-1 (Abrahante *et al*. 2003). Strong *hbl-1* expression can be seen during embryogenesis with hypodermal *hbl-1::gfp::hbl-1 3'UTR* expression decreasing beyond detection at the L3 stage (Abrahante *et al*. 2003) (Fig. 2.4g). RNAi knockdown of *pdi-2, rbd-1,Y71F9AL.9,* and *cey-1* resulted in higher percentages of L3 animals expressing the reporter in the wild type background, potentially indicating a miRNA-independent effect (Fig. 2.4h, Table A.5). Since depletion of these genes did not affect *col-19:gfp* expression or other heterochronic defects in the wild type (Fig. 2.4d), perhaps the extent of *hbl-1* derepression was not strong enough to impact developmental timing. This notion is supported by the observation that *hbl-1* reporter expression in *mir-48 mir-241*(*nDf51*) background is observed at a higher rate (75%, Fig. 2.4h). Knockdown of enhancers of *mir-48 mir-241*(*nDf51*) mutant phenotype derepressed *hbl-1* reporter expression in the *mir-48 mir-241*(*nDf51*) background (Fig. 2.4h, Table A.5). Overall, these findings suggest that our proteomics approach captured proteins that may co-ordinate with *let-7* family miRNAs to repress their target, *hbl-1,* and ultimately coordinate developmental timing.

Depletion of ALG-1 physical interactors altered *lsy-6(ot150)* phenotype

We hypothesized that some of the ALG-1 and/or miRNA putative physical interactors could be factors that are generally required for miRISC activity. To test this, we RNAi depleted them in *lsy-6(ot150)* background. *lsy-6* is essential for cell fate determination of chemosensory ASE neurons (Johnston and Hobert, 2003). lsy-6 represses an ASER cell fate promoting transcription factor *cog-1*, leading to an ASEL neuronal specific gene expression pattern. Loss

of *lsy-6* leads to dysregulated gene expression of *cog-1* and downstream effectors resulting in defective ASEL cell fate which leads to lack of *plim-6::gfp* reporter. However, the reduction of function mutant *lsy-6(ot150)* shows partially penetrant cell fate defective phenotype in approximately 20% of animals (Johnston and Hobert, 2003) (Fig. 2.5a). Knockdown of 8 genes modified *lsy-6(ot150)* defective phenotype (Fig. 2.5b,c, Table A.4) including previously reported conserved AGO interactors *pab-1,* and *larp-1* (Zinovyeva *et al*. 2015) (Fig. 2.5b). Interestingly, we identified two suppressors (*ifg-1,* and *F28B4.3*) of ASEL cell fate defect (Fig. 2.5b,c, Table A.4). To determine whether these candidate factors can influence ASEL cell fate independent of lsy-6 miRNA, we knocked them down in wild-type worms and observed no change in *plim-6::gfp* reporter expression in ASEL cells (Fig. 2.5b,c).

We next determined whether genes that modified *lsy-6* phenotype upon knockdown were important for lsy-6 mediated target activity using *cog-1* reporter system (Palmer *et al*. 2002) (Fig. 2.5d). *cog-1* is expressed in vulval and uterine cells where lsy-6 is absent (Fig. 2.5d, top left panel). When *lsy-6* is ectopically expressed in these tissues under *cog-1* promoter, there is reduced expression of *cog-1* as a result of lsy-6 mediated repression (Palmer *et al*. 2002) (Fig. 2.5d, top right panel). We performed RNAi knockdown of top hits from lsy-6 assay in the *cog-1* reporter strain and observed no difference in *cog-1* expression (Fig. 2.5e, Table A.5), suggesting that these factors do not regulate *cog-1* directly in uterine cells. RNAi knockdown of *F33D11.10* and *psf-1* (enhancers of *lsy-6(ot150)* phenotype) restored *cog-1* expression in the presence of *lsy-6,* suggesting their requirement for lsy-6 mediated *cog-1* repression (Fig. 2.5e). Knockdown of *larp-1* did not restore *cog-1* expression to a statistically significant level (Fig. 2.5e, Table A.5). This could be due to RNAi variability among replicates, or possibly because lsy-6 activity was initially assessed in ASE neurons, while *cog-1* reporter expression was assessed in

uterine tissue. Previously reported tissue-specific composition of miRNA-centered complexes and distinct mechanisms of target suppression support this potential explanation for the observed discrepancy in *larp-1* effects (Dallaire *et al*. 2018). *lsy-6(ot150)* and *cog-1* reporter assays collectively demonstrate that we identified factors that may directly or indirectly coordinate with lsy-6, affecting its target *cog-1* expression.

Overall, depletion of miRNA complex interactors did not produce a phenotype in the absence of the sensitized miRNA mutations (Figs. 2.3b,c, 2.4c,d, 2.5b,c). While we cannot rule out inefficient RNAi knockdown as a possible explanation, we hypothesize that the tested factors are not critical for regulation of miRNA target gene expression, but rather play a modulatory role in miRNA production and/or activity, or influence gene expression downstream of miRNA activity.

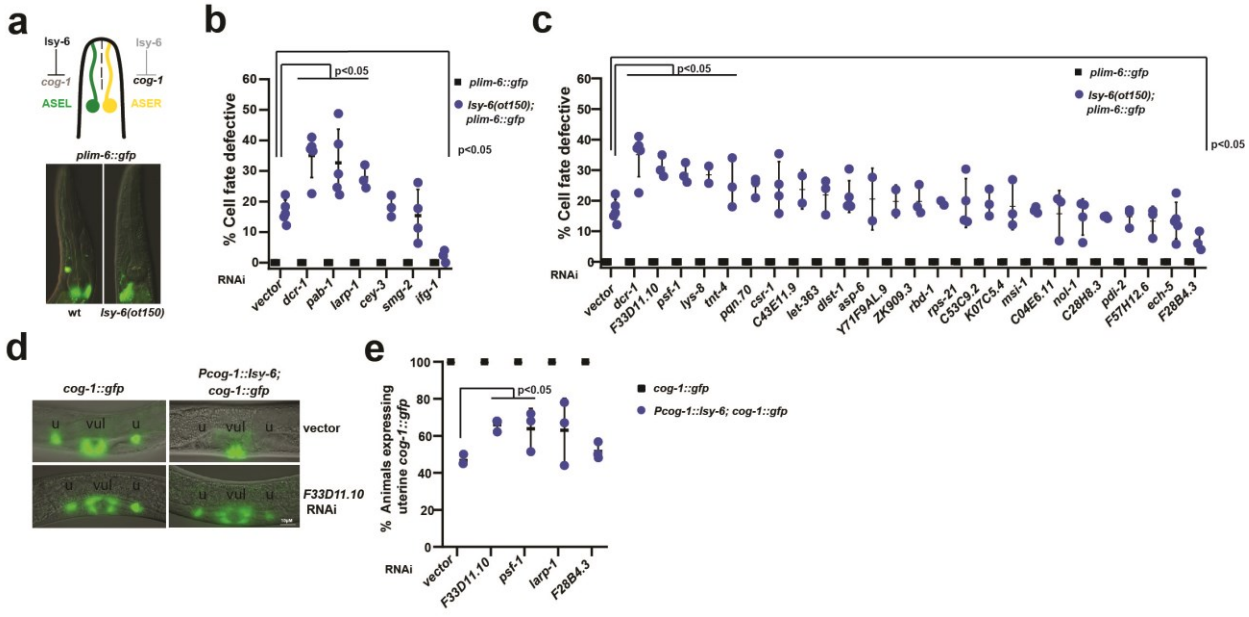

Figure 2.5 ALG-1 and miRNA interactors genetically interact with *lsy-6(ot150)*.

(**a**) lsy-6 determines the asymmetric expression of chemoreceptors in ASER and ASEL neurons, with *plim-6::gfp* expression marking ASEL neuronal cell fate. ASEL cell defective phenotype in the *lsy-6(ot150)* animals can be observed by lack of *plim-6::gfp* expression some of the time (quantified in b). RNAi knockdown of (**b**) conserved AGO (Zinovyeva *et al.* 2015) and (**c**) miRNA/ALG-1 interactors in *plim-6::gfp* or *lsy-6(ot150); plim-6::gfp* animals. Each dot represents an independent RNAi experiment. Statistical significance was determined by One-way ANOVA with post hoc Bonferroni correction. (**d**) *cog-1* expression in uterine cells is repressed by *pcog-1::lsy-6*. RNAi of *F33D11.10* depresses *cog-1::gfp* in that background (quantified in e). (**e**) RNAi of genes that modify *lsy-6(ot150)* phenotype alleviates lsy-6-mediated repression of *cog-1::gfp* in uterine cells. Each dot represents an independent RNAi experiment. T-test was used to determine statistical significance. Vector = empty vector RNAi control.

2.5 Discussion

To better understand miRNA mediated gene regulation, we performed miRNA pulldowns to identify components of miRNA-centered complexes. Our proteomics approach captured 211 miRNA-interacting proteins, some of which were previously reported to precipitate with other miRISC components (Table A.2). Knockdown of 25 out of 39 genes significantly modulated miRNA mutant phenotypes in one or more assays, suggesting that our pulldowns captured proteins that coordinate with miRNAs to affect gene regulation (Fig. 2.6a, Table A.4). Of the 25 hits, knockdown of five genes (*pab-1, let-363, rbd-1, cey-1,* and *lys-8*) and *dcr-1,* a positive control*,* consistently modified miRNA phenotypes in two or more assays (Fig. 2.6a, Table A.4). Of the 22 candidate genes tested, RNAi of six genes modulated *let-7(n2853)* vulval bursting phenotype (Fig. 2.6a, b, Table A.4). Five of these functional interactors were identified in let-7 PD experiments, either in let-7 PD alone or in let-7 PD plus additional precipitation experiments (Fig. 2.6b, Table A.4), suggesting that let-7 interacting factors indeed functionally coordinate with let-7 activity. Knockdown of 16 putative interactors did not modify vulval bursting phenotype of *let-7(n2853)* (Fig. 2.6b), perhaps due to tissue or time specific physical interactions of these proteins with let-7 miRNA or ALG-1 complexes. Such spatio-temporal complex compositions could explain the corresponding lack of activity in vulval tissue. We cannot, however, rule out insufficient RNAi knockdown or non-specific interactions of these proteins with anti-let-7 oligonucleotide. Knockdown of 18/38 candidate genes genetically modified hypodermal and/or seam cell lineage defects of *mir-48 mir-241(nDf51)* mutants (Fig. 2.6c, Table A.4). 12 of these factors were identified in let-7 pulldowns from wild type and/or *mir-48 mir-241; mir-84* mutant backgrounds, suggesting that let-7 PD proteomics captured factors that support let-7 family miRNA activity in developmental timing.

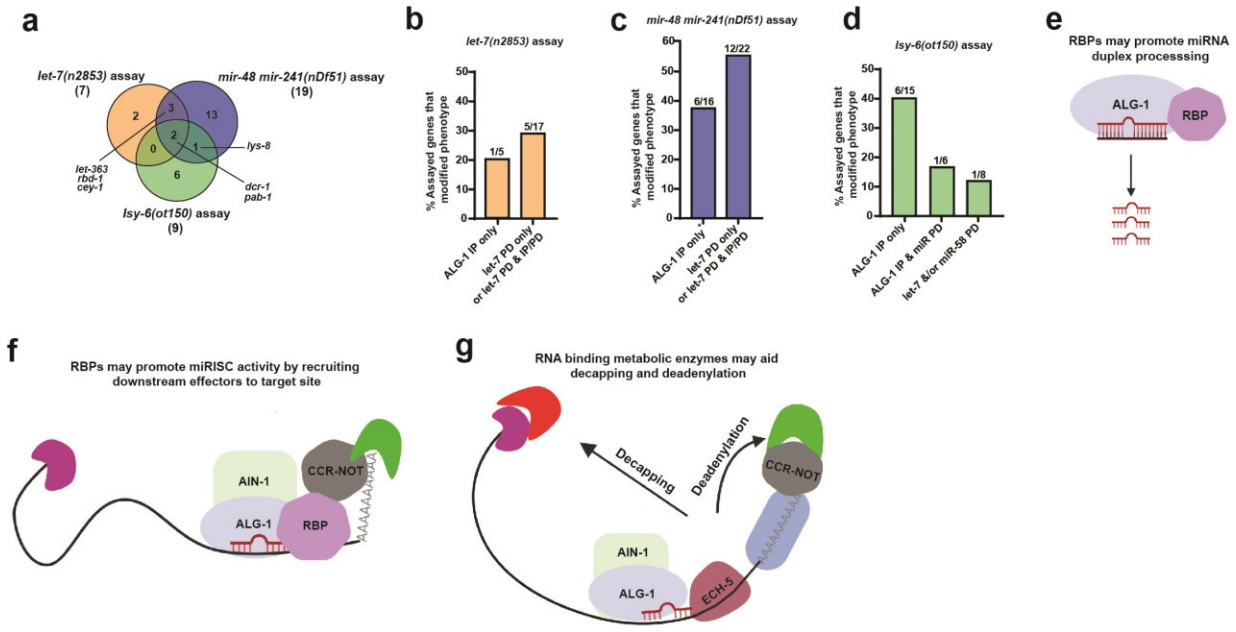

Figure 2.6 Summary of functionally relevant interactors and models for possible mechanisms through which miRNA and ALG-1 interactors affect gene regulation.

(a) Venn diagram showing the overlap of functional hits among the three functional assays. (b–d) Percentages of assayed factors that modulated phenotypes upon their respective gene knockdowns in (b) *let-7(n2853),* (c) *mir-48 mir-241(nDf51),* and (d) *lsy-6(ot150)* assays, with protein physical interaction status shown on the x-axis. *One ALG-1 interactor was also identified in miR-2 pulldown in addition to ALG-1 IP. The number of genes that modulated miRNA phenotypes over total number of genes tested is shown above respective bars. (e–f) RNA binding proteins found interacting with ALG-1 as well as miRNAs could be involved in (e) miRNA duplex processing and/or (f) facilitating miRISC activity on the targets by associating with downstream effectors. (g) Metabolic enzymes with putative RNA binding ability, such as ECH-5, could bind target mRNAs and promote miRISC activity by recruiting deadenylases and decapping proteins. Panels (e,f), and (g) were drawn using BioRender (https://biorender.com).

As *lsy-6* miRNA activity is highly localized and unrelated to miRNAs precipitated in our PD experiments, *lsy-6(ot150)* mutation provided a convenient genetic background to identify which factors may be broadly involved miRNA-mediated gene regulation. Of the eight functional hits from the *lsy-6(ot150)* assay, seven factors were identified as ALG-1 interactors (Fig. 2.6d, Table A.4), consistent with the idea that ALG-1 IP perhaps precipitated proteins with broad specificities. Lack of *lsy-6(ot150)* phenotype modification by knockdown of let-7 and/or miR-58-associated proteins suggests that miRNA-centered complexes may be unique to the specific miRNAs, possibly due to distinct spatial or temporal expression patterns.

Several genes that modified *let-7(n2853)* vulval bursting in our study, *cey-1*, *ifg-1*, *pab-1,* and *rbd-1* (Fig. 2.3b,c, Table A.4), were previously tested in an RNAi screen for suppressors of *let-7(n2853)* vulval bursting, aimed at identifying let-7 target genes (Rausch *et al*. 2015). We observed multiple differences between the results of our RNAi screen, performed at the permissive temperature of 15°C and the previous work, performed at non-permissive 25°C (Rausch *et al*. 2015), which eliminates *let-7* activity. For example, *rbd-1* knockdown enhanced vulval bursting at 15°C (Fig. 2.3c, Table A.4), while it suppressed bursting at 25°C (Rausch *et al*. 2015), suggesting that *rbd-1* may have both let-7 dependent and independent functions. Knockdown of *cey-1* suppressed *let-7(n2853)* vulval bursting at 15°C in our study (Fig. 2.3c, Table A.4), however, no *let-7(n2853)* suppression was observed at 25°C upon *cey-1* knockdown (Rausch *et al*. 2015). These observations suggest that *cey-1* may coordinate with let-7 in target mRNA regulation. Direct comparisons across RNAi studies performed under different conditions can be difficult to interpret and further explorations will be needed to understand the roles of these genes in *let-7*-mediated regulation of gene expression.

How could these putative physical miRNA interactors be coordinating with miRNAs to regulate gene expression? The factors identified in this study could be acting via multiple mechanisms to affect miRNA mutant phenotypes. Some of the miRNA interactors identified in this study have wide-ranging roles in regulation of gene expression. Thus, their knockdown could modify the miRNA reduction-of-function phenotypes directly through miRNA regulation and/or indirectly through regulation of mRNA lifecycle. For example, *pab-1*, a poly(A) binding protein and a homolog of human PABPC1 (Flamand *et al*. 2016), has well established roles in regulating the stability of mRNA transcripts by affecting translation initiation and mRNA stabilization and decay. PAB-1 has been previously shown to interact with miRISC and to aid miRNA-mediated deadenylation (Flamand *et al*. 2016; Zinovyeva *et al*. 2015). The enhancement of miRNA reduction-of-function phenotypes upon *pab-1* knockdown may therefore be a result of miRNA-dependent and/or independent functions of *pab-1,* perhaps through loss of target mRNA deadenylation and subsequent mRNA stabilization.

We used the biological and molecular functions predicted by GO term analysis to consider the possible mode of action for the identified miRNA and miRISC interactors. RNA binding proteins were among the classes of genes enriched in our pulldowns (Fig. 2.2a–h, Table A.3). Through functional assays, we identified nine interactors with predicted and/or experimentally validated RNA binding activity as genetic interactors of miRNA mutants (Table A.4). Interestingly, knockdown of genes encoding all nine RNA binding proteins enhanced miRNA mutant phenotypes, consistent with the recent finding that 3'UTR-binding RBPs generally promote miRISC targeting (Kim *et al*. 2021). Some of these RBPs could play a role in miRNA processing (Fig. 2.6e), some RBPs could potentially facilitate miRISC targeting or activity

(Fig. 2.6f), while other RBPs could regulate localization and stability of miRNAs and/or miRNA targets, ultimately affecting gene regulation.

Translation regulators were also captured in miRNA pulldowns and ALG-1 IP (Table A.1, A.3), with two of them modifying miRNA phenotypes. Depletion of *ifg-1,* encoding translation initiation factor 4G (eIF4G) (Pan *et al*. 2007), suppressed the ASEL cell fate defect of *lsy-6(ot150)* (Fig. 2.5b). Given the potential physical association of IFG-1 with ALG-1 (Zinovyeva *et al*. 2015), it is possible that IFG-1 and miRNAs share common targets; with loss of IFG-1 reducing translation through loss of initiation, thereby suppressing target mRNA overexpression in miRNA reduction of function mutants. RNA helicase F33D11.10 co-precipitated in let-7 pulldown (Table A.1) and was previously identified as an interactor of ALG-1 (Zinovyeva *et al*. 2015). Loss of *F33D11.10* activity enhanced the ASEL cell fate defect of *lsy-6(ot150)* mutant (Fig. 2.5c). RNA helicases have been previously implicated in miRNA processing as well as miRISC activity (Chu *et al*. 2016) and F33D11.10 may be similarly involved in either facilitating miRNA processing, miRISC activity, or both.

A surprising category of interactors identified in our study was the intermediary metabolic enzymes. RNAi depletion of metabolic enzymes DLST-1, OGDH-1 and ECH-5 modified miRNA mutant phenotypes in our study (Figs. 2.3c, 2.4d,f, Table A.4). Several reports have suggested that some metabolic enzymes possess RNA binding functions, previously unidentified due to a lack of conventional RNA binding domains (Beckmann *et al*. 2015; Curtis *et al*. 2021; Rodríguez-Saavedra *et al*. 2021). It is possible that the metabolic enzymes identified in our study possess similar dual roles. For instance, *ech-5* encodes a homolog of human AU RNA binding methylglutaconyl-CoA hydratase (AUH) (Yilmaz *et al*. 2016). In humans, AUH plays a dual role as a hydratase and as an RBP, binding AU-rich elements in the 3′ UTR of mRNAs

(Kurimoto *et al.* 2009). Other ARE-binding proteins have been previously shown to aid in rapid degradation through deadenylation (Otsuka *et al*. 2019). In our study, ECH-5 co-precipitated with let-7 miRNAs and *ech-5* depletion enhanced *let-7(n2853)* vulval bursting phenotype (Fig. 2.3c, Table A.1). Thus, we might speculate ECH-5 could bridge miRISC complex interaction with deadenylation machinery, with loss of *ech-5* exacerbating the target mRNA stabilization in miRNA mutant backgrounds (Fig. 2.6g). How other metabolic genes such as *dlst-1* and *ogdh-1*, key players of TCA cycle (Zhang *et al*. 2020; Castelein *et al*. 2008), influence gene regulation remains unclear. Thorough investigations into molecular mechanisms by which these factors coordinate with miRNAs in gene regulation will be needed.

Interestingly, LET-363, *C. elegans* mTOR was identified as an interactor of all three miRNAs in this study (Fig. 2.1f, Table A.1). RNAi of *let-363* enhanced the vulval bursting of *let-7(n2853)* and suppressed the seam cell lineage defect of *mir-48 mir-241(nDf51)* mutant (Figs. 2.3c, 2.4f, Table A.4). While we did not test for functional *let-363* requirement in our *lsy-6(ot150)* assay, RNAi of *let-363* was previously reported to exacerbate the cell fate specification defect of *lsy-6(ot150)* (Zhang and Zhang, 2013), consistent with a *let-363* role in miRNA-mediated gene regulation. mTOR activation has been reported to downregulate miRNA biogenesis through Mdm2-mediated DROSHA degradation in mice (Ye *et al*. 2015). However, the physical association of LET-363 with miRNAs was surprising. If confirmed, these persistent physical and functional interactions of LET-363 with miRNA-centered complexes should be further explored to establish the mechanistic connection between mTOR and miRNA-mediated gene regulatory activity.

Do miRNAs within the same family associate with same set of protein interactors? *let-7* family miRNAs are well-studied in *C. elegans*. The four most abundant members of the *let-*

7 family, *let-7, mir-48, mir-84* and *mir-241,* are crucial components of the heterochronic pathway, regulating cell fates during larval development (Reinhart *et al*. 2000; Johnston and Hobert, 2003). The miRNAs are thought to function semi-redundantly, with distinct targeting capabilities (Broughton *et al*. 2016). Part of their ability to target unique targets could come from discrete protein interactors adding a layer of specificity between a *let-7* family miRNA and its target. Yet not much is known about the protein interacting partners of individual members of this family. By performing pulldowns with a let-7 specific oligo from wild type and *mir-48 mir-241(nDf51); mir-84(n4037)* background, we began the task of unraveling which interactors may be specific to let-7 itself or other family members (Fig. 2.1h, Table A.1). For example, ECH-5 and C04E6.11 were identified in let-7 pulldowns from both genetic backgrounds, suggesting that they most likely interact with let-7 (Table A.1). RNAi depletion of *ech-5* or *C04E6.11* enhanced the *let-7(n2853)* phenotype but showed no effect on the *mir-48 mir-241(nDf51)* associated phenotypes (Figs. 2.3c, 2.4d). Thus, it is possible that ECH-5 and C04E6.11 specifically interact with, and provide functional support for, let-7 itself. CEY-1 was captured in let-7 pulldowns from both wild type and *mir-48 mir-241; mir-84* mutant background, but depletion of *cey-1* suppressed *let-7(n2853)* vulval bursting and enhanced *mir-48 mir-241(nDf51)* mutant phenotypes (Figs. 2.3c, 2.4d). This suggests that *cey-1* may functionally interact with multiple members of the *let-7* family, potentially through distinct mechanisms. Previously, miR-241 complementary oligo pulldown captured CEY-1 (Dallaire *et al*. 2018), although it remains difficult to assess specificity, as miR-241 oligo may capture other members of the family, similar to let-7 (Zinovyeva *et al*. 2014). Overall, we cannot rule out the possibility that some of the factors precipitating in miRNA pulldowns are non-specifically interacting with the precipitating oligo, rather than with the miRNA-centered complexes. It is also possible that let-7 interactions may be altered in the *mir-*

48 mir-241(nDf51); mir-84(n4037) background. Similarly, the severe developmental timing defect of *mir-48 mir-241(nDf51); mir-84(n4037)* animals could hinder identification of *bona fide* interactors of let-7 in that background. However, the high rate of functional relevance of these factors for miRNA-mediated gene regulation suggests that this approach captures auxiliary factors that may coordinate with miRNAs mediated gene regulation.

2.6 References

Abbott, A. L. *et al.* The let-7 MicroRNA Family Members mir-48, mir-84, and mir-241 Function Together to Regulate Developmental Timing in *Caenorhabditis elegans*. *Dev Cell* 9, 403–414 (2005).

Abrahante, J. E. *et al.* The *Caenorhabditis elegans* hunchback-like Gene lin-57/hbl-1 Controls Developmental Time and Is Regulated by MicroRNAs. *Dev Cell* 4, 625–637 (2003).

Bagga, S. *et al.* Regulation by let-7 and lin-4 miRNAs Results in Target mRNA Degradation. *Cell* 122, 553–563 (2005).

Beckmann, B. M. *et al.* The RNA-binding proteomes from yeast to man harbour conserved enigmRBPs. *Nat Commun* 6, 10127 (2015).

Broughton, J. P., Lovci, M. T., Huang, J. L., Yeo, G. W. & Pasquinelli, A. E. Pairing beyond the Seed Supports MicroRNA Targeting Specificity. *Mol Cell* 64, 320–333 (2016).

Castelein, N., Hoogewijs, D., Vreese, A. D., Braeckman, B. P. & Vanfleteren, J. R. Dietary restriction by growth in axenic medium induces discrete changes in the transcriptional output of genes involved in energy metabolism in *Caenorhabditis elegans*. *Biotechnol J* 3, 803–812 (2008).

Chu, Y.-D., Chen, H.-K., Huang, T. & Chan, S.-P. A novel function for the DEAD-box RNA helicase DDX-23 in primary microRNA processing in *Caenorhabditis elegans*. *Dev Biol* 409, 459–472 (2016).

Curtis, N. J. & Jeffery, C. J. The expanding world of metabolic enzymes moonlighting as RNA binding proteins. *Biochem Soc T* 49, 1099–1108 (2021).

Dallaire, A., Frédérick, P.-M. & Simard, M. J. Somatic and Germline MicroRNAs Form Distinct Silencing Complexes to Regulate Their Target mRNAs Differently. *Dev Cell* 47, 239-247.e4 (2018).

Ding, L., Spencer, A., Morita, K. & Han, M. The Developmental Timing Regulator AIN-1 Interacts with miRISCs and May Target the Argonaute Protein ALG-1 to Cytoplasmic P Bodies in *C. elegans*. *Mol Cell* 19, 437–447 (2005).

Ebrahimi, S. O., Reiisi, S. & Shareef, S. miRNAs, oxidative stress, and cancer: A comprehensive and updated review. *J Cell Physiol* 235, 8812–8825 (2020).

Ecsedi, M., Rausch, M. & Großhans, H. The let-7 microRNA Directs Vulval Development through a Single Target. *Dev Cell* 32, 335–344 (2015).

Flamand, M. N. *et al.* Poly(A)-binding proteins are required for microRNA-mediated silencing and to promote target deadenylation in *C. elegans*. *Nucleic Acids Res* 44, 5924–5935 (2016).

Frohn, A. *et al.* Dicer-dependent and -independent Argonaute2 Protein Interaction Networks in Mammalian Cells*. *Mol Cell Proteomics* 11, 1442–1456 (2012).

Grishok, A. *et al.* Genes and Mechanisms Related to RNA Interference Regulate Expression of the Small Temporal RNAs that Control *C. elegans* Developmental Timing. *Cell* 106, 23–34 (2001).

Guil, S. & Cáceres, J. F. The multifunctional RNA-binding protein hnRNP A1 is required for processing of miR-18a. *Nat Struct Mol Biol* 14, 591–596 (2007).

Hammell, C. M., Lubin, I., Boag, P. R., Blackwell, T. K. & Ambros, V. nhl-2 Modulates MicroRNA Activity in Caenorhabditis elegans. *Cell* 136, 926–938 (2009).

Han, J. *et al.* Molecular Basis for the Recognition of Primary microRNAs by the Drosha-DGCR8 Complex. *Cell* 125, 887–901 (2006).

Huang, D. W., Sherman, B. T. & Lempicki, R. A. Systematic and integrative analysis of large gene lists using DAVID bioinformatics resources. *Nat Protoc* 4, 44–57 (2009).

Hutvágner, G. *et al.* A Cellular Function for the RNA-Interference Enzyme Dicer in the Maturation of the let-7 Small Temporal RNA. *Science* 293, 834–838 (2001).

Iwasaki, S. *et al.* Hsc70/Hsp90 Chaperone Machinery Mediates ATP-Dependent RISC Loading of Small RNA Duplexes. *Mol Cell* 39, 292–299 (2010).

Jan, C. H., Friedman, R. C., Ruby, J. G. & Bartel, D. P. Formation, Regulation and Evolution of Caenorhabditis elegans 3′UTRs. *Nature* 469, 97–101 (2011).

Jannot, G., Vasquez-Rifo, A. & Simard, M. J. Argonaute Proteins, Methods and Protocols. *Methods Mol Biology* 725, 233–249 (2011).

Johnston, R. J. & Hobert, O. A microRNA controlling left/right neuronal asymmetry in *Caenorhabditis elegans*. *Nature* 426, 845–849 (2003).

Kamath, R. S. & Ahringer, J. Genome-wide RNAi screening in Caenorhabditis elegans. *Methods* 30, 313–321 (2003).

Kim, J. K. *et al.* Functional Genomic Analysis of RNA Interference in *C. elegans*. *Science* 308, 1164–1167 (2005).

Kim, K. K., Yang, Y., Zhu, J., Adelstein, R. S. & Kawamoto, S. Rbfox3 Controls the Biogenesis of a Subset of MicroRNAs. *Nat Struct Mol Biol* 21, 901–910 (2014).

Kim, S. *et al.* The regulatory impact of RNA-binding proteins on microRNA targeting. *Nat Commun* 12, 5057 (2021).

Kundu, P., Fabian, M. R., Sonenberg, N., Bhattacharyya, S. N. & Filipowicz, W. HuR protein attenuates miRNA-mediated repression by promoting miRISC dissociation from the target RNA. *Nucleic Acids Res* 40, 5088–5100 (2012).

Kurimoto, K. *et al.* AU-rich RNA-binding induces changes in the quaternary structure of AUH. *Proteins Struct Funct Bioinform* 75, 360–372 (2009).

Kwak, P. B. & Tomari, Y. The N domain of Argonaute drives duplex unwinding during RISC assembly. *Nat Struct Mol Biol* 19, 145–151 (2012).

Landthaler, M. *et al.* Molecular characterization of human Argonaute-containing ribonucleoprotein complexes and their bound target mRNAs. *Rna* 14, 2580–2596 (2008).

Lee, Y. *et al.* The nuclear RNase III Drosha initiates microRNA processing. *Nature* 425, 415–419 (2003).

Li, L. & Zinovyeva, A. Y. Protein Extract Preparation and Co-immunoprecipitation from *Caenorhabditis elegans*. *J Vis Exp* (2020) doi:10.3791/61243.

Li, L., Veksler-Lublinsky, I. & Zinovyeva, A. HRPK-1, a conserved KH-domain protein, modulates microRNA activity during *Caenorhabditis elegans* development. *Plos Genet* 15, e1008067 (2019).

Long, X. *et al.* TOR Deficiency in C. elegans Causes Developmental Arrest and Intestinal Atrophy by Inhibition of mRNA Translation. *Curr Biol* 12, 1448–1461 (2002).

Lucas, M. P. de, Sáez, A. G. & Lozano, E. miR-58 family and TGF-β pathways regulate each other in Caenorhabditis elegans. *Nucleic Acids Res* 43, 9978–9993 (2015).

Ma, F., Zhang, X. & Yin, K.-J. MicroRNAs in central nervous system diseases: A prospective role in regulating blood-brain barrier integrity. *Exp Neurol* 323, 113094 (2019).

MacRae, I. J., Zhou, K. & Doudna, J. A. Structural determinants of RNA recognition and cleavage by Dicer. *Nat Struct Mol Biol* 14, 934–940 (2007).

Marco, A., Hooks, K. & Griffiths-Jones, S. Evolution and function of the extended miR-2 microRNA family. *Rna Biol* 9, 242–248 (2012).

Mayya, V. K. *et al.* microRNA-mediated translation repression through GYF-1 and IFE-4 in C. elegans development. *Nucleic Acids Res* 49, gkab162- (2021).

Meijer, H. A., Smith, E. M. & Bushell, M. Regulation of miRNA strand selection: follow the leader? *Biochem Soc T* 42, 1135–1140 (2014).

Nishihara, T., Zekri, L., Braun, J. E. & Izaurralde, E. miRISC recruits decapping factors to miRNA targets to enhance their degradation. *Nucleic Acids Res* 41, 8692–8705 (2013).

O'Hern, P. J. *et al.* Decreased microRNA levels lead to deleterious increases in neuronal M2 muscarinic receptors in Spinal Muscular Atrophy models. *Elife* 6, e20752 (2017).

Otsuka, H., Fukao, A., Funakami, Y., Duncan, K. E. & Fujiwara, T. Emerging Evidence of Translational Control by AU-Rich Element-Binding Proteins. *Frontiers Genetics* 10, 332 (2019).

Palmer, R. E., Inoue, T., Sherwood, D. R., Jiang, L. I. & Sternberg, P. W. *Caenorhabditis elegans cog-1* Locus Encodes GTX/Nkx6.1 Homeodomain Proteins and Regulates Multiple Aspects of Reproductive System Development. *Dev Biol* 252, 202–213 (2002).

Pan, K. Z. *et al.* Inhibition of mRNA translation extends lifespan in *Caenorhabditis elegans*. *Aging Cell* 6, 111–119 (2007).

Parry, D. H., Xu, J. & Ruvkun, G. A Whole-Genome RNAi Screen for *C. elegans* miRNA Pathway Genes. *Curr Biol* 17, 2013–2022 (2007).

Pasquinelli, A. E. *et al.* Conservation of the sequence and temporal expression of let-7 heterochronic regulatory RNA. *Nature* 408, 86–89 (2000).

Porta-de-la-Riva, M., Fontrodona, L., Villanueva, A. & Cerón, J. Basic *Caenorhabditis elegans* Methods: Synchronization and Observation. *J Vis Exp* e4019 (2012) doi:10.3791/4019.

Rausch, M., Ecsedi, M., Bartake, H., Müllner, A. & Großhans, H. A genetic interactome of the let-7 microRNA in *C. elegans*. *Dev Biol* 401, 276–286 (2015).

Reinhart, B. J. *et al.* The 21-nucleotide let-7 RNA regulates developmental timing in Caenorhabditis elegans. *Nature* 403, 901–906 (2000).

Ren, Z., Veksler-Lublinsky, I., Morrissey, D. & Ambros, V. Staufen Negatively Modulates MicroRNA Activity in Caenorhabditis elegans. *G3 Genes Genomes Genetics* 6, 1227–1237 (2016).

Rodríguez-Saavedra, C. *et al.* Moonlighting Proteins: The Case of the Hexokinases. *Frontiers Mol Biosci* 8, 701975 (2021).

Snel, B., Lehmann, G., Bork, P. & Huynen, M. A. STRING: a web-server to retrieve and display the repeatedly occurring neighbourhood of a gene. *Nucleic Acids Res* 28, 3442–3444 (2000).

Srikantan, S., Tominaga, K. & Gorospe, M. Functional Interplay between RNA-Binding Protein HuR and microRNAs. *Curr Protein Pept Sc* 13, 372–379 (2012).

Subasic, D. *et al.* Cooperative target mRNA destabilization and translation inhibition by miR-58 microRNA family in *C. elegans*. *Genome Res* 25, 1680–1691 (2015).

Tabb, D. L., McDonald, W. H. & Yates, J. R. DTASelect and Contrast: Tools for Assembling and Comparing Protein Identifications from Shotgun Proteomics. *J Proteome Res* 1, 21–26 (2002).

Vella, M. C., Choi, E.-Y., Lin, S.-Y., Reinert, K. & Slack, F. J. The *C. elegans* microRNA let-7 binds to imperfect let-7 complementary sites from the lin-41 3′UTR. *Gene Dev* 18, 132–137 (2004).

Wu, E. *et al.* A continuum of mRNP complexes in embryonic microRNA-mediated silencing. *Nucleic Acids Res* 45, 2081–2098 (2017).

Wu, E. *et al.* Pervasive and Cooperative Deadenylation of 3′UTRs by Embryonic MicroRNA Families. *Mol Cell* 40, 558–570 (2010).

Ye, P. *et al.* An mTORC1-Mdm2-Drosha axis for miRNA biogenesis in response to glucose- and amino acid-deprivation. *Mol. Cell.* 57, 708–720 (2015)

Yilmaz, L. S. & Walhout, A. J. M. A *Caenorhabditis elegans* Genome-Scale Metabolic Network Model. *Cell Syst* 2, 297–311 (2016).

Zhang, L. *et al.* Systematic Identification of C. elegans miRISC Proteins, miRNAs, and mRNA Targets by Their Interactions with GW182 Proteins AIN-1 and AIN-2. *Mol Cell* 28, 598–613 (2007).

Zhang, P. & Zhang, H. Autophagy modulates miRNA-mediated gene silencing and selectively degrades AIN-1/GW182 in *C. elegans*. *Embo Rep* 14, 568–576 (2013).

Zhang, Z. *et al.* Broadly conserved roles of TMEM131 family proteins in intracellular collagen assembly and secretory cargo trafficking. *Sci Adv* 6, eaay7667 (2020).

Zhou, R. *et al.* Comparative Analysis of Argonaute-Dependent Small RNA Pathways in Drosophila. *Mol Cell* 32, 592–599 (2008).

Zinovyeva, A. Y., Bouasker, S., Simard, M. J., Hammell, C. M. & Ambros, V. Mutations in Conserved Residues of the *C. elegans* microRNA Argonaute ALG-1 Identify Separable Functions in ALG-1 miRISC Loading and Target Repression. *Plos Genet* 10, e1004286 (2014).

Zinovyeva, A. Y., Veksler-Lublinsky, I., Vashisht, A. A., Wohlschlegel, J. A. & Ambros, V. R. Caenorhabditis elegans ALG-1 antimorphic mutations uncover functions for Argonaute in

microRNA guide strand selection and passenger strand disposal. *Proc National Acad Sci* 112, E5271–E5280 (2015).

Chapter 3 - hnRNPA1/2 homolog *hrpa-1* coordinates with miRNAs to regulate gene expression during *C. elegans* development.

This chapter is a part of a submitted manuscript preprint-

Hebbar, S., Panzade, G., & Zinovyeva, A. Y. (2022) hnRNPA1/2 homolog *hrpa-1* coordinates with miRNAs to regulate gene expression during *C. elegans* development (submitted to *bioRxiv*).

3.1 Abstract

microRNAs (miRNAs) are small non-coding RNAs that play crucial roles in development and in disease. miRNAs associate with Argonaute proteins to form miRNA Induced Silencing Complexes (miRISCs), which post-transcriptionally repress gene expression. miRNA-mediated gene repression itself is subject to regulation by factors that can affect miRNA biogenesis or function. We previously identified HRPA-1, an hnRNPA/B homolog, as a putative physical interactor of miRNAs. Here, we report characterizations of both physical and genetic interactions between HRPA-1 and miRISC components. We confirmed HRPA-1 precipitation in let-7 and miR-58 pulldowns and detected an interaction between HRPA-1 and Argonaute. Deletion of *hrpa-1* in a *mir-48 mir-241(nDf51)* background enhanced the *mir-48 mir-241* developmental defects, suggesting that *hrpa-1* may be important for *let-7* family miRNA activity. Similarly, loss of *hrpa-1* strongly enhanced developmental defects associated with two other miRNA mutants, *lsy-6(ot150)* and *let-7(n2853).* Depletion of HRPA-1 modestly disrupted miRNA levels and affected global gene expression profiles. We identified a potential target of *hrpa-1*, *R06C1.4,* whose knockdown partially recapitulates the *hrpa-1(-)* effects on miRNA mutant phenotypes. Overall, we demonstrate *hrpa-1* and *R06C1.4* roles in *C. elegans* developmental timing regulation and propose models describing possible coordinating modes of gene regulation by HRPA-1 and miRNAs.

3.2 Introduction

Gene regulatory mechanisms orchestrate developmental and physiological processes by controlling spatiotemporal gene expression programs. microRNAs (miRNAs) and RNA binding proteins (RBPs) are essential components of the gene regulatory machinery, with both classes of

molecules post-transcriptionally controlling gene expression. miRNAs bind target mRNAs in the 3' UTR region via partial complementary base pairing, placing the miRNA induced silencing complex (miRISC) on the target RNAs to initiate translational inhibition and mRNA destabilization. RBPs exert their gene-regulatory influence through regulation of the RNA lifecycle. Coordination between miRNAs and RBPs contributes to the gene regulatory outcomes of gene expression programs. Heterogenous nuclear ribonucleoproteins (hnRNPs) are a family of closely related RNA binding proteins that associate with different classes of RNAs (Dreyfuss *et al.* 1993). HnRNPs harbor modular RNA binding domains and Proline or Glycine-rich regions (Dreyfuss *et al.* 2002). Members of this RBP family have been reported to affect alternative splicing, mRNA localization and mRNA stability among other processes (as reviewed in Geuens *et al.* 2016). A few prominent members of the family such as hnRNPA1, and hnRNPA2B1 have also been shown to bind DNA within the telomeric ends to regulate their stability (Jean-Philippe *et al.* 2013)**.**

hnRNPs have also been implicated in miRNA-mediated gene regulation (Li *et al.* 2019; Shin *et al.* 2017; Fan *et al.* 2015; Guil and Ca´ceres, 2007; Michlewski and Ca´ceres, 2010; Kooshapaur *et al.* 2018). hnRNPK (Shin *et al*. 2017; Fan *et al.* 2015) and its *C. elegans* homolog, HRPK-1 (Li *et al.* 2019) have been shown to impact miRNA-mediated gene regulation, albeit through potentially distinct mechanisms. hnRNPA2B1 was identified as a reader of m6A RNA modification that binds to m6A modified primary miRNAs, among other RNAs, and recruits the protein complex responsible for miRNA processing in the nucleus (Alarco´ *et al.* 2015). Sumoylated hnRNPA2B1 regulates sorting of miRNAs into exosomes, potentially influencing miRNA mediated cell-cell signaling (Villarrova-Beltri *et al.* 2013). hnRNPA1 has also been reported to regulate processing of primary miRNAs pri-miR-18a and pri-let-7 (Guil and Ca´ceres,

2007; Michlewski and Ca´ceres, 2008; Kooshapaur *et al.* 2018). While depletion of hnRNPA1 led to reduction in the levels of miR-18, let-7 levels were found to increase in Hela cells lacking hnRNPA1 (Guil and Ca´ceres, 2007; Michlewski and Ca´ceres, 2008; Kooshapaur *et al.* 2018). However, since changes in mature miRNA levels do not always correlate with changes in miRNA function *in vivo,* further characterization of hnRNPA1 and its homologs' roles in gene regulatory events is needed.

We previously identified HRPA-1 in 2'-O methyl oligonucleotide-mediated let-7 and miR-58 pulldowns (Hebbar *et al.* 2022). HRPA-1 was previously reported to be a homolog of hnRNPA1 (Jeong *et al.* 2004), however, recent reports suggest HRPA-1 to be a closer homolog of hnRNPA2B1 (Ryan and Hart, 2021; Ryan *et al*. 2021). Like its human homologs, HRPA-1 has been shown to regulate telomere ends (Jeong *et al*. 2004) and alternative splicing (Barberan-Soler *et al*. 2011). Dysregulation of both human and *C. elegans* hnRNPA/B proteins have been implicated in neurodegeneration (Ryan and Hart, 2021; Ryan *et al*. 2021; Clarke *et al.* 2021). Another key feature that appears to be conserved among these proteins is their ability to form phase separations *in vitro* (Ritsch *et al.* 2022; Ryan *et al*. 2021). HRPA-1 has also been reported to form aggregates under stress in specific tissues when expressed from tissue specific promoters (Lechler and David, 2017; Ryan *et al.* 2021). The relatively high degree of sequence similarity between the hnRNPA/B proteins and HRPA-1 makes *C. elegans* a great system to evaluate hnRNP roles in developmental processes *in vivo*. In this study, we report our investigation into the role of HRPA-1 in miRNA-mediated gene regulation and the associated developmental processes. We found that loss of *hrpa-1* enhanced developmental defects of multiple reduction-of-function miRNA mutants, dysregulated mature miRNAs levels, and disrupted gene expression. Overall, we propose several

models describing how HRPA-1 may contribute to miRNA-mediated gene regulation during *C. elegans* development.

3.3 Materials and Methods

Strain maintenance

All *C. elegans* strains were maintained on NGM and fed with *E. coli* strain OP50. Strains were maintained at 20°C unless otherwise noted.

Strain name	Genotype
N2	Wild type
MT7626	*let-7(n2853)*
VT1367	*col-19::gfp (maIs105)*
VT1296	*mir-48 mir-241(nDf51) col-19::gfp (maIs105)*
OH3646	*lsy-6(ot150); otIs114 [Plim-6-gfp + rol-6(su1006)]*
OH7310	*otIs114 [Plim-6-gfp + rol-6(su1006)]*
PS3662	*syIs63[cog-1::gfp + unc-119(+)]*
OH7310	*otIs193 [cog-1p::lsy-6 + rol-6(su1006)] syIS63[cog-1::gfp + unc-119(+)]*
UY260	*hrpa-1 (zen-192[hrpa-1::linker::AID::TEV::FLAG]); unc-119(ed3); ieSi57 [Peft-3::TIR1::mRuby::unc-54 3'UTR, cb-unc-119(+)] II*
UY500	*R06C1.4(zen214)*
UY287	*hrpa-1(ok963)/tmc25; mir-48 mir-241(nDf51) col-19::gfp (maIs105)*
UY306	*hrpa-1(ok963)/tmc25; col-19::gfp (maIs105)*
UY292	*hrpa-1(ok963)/tmc25; lsy-6(ot150); otIs114 [Plim-6-gfp + rol-6(su1006)]*

UY518	*hrpa-1(ok963)/tmc25; otIs114 [Plim-6-gfp + rol-6(su1006)]*
UY293	*hrpa-1(syb1830 [hrpa-1::linker::GFP])*
UY430	*hrpa-1(syb1830 [hrpa-1::linker::GFP]) pgl-1 (gg547[pgl-1::3X FLAG::tagRFP]).*
UY519	*R06C1.4(zen219[R06C1.4::linker::V5])*
UY520	*R06C1.4(zen219[R06C1.4::linker::V5]); hrpa-1(zen-192[hrpa-1::linker::AID::TEV::FLAG])*
UY517	*R06C1.4(zen214); mir-48 mir-241(nDf51) col-19::gfp (maIs105)*
HW1113	*xeSi78[Pdpy-30::GFP (PEST)-H2B::lin-41 3' UTR, xeSi36 [Pdpy-30::mCherry::H2B::artificial 3' UTR*
HW1114	*xeSi78[Pdpy-30::GFP (PEST)-H2B::lin-41 3' UTR (xeSi78), Pdpy-30::mCherry::H2B::artificial 3' UTR (xeSi36); let-7(n2853)*
HW1159	*xeSi87[Pdpy-30::GFP(PEST)-H2B::lin-41deltaLCS 3'UTR, unc-119 (+)], xeSi36[Pdpy-30::mCherry::H2B::artificial 3'UTR, unc-119(+)]*

Table 3.1 List of strains used in this study

RNAi and phenotypic assessments

For all phenotypic assays using *hrpa-1(ok963)* mutants, *hrpa-1(ok963)/hrpa-1(ok963)* progeny of *hrpa-1(ok963)/tmc25* parent in wild type or miRNA mutant backgrounds *(lsy-6(ot150)* or *mir-48 mir241(nDf51))* were scored. For ASEL cell fate assay, homozygous *hrpa-1(ok963); lsy-6 (ot150)* animals lacking the *plim-6::gfp* reporter expression in ASEL neurons were scored as "cell fate defective". RNAi knockdown was performed as previously described (Kamath *et al*. 2003). Empty vector and *dcr-1* RNAi were used as negative and positive controls respectively. For the let-7 vulval bursting assay, N2 or *let-7(n2853)* embryos obtained through bleaching were placed on RNAi plates and grown at 15°C. Vulval bursting was scored in day 1 adults. For *cog-1* assay, *cog-1::gfp* or *pcog-1::lsy-6; cog-1::gfp* animals were transferred as L1s on RNAi plates

and F1 progeny were scored at L4 stage for *cog-1::gfp* expression in uterine cells. Animals lacking reporter expression in one or both uterine cells were scored as abnormal.

For RNAi based assay, *mir-48 mir-241(nDf51) col-19::gfp (maIs105)* or *col-19::gfp (maIs105)* animals were placed on RNAi plates at L3 stage and the hypodermal and seam cell *col-19::gfp* expression were scored in F1 young adult animals. Seam cell numbers were scored by counting the number of seam cells between the pharynx and the anus.

CRISPR-based genome editing

CRISPR/Cas9 based gene editing was performed by carrying out microinjections as previously described (Mello *et al*. 1991). Strains were generated by injecting RNP injection mix consisting of Alt-R Cas9 (IDT, cat# 1081058), *dpy-10* crRNA, gene specific crRNAs, and tracer RNA (IDT, cat# 1072532). Endogenously tagged *R06C1.4::V5* was generated by inserting coding sequences of V5 tag into the C-terminus of *R06C1.4* locus just before the stop codon through CRISPR/Cas9 mediated homologous recombination. *GFP* insertion at the endogenous *hrpa-1* locus to generate *hrpa-1 hrpa-1::linker::GFP* was done by SunyBiotech.

HRPA-1 depletion, RNA extraction, Small RNA and RNA seq

HRPA-1 was depleted using RNAi and auxin treatment. Indole-3-acetic acid (IAA) was purchased from ThermoFisher (Product #I3750). IAA treatment was performed as previously described (Zhang *et al.* 2015). For HRPA-1 depletion, *hrpa-1::linker::AID*::TEV::FLAG* embryos obtained through bleaching were transferred to empty vector control or *hrpa-1* RNAi plates and maintained at 20ºC until the L4 stage. RNAi-treated L4 larvae were then transferred to either control or 1mM IAA plates for 3 hours before collecting the

treated animals for downstream experiments. Western blot experiments after RNAi and IAA treatment were performed by picking 50 worms directly into the 2x Laemmli protein loading buffer and boiled at 95°C for 5 minutes.

RNA from L4 staged animals from control and *hrpa-1*-depleted conditions were extracted as previously described (Li *et al.* 2019), except worm pellets resuspended in Trizol were vortexed for 10 mins before proceeding to phenol-chloroform extraction step. Small RNA and RNAseq was performed on the same set of RNA. For small RNA library preparation, small RNA size selection was performed as previously described (Gu *et al.* 2011). NEXTflex Small RNA Library Prep kit v3 (Bioo Scientific) was used to prepare libraries according to the manufacturer's instructions, followed by size selection of final PCR products as previously described (Gu *et al.* 2011). TruSeq stranded RNA-seq library prep was employed to prepare RNA libraries. All libraries were sequenced using the Illumina Nextseq500 platform at the Kansas State Genomics Core.

Small RNA data analysis

Small RNAseq reads were checked for quality before and after filtering using FastQC v0.11.8 (https://www.bioinformatics.babraham.ac.uk/projects/fastqc). Cutadapt tool was used to: (1) clip the adapter sequence from 3' end (-a ATCTCGTATGCCGTCTTCTGCTTG -e 0.1); (2) split reads into libraries using fastx_barcode splitter utility (http://hannonlab.cshl.edu/fastx_toolkit/index.html) based on their barcode index sequences and concatenate files that belong to the same barcode; (3) clip the remaining 3' end and 5' adapter sequences (-a TGGAATTCTCGGGTGCCAAGGAACTCCAGTCAC -e 0.1); (4) trim the first and last 4 random bases, and (5) select reads with a final length ranging between 17-29 nt for further analysis. Reads were mapped to *C. elegans* genome (WS279) using bowtie v1.2.2

(Langmead *et al*. 2009) allowing three mismatches in the alignment. Mature miRNA expression was quantified using the miRDeep2 pipeline (Friedländer *et al*. 2012). The DESeq2 package in R was used to perform differential expression analysis (Anders and Huber, 2010).

RNAseq read processing and data analysis.

FastQC v0.11.8 was used to assess quality of paired end RNA seq reads. Trimmomatic tool was used for quality filtering and adapter trimming. Filtered reads were mapped to *C. elegans* reference genome (WS279) using STAR aligner (Doblin *et al*. 2013). Stringtie transcript assembler was used to construct scaffold and contigs to assemble the transcripts. Normalized expression for each gene in the assembled transcriptome was quantified using featureCounts program (Subread package) (Liao *et al*. 2014). DESeq2 package in R was used to perform differential expression analysis (Anders and Huber, 2010).

Protein extract preparation, miRNA pulldown and immunoprecipitation experiments

Protein extracts from mixed stage animals were prepared as previously described (Li and Zinovyeva, 2020). 2'O-methylated oligonucleotide-mediated miRNA pulldown was performed as previously described, using 1mg total protein for each pulldown (Jannot *et al*. 2011). HRPA-1::FLAG immunoprecipitation was performed using the anti-FLAG antibody-conjugated ChromoTek DYKDDDDK Fab-Trap™ Agarose beads (cat# ffa-10) according to the manufacturer's protocol. Lysis and wash buffers for these immunoprecipitations were prepared as previously described (Li and Zinovyeva, 2020). Lysates with equal amounts of total protein from N2 and *hrpa-1::AID*::TEV::FLAG* strains were used for FLAG IP. Immunoprecipitation was performed for 1h at 4°C followed by 4 washes with the Wash buffer. 10% of the input was used

for western blot. HRPA-1::AID*::TEV::FLAG was detected using Monoclonal Anti-FLAG M2-Peroxidase (HRP) antibody (A8592-2MG) from Sigma-Aldrich at a 1:1000 dilution. R06C1.4::V5 was detected using the Anti-V5 antibody from Invitrogen (MA5-32053) at a 1:1000 dilution. ALG-1 was detected using custom generated anti-ALG-1 monoclonal antibody (Zinovyeva *et al.* 2014). As a loading control, mouse Anti-TUBULIN antibody from Sigma-Aldrich (T6074) was used at a 1:5000 dilution to detect tubulin.

FLAG-based RNA immunoprecipitation experiments were performed using lysates from N2 and *hrpa-1::AID*::TEV::FLAG* strain. Lysates with equal amount of total protein was used across both samples for immunoprecipitation, RNA extraction, and western blots. Following immunoprecipitation, 25% of the suspension was used for western blot and the rest was used for total RNA extraction using the phenol/chloroform method.

Western blot detection of HRPA-1 from mutants

Western blot analyses for detection of HRPA-1 from *hrpa-1(ok963)* and *hrpa-1(ok597)* mutants were performed by directly picking ~50 worms into 2x Laemmli protein loading buffer, with custom Rabbit polyclonal anti-HRPA-1 antibody (Jeong *et al.* 2004) used for detection.

RT-qPCR

RNA quantification following FLAG IP was performed by RT-qPCR using the one-step QuantiNova SYBR-Green RT-PCR kit (cat# 208152) according to the manufacturer's protocol. ABI 7500 Real-Time PCR System was used to perform all the RT-qPCR experiments. Ct values were adjusted to account for input and IP RNA dilutions. To calculate % input, we first normalized the Ct value for IP RNAs with their respective input RNAs to obtain ΔCt. Fold enrichment was

determined by ΔΔCt method by further normalizing *hrpa-1::AID*::TEV::FLAG* RIP fraction to our negative control (IP fraction from N2).

Microscopy and statistical analyses

Phenotypes were scored using a fluorescence-equipped Leica DM6 upright microscope and images were captured using Leica DM6B camera. Images were processed using the Leica Application Suite X (3.4.1.17822) software. HRPA-1::GFP images were assembled using Adobe Illustrator. Student t-test was used to determine statistical significance for RNAi based assays (hypodermal *col-19::gfp*, seam cell number analysis, vulval bursting assay and *cog-1* reporter assay). Chi-square test was performed to determine statistical significance for all other assays. GraphPad Prism (9.2.0 (332)) software was used to perform all of the statistical analyses.

3.4 Results

We previously characterized miRNA-interacting protein complexes to identify factors that coordinate with miRNAs to regulate gene expression (Hebbar *et al.* 2022). HRPA-1, an RNA binding protein, was captured in 2-O'methylated oligonucleotide mediated pulldowns of both let-7 and miR-58 miRNAs (Fig 3.1A, Hebbar *et al.* 2022). To begin to understand the role of HRPA-1 in miRNA mediated gene regulation, we first sought to confirm the precipitation of HRPA-1 in 2'-O-methyl oligonucleotide-mediated miRNA pulldowns. let-7- and miR-58-specific oligos, but not the scrambled control oligo, precipitated FLAG-tagged HRPA-1 from an endogenously tagged *hrpa-1::AID*::TEV::FLAG* strain (Fig 3.1B). In addition, immunoprecipitation of HRPA-1::AID*::TEV::FLAG co-precipitated the miRISC component, ALG-1 (Fig 3.1C). This is consistent with previous detection of HRPA-1 in ALG-1 IP through mass-spec analysis, with

average fold enrichment of 2.94 (Zinovyeva *et al*. 2015). The small amount of ALG-1 precipitating in HRPA-1::AID*::TEV::FLAG IP, as well as the mild enrichment observed in ALG-1 mass spec (Zinovyeva *et al*. 2015) suggest that HRPA-1 interaction with ALG-1 may be transient and may be RNA-dependent.

To assess genetic interactions between *hrpa-1* and miRNAs of interest, we confirmed that the existing *hrpa-1* deletion mutants, *hrpa-1(ok963)* (Jeong *et al.* 2004) and *hrpa-1(ok597)* (Ryan *et al.* 2021) are strong loss of function/null based on the molecular nature of the alleles and the lack of detectable HRPA-1 protein (Fig 3.1D, E). For subsequent functional analyses, we used the larger of the two deletions, *hrpa-1(ok963).*

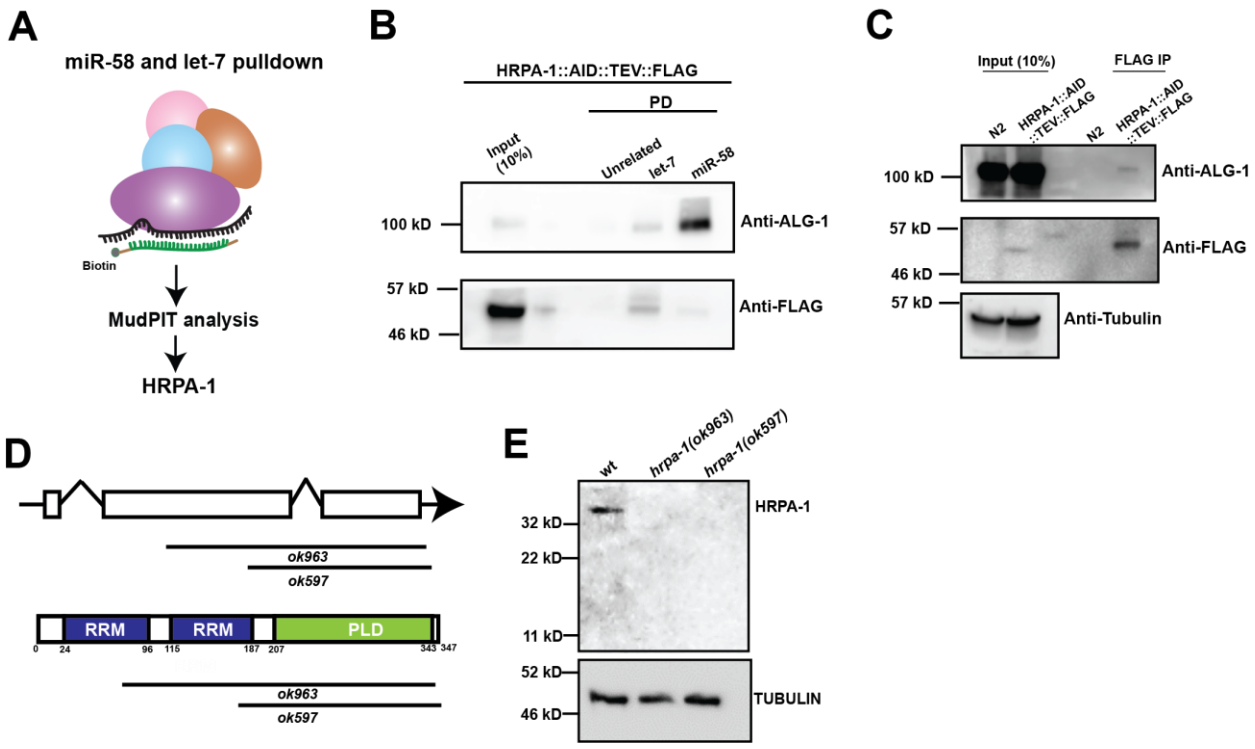

Figure 3.1 HRPA-1 was captured in 2' O-methyl oligonucleotide-mediated let-7 and miR-58 pulldowns.

(A) HRPA-1 was previously captured in let-7 and miR-58 pulldown experiments (Hebbar *et al.* 2022). (B) Detection of HRPA-1 and ALG-1 in Western blot following 2'-O-methylated oligonucleotide-mediated miRNA pulldowns (PD) from *hrpa-1::AID::TEV::FLAG* animals. (C) HRPA-1 immunoprecipitation co-precipitates ALG-1. (D) A schematic of *hrpa-1* gene structure, protein domains, and available *hrpa-1* deletion mutations. RRM- RNA Recognition Motif, PLD- Prion like Domain. (E) *hrpa-1* mutants do not produce detectable protein by Western blot analysis.

***hrpa-1(ok963)* genetically interacts with *let-7* family miRNA mutants.**

HRPA-1 co-precipitated in a let-7 complementary oligonucleotide pulldown, which captures multiple members of the *let-7* family of miRNAs (Zinovyeva *et al.* 2014). We wanted to determine whether *hrpa-1* is functionally important for the *let-7* family miRNAs. *let-7* family miRNAs, let-7, miR-48, miR-241, and miR-84 are integral components of the heterochronic pathway that controls the temporal progression of *C. elegans* post-embryonic developmental programs (Reinhart *et al.* 2000; Abbott *et al.* 2005). Highly conserved *let-7* plays crucial roles during *C. elegans* L4 larval to adult transition (Reinhart *et al*. 2000). In addition to governing hypodermal development, *let-7* also regulates vulval development, primarily by repressing *lin-41* in vulval precursor cells (Ecsedi *et al.* 2015). Loss of *let-7* leads to derepression of *lin-41,* which results in a burst vulva phenotype (Reinhart *et al.* 2000). A temperature sensitive *let-7(n2853)* mutant has a partially penetrant vulval bursting phenotype at permissive temperature (15ºC), making it amenable to genetic perturbations (Fig 3.2A, Vella *et al.* 2004). Knockdown of *hrpa-1* in *let-7(n2853)* mutant at 15ºC enhanced the vulval bursting phenotype, suggesting that *hrpa-1* may directly or indirectly facilitate let-7 mediated target repression during vulval development (Fig 3.2B, Table B.2).

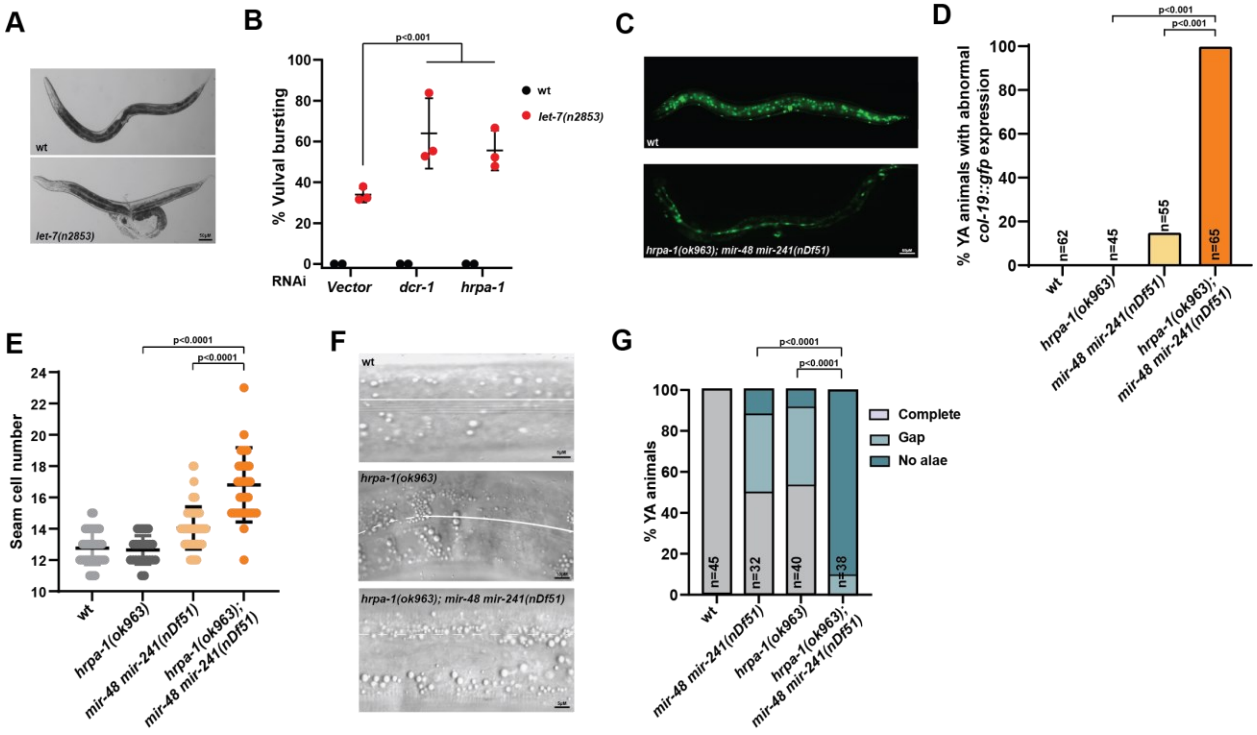

Figure 3.2 Loss of *hrpa-1* enhances the developmental defects associated with *let-7* family miRNA mutants.

(A) *let-7(n2853)* animals show a partially penetrant vulval bursting phenotype at 15ºC. (B) RNAi knockdown of *hrpa-1* enhances the vulval bursting phenotype at 15ºC. (C) *mir-48 mir-241(nDf51)* young adults show delayed hypodermal expression of *col-19::gfp* reporter. *hrpa-1(ok963)* enhances the (D) abnormal hypodermal *col-19::gfp* expression, (E) seam cell lineage defect, and (F-G) alae formation defect of *mir-48 mir-241(nDf51)* animals. Solid lines indicate alae, dashed lines indicate regions lacking discernable alae. T-test was used to determine the statistical significance for let-7 vulval bursting and seam cell number analyses. Chi-square was used to analyze hypodermal *col-19::gfp* and alae defect assays.

To evaluate the possibility of HRPA-1 regulating miRNA targets in a miRNA-independent manner, we determined the effect of *hrpa-1* knockdown on a well-established let-7 target, *lin-41,* whose dysregulation leads to vulval bursting (Ecsedi *et al*. 2015). A fluorescent reporter-based quantification of *lin-41_3'UTR* levels (Ecsedi *et al*. 2015) in wild type and *let-7(n2853)* at non-permissive temperature (20ºC) did not show any changes in reporter level upon *hrpa-1* knockdown (Fig B.1, Table B.2). Further, *lin-41deltaLCS 3'UTR* reporter, which harbors let-7 complementary site deletion, showed no changes in reporter levels upon *hrpa-1* knockdown (Fig B.1, Table B.2). These observations suggest that *hrpa-1* does not regulate *lin-41* on its own and the enhancement of vulval bursting in *let-7(n2853)* assay may be due to derepression of let-7-mediated *lin-41* repression.

miR-48, miR-241 and miR-84 redundantly target *hbl-1* for repression during L2-L3 transition, ensuring the timely division and differentiation patterns of *C. elegans* seam cells (Abbott *et al*. 2005). Complete loss of these miRNAs leads to reiteration of L2 specific cell divisions and delayed expression of the adult-specific marker *col-19::gfp* (Abbott *et al.* 2005). Partial deletion mutant *mir-48 mir-241(nDf51)* shows incompletely penetrant delayed development of the hypodermal tissue, as assayed by *col-19::gfp* expression in the seam cells and the hypodermis (Fig 3.2C, Abbott *et al.* 2005). Deletion of *hrpa-1* in this background enhanced the heterochronic defects of *mir-48 mir-241(nDf51)* mutant (Fig 3.2D, E, Table B.3), observed through delayed *col-19::gfp* expression in hypodermal cells (Fig 3.2D) and increased seam cell numbers in young adult animals (Fig 3.2E). Loss of *hrpa-1* alone did not delay hypodermal development or affect seam cell number (Fig 3.2D, E, Table B.3). However, *hrpa-1(ok963)* mutants showed alae formation defects and deleting *hrpa-1* in *mir-48 mir-241(nDf51)* background

further enhanced these alae formation defects (Fig 3.2F, G, Table B.3), suggesting that *hrpa-1* is involved in developmental processes controlled by the *let-7* family miRNAs.

Loss of *hrpa-1* enhanced developmental defect associated with *lsy-6(ot150).*

To determine whether *hrpa-1* broadly coordinates with miRNAs to regulate *C. elegans* development, we examined the effects of *hrpa-1(ok963)* on *lsy-6* miRNA activity. *lsy-6* functions to specify asymmetric cell fates of chemosensory neurons. *lsy-6* specifies ASEL cell fate by repressing *cog-1* which encodes an ASER promoting transcription factor (Johnston and Hobert, 2003). Loss of lsy-6 activity results in derepression of *cog-1* leading to defective specification of ASEL cell fate, which can be tracked using a *plim-6::gfp* reporter (Johnston and Hobert, 2003). A hypomorphic mutant, *lsy-6(ot150)*, shows a partially penetrant cell fate defective phenotype (Fig 3.3A, B). *hrpa-1(ok963)* enhanced the *lsy-6(ot150)* cell defective phenotype but did not produce an ASE cell fate defect on its own (Fig 3.3B, Table B.3). To determine whether *hrpa-1* is important for lsy-6 mediated *cog-1* repression, we utilized the *cog-1* reporter strains (Palmer *et al*. 2002). *cog-1* is normally expressed in the vulval and uterine cells (Palmer *et al*. 2002). Uterine *cog-1::gfp* expression is repressed in the reporter strain that expresses *lsy-6* under *cog-1* promoter (Fig 3.3C, Palmer *et al*. 2002). Knockdown of *hrpa-1* alone did not affect *cog-1::gfp* expression (Fig 3.3D, Table B.2). However, RNAi of *hrpa-1* in the *pcog-1::lsy-6; cog-1::gfp* reporter strain derepressed *cog-1::gfp* in the uterine cells (Fig 3.3D, Table B.2), suggesting that *hrpa-1* may be important for lsy-6-mediated *cog-1* repression in that tissue.

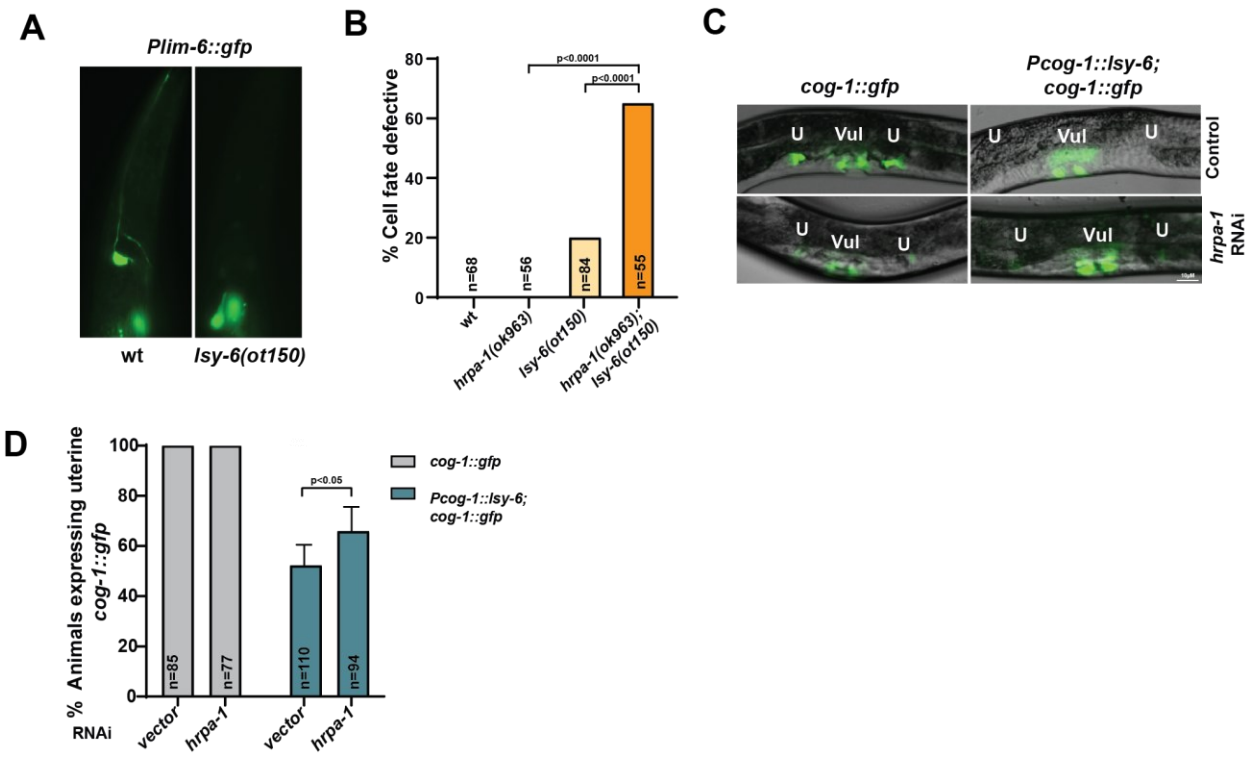

Figure 3.3 *hrpa-1* is functionally important for lsy-6 miRNA activity.

(A) *lsy-6(ot150)* mutants show partially penetrant defective ASEL neuronal cell fate phenotype. (B) *hrpa-1(ok963)* enhanced the ASEL cell defective phenotype of *lsy-6(ot150)* animals. (C-D) *cog-1* expression in the uterine cells is repressed when *lsy-6* is expressed in the same tissue. Depletion of *hrpa-1* leads to derepression of lsy-6 mediated *cog-1* repression in the uterine cells (C), quantified in (D). Chi-square and T-test were used to determine the statistical significance of ASEL cell fate assay and *cog-1* reporter assay respectively.

HRPA-1 is ubiquitously expressed.

To determine the spatial and temporal expression pattern of HRPA-1, we tagged the 3' end of the endogenous *hrpa-1* gene with GFP. HRPA-1::GFP was strongly nuclear and showed ubiquitous expression across somatic and germline tissues throughout *C. elegans* development (Fig 3.4A-C). Weak cytoplasmic GFP signal was detected in the intestine (Fig 3.4C). Our finding is consistent with a previous report describing nuclear expression of HRPA-1 assessed by a multicopy extrachromosomal *hrpa-1* transgene (Joeng *et al.* 2004). In addition, previously, RFP/mCherry tagged *hrpa-1* transgenes expressed under tissue specific promoters have been reported to form cytoplasmic puncta in pharynx and aggregates in neurons under stress (Lechler and David, 2017; Ryan *et al.* 2021). To determine whether endogenous promoter driven HRPA-1 also forms aggregates under stress, we subjected *hrpa-1::gfp* animals to heat stress at 35ºC for 30 min. Heat stress induced HRPA-1::GFP localization to the perinuclear region forming puncta which overlapped with PGL-1::tagRFP signals (Fig 3.4D, D'), a key component of P-granules crucial for post transcriptional gene regulation.

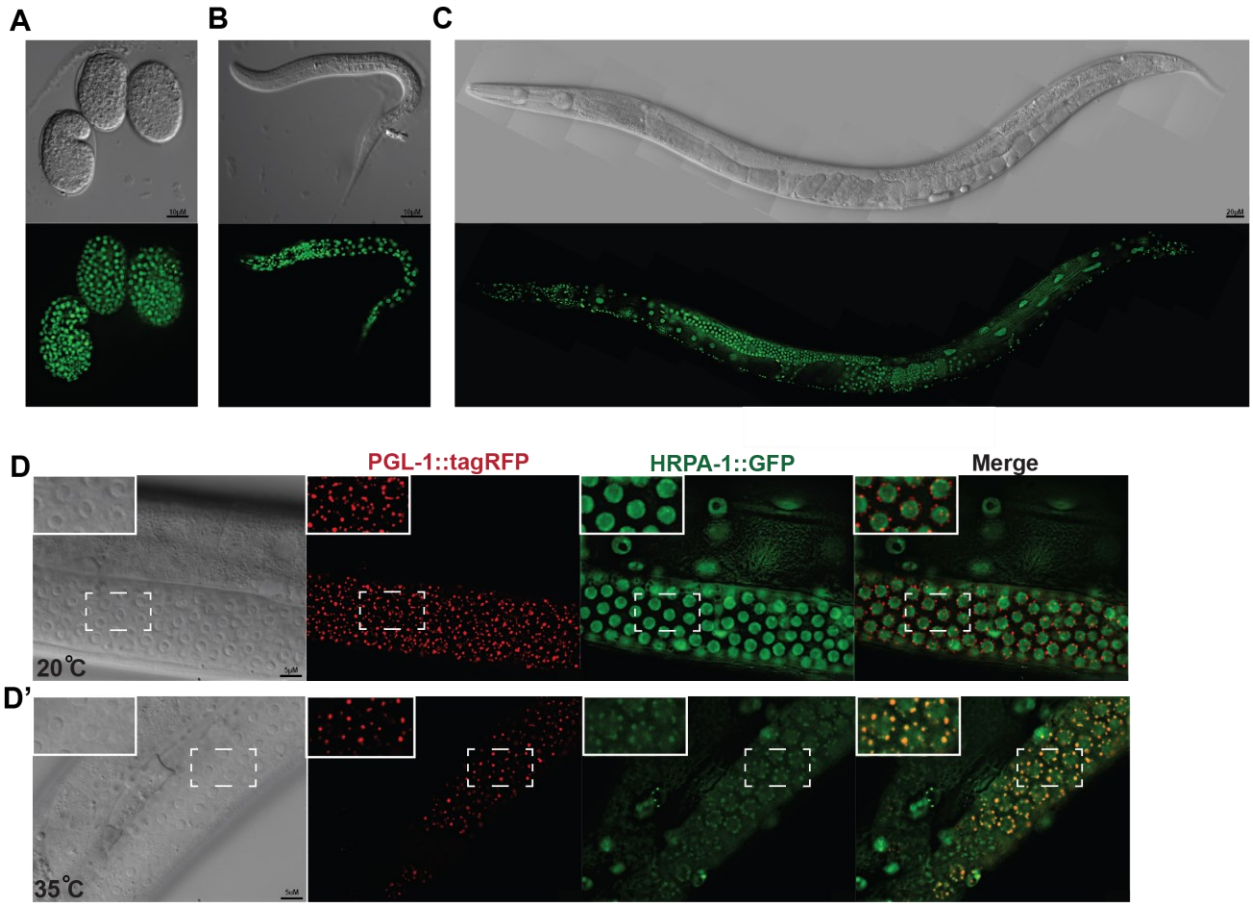

Figure 3.4 HRPA-1::GFP is expressed in the nucleus and localizes to the germline perinuclear region upon heat stress.

Endogenously tagged HRPA-1::GFP expression in (A) embryos, (B) L2 stage larvae, and (C) adults. HRPA-1::GFP is strongly expressed in the nucleus in somatic tissues and in the germline. (D, D') HRPA-1::GFP expression pattern in the germline at 20ºC and (D') at 35ºC. HRPA-1::GFP localizes to the perinuclear region upon heat shock, colocalizing with PGL-1::tagRFP (D').

Depletion of *hrpa-1* altered miRNAs abundance profiles and dysregulated gene expression.

A functional requirement of *hrpa-1* in miRNA-mediated gene regulation could stem from HRPA-1's role in miRNA biogenesis and/or miRNA activity. To determine HRPA-1 involvement in miRNAs biogenesis, we assessed levels of mature miRNAs following HRPA-1 depletion. *hrpa-1(-/-)* animals show severe developmental defects including embryonic lethality, reduced brood size, and larval arrest (Barberan-Soler *et al.* 2011; Ryan and Hart, 2021, Hills-Muckey *et al.* 2022). Thus, to deplete HRPA-1, we subjected *hrpa-1::AID*::TEV::FLAG* animals to both RNAi treatment and IAA induced protein depletion (Fig 3.5A), since neither knockdown alone resulted in robust depletion (Fig 3.5B,C). Small RNAseq from HRPA-1-depleted L4 animals revealed that expression levels of most miRNAs were unaffected by loss of HRPA-1 (Fig 3.5D). Expression levels of 19 miRNAs were disrupted by loss of HRPA-1, with the levels of 11 miRNAs upregulated (ex: miR-320, miR-243) and 8 downregulated (ex: miR-1817), suggesting that HRPA-1 function may be required for biogenesis or stability of these miRNAs (Fig 3.5D, Table B.4). Levels of let-7 and miR-58 miRNAs were unaffected (Fig 3.5D, Table B.4).

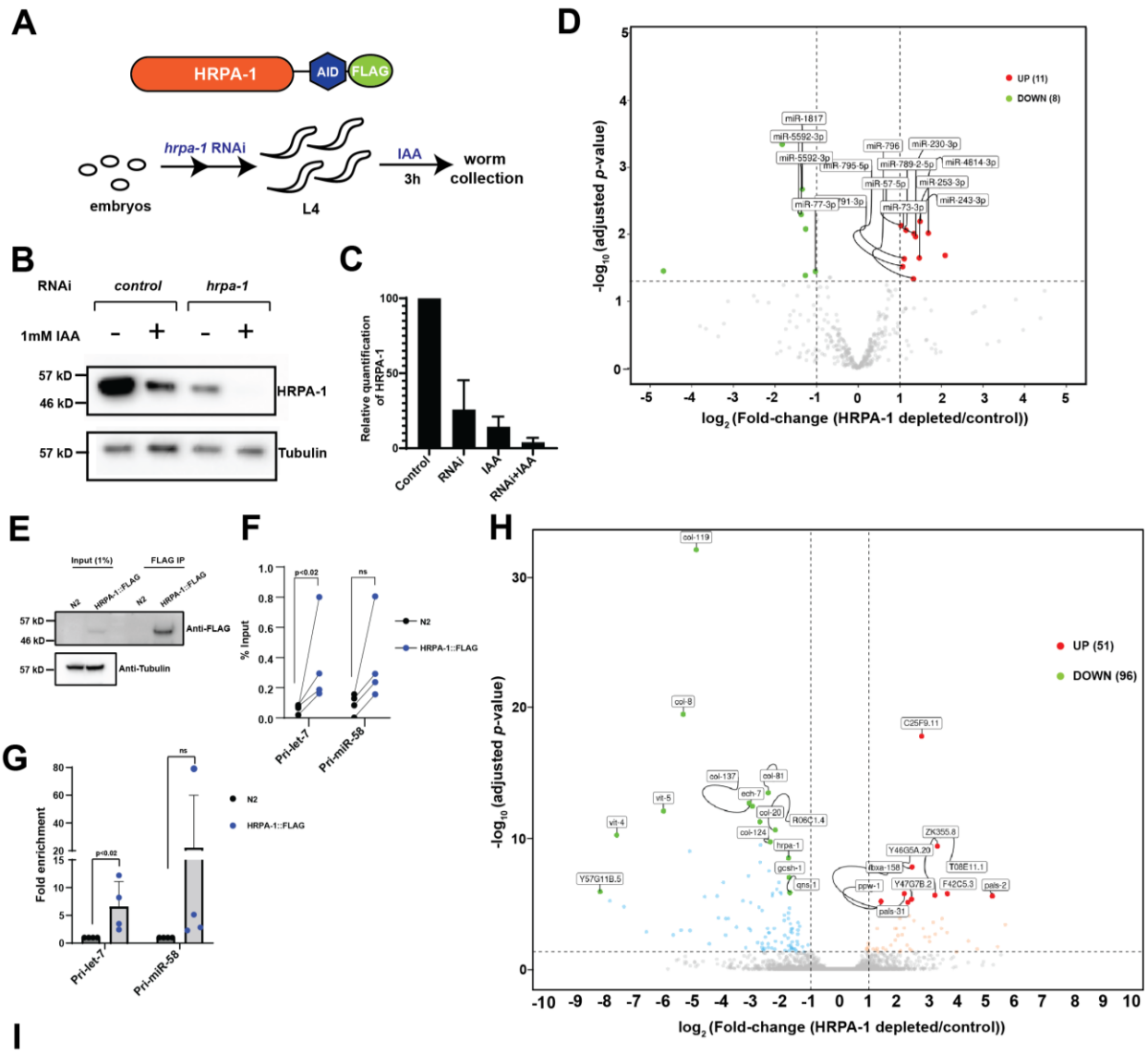
A
HRPA-1
AID
FLAG
hrpa-1 RNAi
IAA
3h
worm collection
embryos
L4
B
RNAi
control
hrpa-1
1mM IAA
57 kD
46 kD
HRPA-1
57 kD
Tubulin
C
Relative quantification of HRPA-1
Control
RNAi
IAA
RNAi+IAA
D
UP (11)
DOWN (8)
-log10 (adjusted p-value)
log2 (Fold-change (HRPA-1 depleted/control))
E
Input (1%)
FLAG IP
N2
HRPA-1::FLAG
Anti-FLAG
Anti-Tubulin
F
% Input
p<0.02
ns
Pri-let-7
Pri-miR-58
G
Fold enrichment
H
UP (51)
DOWN (96)
I
log2 (Fold-change (HRPA-1 depleted/conrol))

Figure 3.5 HRPA-1 depletion disrupts mature miRNA and gene expression levels.
(A-C) HRPA-1 was depleted using combined RNAi and IAA treatment from *hrpa-1::AID*::TEV::FLAG* animals. (A) A schematic of RNAi and IAA treatment performed to deplete HRPA-1. (B) Representative western blot image and (C) quantification of protein depletion achieved in the respective treatment conditions. (D) HRPA-1 depletion alters miRNA abundances as assayed by small RNAseq analysis. (E-G) Anti-FLAG immunoprecipitation from *hrpa-1::AID*::TEV::FLAG* or N2 (control) animals (E), followed by RT-qPCR quantification of bound pri-let-7 and pri-miR-58 RNA, shown as percent input (F) or fold enrichment over control (G). Paired T-test was used to determine statistical significance. (H) Depletion of HRPA-1 led to a disruption of gene expression as assayed by RNAseq analysis. (I) Some of the differentially expressed genes are predicted targets of miRNAs whose levels were disrupted by loss of HRPA-1. Lollipop plots showing $\log_2$(fold) changes in expression levels of miRNAs and their predicted targets, whose expression was altered in HRPA-1-depleted samples.

One of the human homologs of HRPA-1, hnRNPA1, associates with primary miRNAs *in vitro.* Since HRPA-1 was identified in miRNA complementary pulldown experiments that could, in theory, capture primary miRNAs, we sought to determine whether HRPA-1 IP may precipitate *let-7* and *mir-58* primary miRNAs. We performed an anti-FLAG based immunoprecipitation using *hrpa-1::AID*::TEV::FLAG* and N2 (negative control) lysates (Fig 3.5E). Real-time qPCR quantification of precipitated RNA showed a relative enrichment for pri-let-7 in HRPA-1 IP over our negative control (Fig 3.5F, G), suggesting that HRPA-1 may associate with pri-let-7. Pri-miR-58 was enriched, albeit not to statistically significant levels due to high variation Pri-miR-58 was enriched, albeit not to statistically significant levels due to high variation (Fig 3.5F, G).

To gain insight into the effects of *hrpa-1* depletion on global gene expression, we performed RNAseq on the RNA extracted from genotype *hrpa-1::AID*::TEV::FLAG* L4 animals treated with *hrpa-1* RNAi and auxin (Fig 3.5A). 147 genes were differentially expressed in HRPA-1-depleted animals, with 96 genes downregulated and 51 genes upregulated (Fig 3.5H, Table B.5). Since intronic miRNA transcription depends on their host gene and the splicing machinery (Kim and Kim, 2007), we wondered whether the changes in levels of intronic miRNAs were a result of changes in host gene transcription/processing. Expression levels of genes hosting intronic miRNAs were not affected by depletion of HRPA-1 (Fig B.2, Table B.4, B.5), suggesting that the modest changes observed in intronic miRNA levels were not due to effects of *hrpa-1* on host gene transcription.

Since disruption of miRNA-mediated target repression could be the underlying cause of differential expression of some of the genes following depletion of HRPA-1, we asked whether genes disrupted upon loss of HRPA-1 were predicted targets of miRNAs affected by depletion of HRPA-1 (Fig 3.5I). We found that some of the predicted targets of upregulated miRNAs (such as

miR-230, miR-243, miR-253, and miR-789-2) were downregulated by loss of HRPA-1 (Fig 3.5I). These targets included collagens (*col-19, col-8,* and *col-124,* among others) and other genes such as *R06C1.4, clec-4, acdh-1*, and *pmp-5* (Fig 3.5I).

_R06C1.4_ acts downstream of _hrpa-1_ and depletion of _R06C1.4_ partially recapitulates _hrpa-1_ loss-of-function phenotypes in _mir-48 mir-241(nDf51)_ background.

Genes dysregulated by depletion of HRPA-1 could be the underlying cause of the enhanced developmental defects observed in miRNA mutant backgrounds upon loss of *hrpa-1*. To test this, we performed RNAi knockdown of top genes downregulated upon *hrpa-1* depletion (excluding collagen and vitellogenin genes). While *R06C1.4* and *ego-1* RNAi on their own did not result in developmental timing defects (Fig 3.6A, B), depletion of *R06C1.4* and *ego-1* in *mir-48 mir-241(nDf51)* background partially recapitulated the enhanced the developmental timing phenotype observed in *mir-48 mir-241; hrpa-1* animals (Fig 3.6A, B, Table B.2). Knockdown of either of these genes did not alter the vulval bursting phenotype in *let-7(n2853)* assay at 15℃ (Fig B.3). To confirm the *R06C1.4* RNAi knockdown phenotype, we used CRISPR/Cas9 to delete the *R06C1.4* genomic locus (Fig 3.6C). *R06C1.4(zen214)* enhanced delayed hypodermal *col-19::gfp* expression and increased the seam cell number observed in *mir-48 mir-241* young adults (Fig 6D, E, Table B.3), confirming the *R06C1.4* RNAi effects in *mir-48 mir-241(nDf51)* background (Fig 3.6A, B, Table B.3).

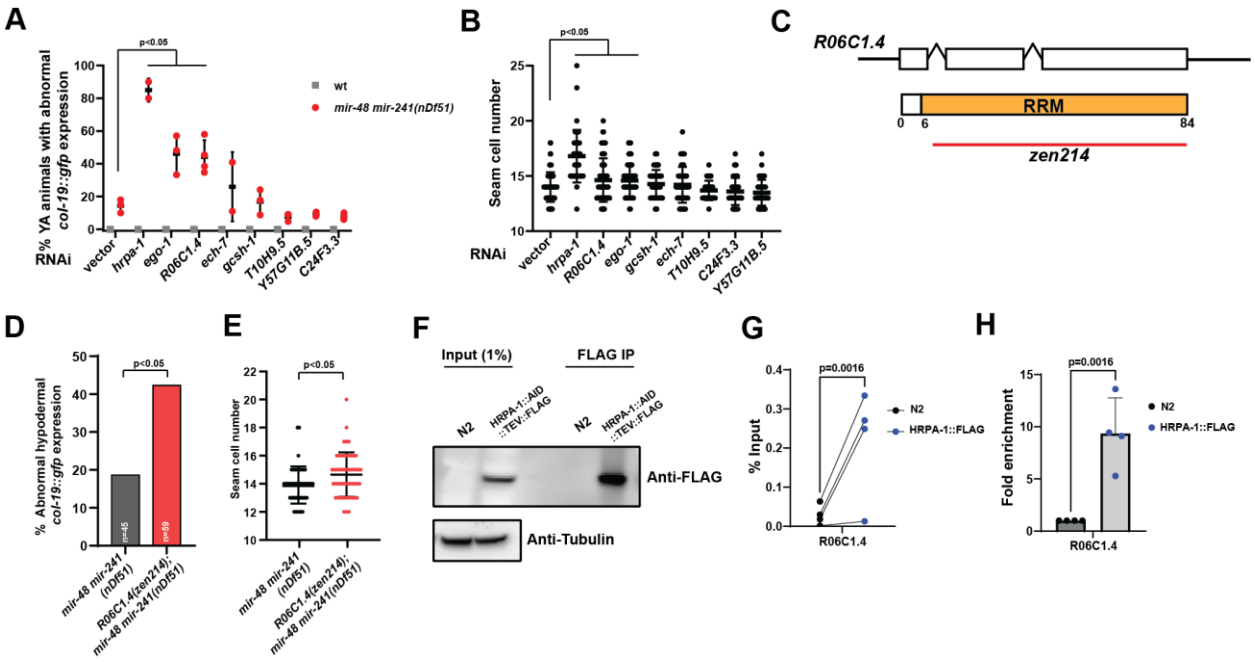

Figure 3.6 *R06C1.4* depletion partially recapitulates hrpa-1 loss of function phenotype in *mir-48 mir-241(nDf51)* backgrounds.

(A-B) RNAi knockdown of top non-collagen genes downregulated by loss of HRPA-1 in *mir-48 mir-241(nDf51)* background partially recapitulates (A) abnormal *col-19:gfp* expression and (B) seam cell number defect produced by *hrpa-1* depletion in *mir-48 mir-241* mutant animals. (C) *R06C1.4* gene and protein structure schematics. RRM–RNA Recognition Motif. Deletion allele, *R06C1.4(zen214)*, was generated using CRISPR/Cas9 genome editing deletes most of the *R06C1.4* gene. (D, E) *R06C1.4(zen214)* enhances the abnormal hypodermal *col-19::gfp* expression and seam cell lineage defect in *mir-48 mir-241(nDf51)* background. (F-H) Anti-FLAG immunoprecipitation from *hrpa-1::AID*::TEV::FLAG* or N2 (control) animals (E), followed by RT-qPCR quantification of bound R06C1.4 RNA, shown as percent input (F) or fold enrichment over control (G).

R06C1.4 appears to play a role in facilitating HRPA-1 function on miRNA-mediated developmental process. Since *R06C1.4* was downregulated upon *hrpa-1* depletion (Fig 3.5H), we wondered whether HRPA-1 could directly interact with *R06C1.4* mRNA. HRPA-1 IP significantly enriched for *R06C1.4* mRNA compared to N2 control, supporting a potential model for posttranscriptional regulation of *R06C1.4* RNA by HRPA-1 (Fig 3.6 G,H). The yeast homolog of R06C1.4, Rna15, is a component of cleavage and polyadenylation factor I (CFI) that is involved in 3' end processing of precursor mRNAs (Fig B.4A). Yeast hnRNP homolog, HRP1, is also a component of this complex (Gordon *et al.* 2011). To explore all avenues of HRPA-1 effects on *R06C1.4*, we wondered whether HRPA-1 could physically associate with R06C1.4 and perhaps be involved in 3' end processing of primary miRNAs, in addition to feeding back onto *R06C1.4* expression. However, an anti-FLAG immunoprecipitation from *hrpa-1::AID*::TEV::FLAG* worms expressing R06C1.4::V5 did not co-precipitate R06C1.4 (Fig B.4B). Thus, our data suggest that HRPA-1 does not form a physical complex with R06C1.4.

3.5 Discussion

Heterogenous nuclear ribonucleoproteins have been implicated in several gene regulatory processes (reviewed in Geuens *et al.* 2016). Despite being extensively studied in different species, their complete functional profile is not entirely understood. The *C. elegans* hnRNPA/B family homolog, HRPA-1, has been previously reported to regulate telomere length, alternative splicing, and longevity (Jeong *et al.* 2004; Barberan-Soler *et al.* 2011). In this study, we report a role for *hrpa-1* in miRNA mediated gene regulation.

We previously identified HRPA-1 in miR-58 and let-7 pulldowns (Hebbar *et al*. 2022) and we confirm the co-precipitation in this study (Fig 3.1B). While these data are suggestive of a direct

interaction with mature let-7 and miR-58, we cannot rule out a potential interaction with primary or precursor miRNAs. Findings from HRPA-1 IP in this study (Fig 3.1C) and previously reported ALG-1 IP (Zinovyeva *et al.* 2015) indicate that HRPA-1 may transiently interact with ALG-1. The observed weak interaction between ALG-1 and HRPA-1 may be RNA-dependent, possibly stemming from HRPA-1 and miRISC binding to proximal binding sites on the targets. However, HRPA-1 was not previously identified in AIN-1 or AIN-2 immunoprecipitations (Zhang *et al*. 2007; Dallarie *et al*. 2018), suggesting HRPA-1 might not interact with mature miRISC, or may do so very transiently. Taken together, these observations indicate that HRPA-1 may interact with miRNA biogenesis intermediates prior to miRISC formation or may interact with miRISC, but transiently.

Can subcellular HRPA-1 localization inform us of its function?

The ubiquitous expression of HRPA-1::GFP suggests a role for this protein in multiple developmental processes (Fig 3.4A). A strong nuclear expression is consistent with the subcellular localization of its orthologs in humans, flies (Dreyfuss *et al.* 1993; Borah *et al*. 2008). The human homologs, hnRNPA1 and hnRNPA2/B1, have been reported to shuttle between nucleus and cytoplasm (Izaurralde *et al.* 1997). It's possible that the cytoplasmic signal of our endogenous HRPA-1::GFP reporter was difficult to detect in part due to strong nuclear signal (Fig 3.4). Previously, *in vivo* proximity-based proteomics found HRPA-1 to be enriched in the nucleus while also reporting cytoplasmic HRPA-1 localization in a few tissues, including epidermis, intestine, and body wall muscle (Reinke *et al.* 2017). Thus, it is possible that while the bulk of HRPA-1 localizes to the nucleus, HRPA-1 is present in the cytoplasm, where it may associate with the cytoplasmic miRNA machinery or the miRNA targets.

What is the underlying mechanism for *hrpa-1* genetic interactions with miRNAs?

While the physical association between HRPA-1 and miRNAs/miRISC requires future work to be resolved, we show that *hrpa-1(ok963)* genetically interacts with multiple miRNA sensitized backgrounds (Figs. 3.2, 3.3). Loss of *hrpa-1* significantly enhanced the developmental defects associated with *let-7(n2853), mir-8 mir-241(nDf51),* and *lsy-6(ot150)* mutants (Figs. 3.2, 3.3, Table B.2, B.3). This observation suggests that HRPA-1 is normally involved in promoting miRNA activity during development and HRPA-1 activity may be broadly important for gene regulation, spanning many miRNAs' developmental functions. HRPA-1 could affect miRNA biogenesis and/or activity and we tested the former hypothesis by assessing miRNA levels in HRPA-1-depleted animals. Surprisingly, HRPA-1 depletion did not significantly affect the levels of let-7, miR-58, or other miRNAs (Fig 3.5D, Table B.4) responsible for the developmental phenotypes observed in *hrpa-1(ok963); miRNA(reduction of function)* animals (Fig 3.2, 3.3). This could indicate that HRPA-1 is not critical for biogenesis of these miRNAs but may rather be required for efficient miRNA-target repression activity (Fig 3.7A) or may indirectly coordinate with miRNAs to regulate developmental gene expression programs. However, it is also possible that our *hrpa-1* RNAi/IAA depletion was not sufficient to cause a wide-spread disruption in mature miRNA levels (Fig 3.5C). While animals were hatched onto *hrpa-1* RNAi, the additional three-hour IAA treatment was likely not sufficient to further affect levels of the existing mature miRNAs, considering the long miRNA half-life (Miki *et al.* 2014ai; Vieux *et al.* 2021). Supporting this notion is the fact that we observed a mild accumulation of pri-let-7 in HRPA-1-depleted RNA (1.65 fold) (Fig B.5). Given the rapid processing rates of miRNA intermediates, primary miRNAs could be more responsive to dysregulation of HRPA-1 mediated processes than mature miRNAs in our approach. In addition, we did observe an enrichment for pri-let-7 in HRPA-1::FLAG IP (Fig

3.5E), suggesting that HRPA-1 role in primary miRNA processing could be similar to its human homolog (Guil and Ca´ceres, 2007; Michlewski and Ca´ceres, 2008). Thus, it is possible that HRPA-1 affects *let-7* processing in specific tissues and our small RNA seq was not sensitive enough to detect such tissue-specific changes in mature let-7 levels.

Potential gene regulatory targets of HRPA-1

Depletion of *hrpa-1* did alter levels of 20 mature miRNAs, suggesting a role in biogenesis or stability (Fig 3.5D), perhaps through effects on primary miRNA processing either by promoting or inhibiting microprocessor activity (Fig 3.7B). Interestingly, predicted targets of some of the upregulated miRNAs were downregulated in *hrpa-1* animals, supporting the hypothesis that developmental effects of *hrpa-1* loss could at least in part be brought on by miRNA biogenesis/stability misregulation.

Among the miRNA-target pairs predicted by TargetScan, depletion of HRPA-1 resulted in dysregulation of the miR-230-R06C1.4 pair (Fig 3.5D,H,I). Mature miR-230 levels were upregulated in *hrpa-1*-depleted animals (Fig 3.5D), while levels of the *R06C1.4* mRNA went down (Fig 3.5H). *R06C1.4* knockdown partially recapitulated *hrpa-1* loss of function phenotype in miRNA mutant background (Fig 3.6 A,B,D). Thus, downregulation of R06C1.4 upon of depletion of HRPA-1 could be via HRPA-1 effects on miR-230 biogenesis and/or stability (Fig 3.7B'). HRPA-1 could also be involved in *R06C1.4* regulation independent of miR-230, as evidenced by enrichment for *R06C1.4* mRNA in HRPA-1 IP (Fig 3.7B'').

Overall, we present evidence for HRPA-1 functional requirement in several miRNA-mediated developmental processes and identify potential mRNA and miRNA targets of HRPA-1, including *R06C1.4*. We propose HRPA-1 may interface with multiple gene regulatory machineries, similar to its human homologs. Whether *hrpa-1* coordinates with miRNAs through direct mechanisms

(such as miRNA biogenesis) to regulate gene expression in *C. elegans* remains to be resolved and will be a subject of interest for future studies.

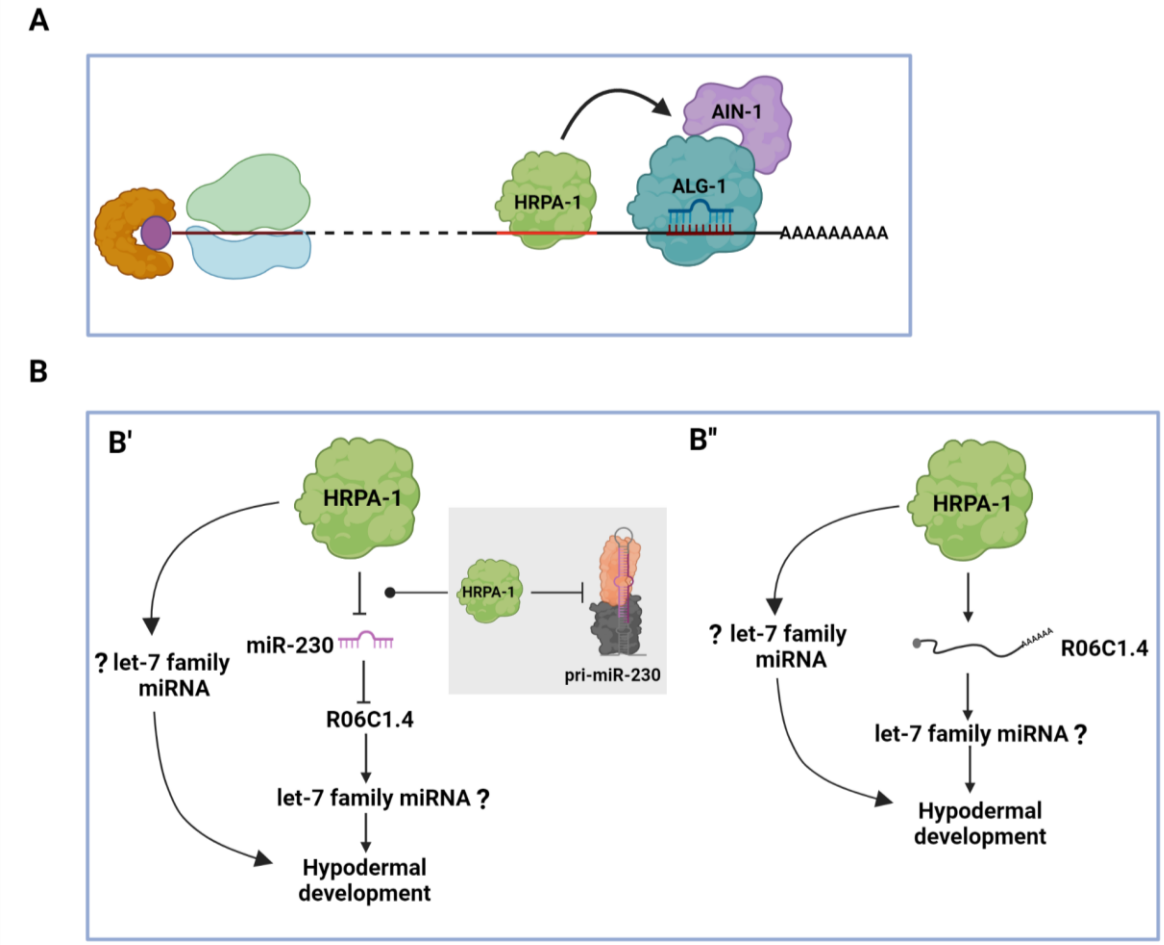

Figure 3.7 Models representing HRPA-1's roles in miRNA mediated gene regulation
(A) For miRNAs whose levels were unaffected by loss of *hrpa-1*, we propose a role for in promoting miRISC target binding and repression. (B) Models for regulation of R06C1.4 by HRPA-1 and its role in regulation of developmental gene expression programs by HRPA-1. (B') Regulation of R06C1.4 could be through modulation of biogenesis of miR-230 by HRPA-1. (B'') HRPA-1 could be regulating R06C1.4 in a miRNA independent manner which could have an impact on miRNAs that regulate hypodermal development. Models drawn using BioRender (biorender.com).

3.6 References

Abbott, A. L. *et al.* The let-7 MicroRNA Family Members mir-48, mir-84, and mir-241 Function Together to Regulate Developmental Timing in *Caenorhabditis elegans*. *Dev Cell* 9, 403–414 (2005).

Alarcón, C. R. *et al.* HNRNPA2B1 Is a Mediator of m6A-Dependent Nuclear RNA Processing Events. *Cell* 162, 1299–1308 (2015).

Anders, S. & Huber, W. Differential expression analysis for sequence count data. *Genome Biol* 11, R106–R106 (2010).

Barberan-Soler, S., Medina, P., Estella, J., Williams, J. & Zahler, A. M. Co-regulation of alternative splicing by diverse splicing factors in Caenorhabditis elegans. *Nucleic Acids Res* 39, 666–674 (2011).

Borah, S., Wong, A. C. & Steitz, J. A. Drosophila hnRNP A1 homologs Hrp36/Hrp38 enhance U2-type versus U12-type splicing to regulate alternative splicing of the prospero twintron. *Proc National Acad Sci* 106, 2577–2582 (2009).

Clarke, J. P., Thibault, P. A., Salapa, H. E. & Levin, M. C. A Comprehensive Analysis of the Role of hnRNP A1 Function and Dysfunction in the Pathogenesis of Neurodegenerative Disease. *Frontiers Mol Biosci* 8, 659610 (2021).

Dallaire, A., Frédérick, P.-M. & Simard, M. J. Somatic and Germline MicroRNAs Form Distinct Silencing Complexes to Regulate Their Target mRNAs Differently. *Dev Cell* 47, 239-247.e4 (2018).

Dobin, A. *et al.* STAR: ultrafast universal RNA-seq aligner. *Bioinformatics* 29, 15–21 (2013).

Dreyfuss, G., Kim, V. N. & Kataoka, N. Messenger-RNA-binding proteins and the messages they carry. Nat Rev Mol Cell Bio 3, 195–205 (2002).

Dreyfuss, G., Matunis, M. J., Pi ol-Roma, S., & Burd, C. G. hnRNP proteins and the biogenesis of mRNA. *Annu rev biochem,* 62, 289-289 (1993).

Ecsedi, M., Rausch, M. & Großhans, H. The let-7 microRNA Directs Vulval Development through a Single Target. *Dev Cell* 32, 335–344 (2015).

Fan, B. *et al.* Heterogeneous Ribonucleoprotein K (hnRNP K) Binds miR-122, a Mature Liver-Specific MicroRNA Required for Hepatitis C Virus Replication*. *Mol Cell Proteomics* 14, 2878–2886 (2015).

Friedländer, M. R., Mackowiak, S. D., Li, N., Chen, W. & Rajewsky, N. miRDeep2 accurately identifies known and hundreds of novel microRNA genes in seven animal clades. *Nucleic Acids Res* 40, 37–52 (2012).

Geuens, T., Bouhy, D., & Timmerman, V. The hnRNP family: insights into their role in health and disease. Human genetics, 135, 851-867 (2016).

Gu, W., Claycomb, J., Batista, P., Mello, C., Conte, D. Cloning Argonaute-Associated Small RNAs from Caenorhabditis elegans. In: Hobman TC, Duchaine TF, editors. *Methods in Molecular Biology*. Humana Press. pp. 251–280–280 (2011).

Guil, S. & Cáceres, J. F. The multifunctional RNA-binding protein hnRNP A1 is required for processing of miR-18a. *Nat Struct Mol Biol* 14, 591–596 (2007).

Guil, S., Long, J. C. & Cáceres, J. F. hnRNP A1 Relocalization to the Stress Granules Reflects a Role in the Stress Response. *Mol Cell Biol* 26, 5744–5758 (2006).

Hebbar, S. *et al.* Functional identification of microRNA-centered complexes in C. elegans. *Sci Rep-uk* 12, 7133 (2022).

Hills-Muckey, K. *et al.* An engineered, orthogonal auxin analog/ At TIR1(F79G) pairing improves both specificity and efficacy of the auxin degradation system in Caenorhabditis elegans. *Genetics* 220, (2021).

Izaurralde, E. *et al.* A Role for the M9 Transport Signal of hnRNP A1 in mRNA Nuclear Export. *J Cell Biology* 137, 27–35 (1997).

Jannot, G., Vasquez-Rifo, A. & Simard, M. J. Argonaute Proteins, Methods and Protocols. *Methods Mol Biology* 725, 233–249 (2011).

Jean-Philippe, J., Paz, S. & Caputi, M. hnRNP A1: The Swiss Army Knife of Gene Expression. *Int J Mol Sci* 14, 18999–19024 (2013).

Joeng, K. S., Song, E. J., Lee, K.-J. & Lee, J. Long lifespan in worms with long telomeric DNA. *Nat Genet* 36, 607–611 (2004).

Johnston, R. J. & Hobert, O. A microRNA controlling left/right neuronal asymmetry in *Caenorhabditis elegans*. *Nature* 426, 845–849 (2003).

Kamath, R. S. & Ahringer, J. Genome-wide RNAi screening in Caenorhabditis elegans. *Methods* 30, 313–321 (2003).

Kim, Y. & Kim, V. N. Processing of intronic microRNAs. *Embo J* 26, 775–783 (2007).

Kooshapur, H. *et al.* Structural basis for terminal loop recognition and stimulation of pri-miRNA-18a processing by hnRNP A1. *Nat Commun* 9, 2479 (2018).

Lechler, M. C. & David, D. C. More stressed out with age? Check your RNA granule aggregation. *Prion* 11, 313–322 (2017).

Lechler, M. C. *et al.* Reduced Insulin/IGF-1 Signaling Restores the Dynamic Properties of Key Stress Granule Proteins during Aging. *Cell Reports* 18, 454–467 (2017).

Li, L. & Zinovyeva, A. Y. Protein Extract Preparation and Co-immunoprecipitation from Caenorhabditis elegans. *J Vis Exp* (2020) doi:10.3791/61243.

Li, L., Veksler-Lublinsky, I. & Zinovyeva, A. HRPK-1, a conserved KH-domain protein, modulates microRNA activity during Caenorhabditis elegans development. *Plos Genet* 15, e1008067 (2019).

Liao, Y., Smyth, G. K. & Shi, W. featureCounts: an efficient general-purpose program for assigning sequence reads to genomic features. *Bioinformatics* 30, 923–930 (2014).

Mello, C. C., Kramer, J. M., Stinchcomb, D., & Ambros, V. Efficient gene transfer in C. elegans: extrachromosomal maintenance and integration of transforming sequences. *The EMBO journal*, 10, 3959-3970 (1991).

Michlewski, G. & Cáceres, J. F. Antagonistic role of hnRNP A1 and KSRP in the regulation of let-7a biogenesis. *Nat Struct Mol Biol* 17, 1011–1018 (2010).

Miki, T. S., Rüegger, S., Gaidatzis, D., Stadler, M. B., & Großhans, H. Engineering of a conditional allele reveals multiple roles of XRN2 in Caenorhabditis elegans development and substrate specificity in microRNA turnover. *Nucleic acids research* 42, 4056-4067. (2014).

Palmer, R. E., Inoue, T., Sherwood, D. R., Jiang, L. I. & Sternberg, P. W. *Caenorhabditis elegans cog-1* Locus Encodes GTX/Nkx6.1 Homeodomain Proteins and Regulates Multiple Aspects of Reproductive System Development. *Dev Biol* 252, 202–213 (2002).

Reinhart, B. J. *et al.* The 21-nucleotide let-7 RNA regulates developmental timing in Caenorhabditis elegans. *Nature* 403, 901–906 (2000).

Reinke, A. W., Mak, R., Troemel, E. R., & Bennett, E. J. In vivo mapping of tissue-and subcellular-specific proteomes in Caenorhabditis elegans. *Science advances*, 3, e1602426 (2017).

Ritsch, I. *et al.* Phase separation of hnRNP A1 upon specific RNA-binding observed by magnetic resonance. *Biorxiv* 2022.03.21.485092 (2022) doi:10.1101/2022.03.21.485092.

Ryan, V. H. & Hart, A. C. sym-2 loss-of-function causes glutamatergic neurodegeneration after oxidative stress. *Micropublication Biology* 2021, 10.17912/micropub.biology.000363 (2021).

Ryan, V. H. *et al.* Tyrosine phosphorylation regulates hnRNPA2 granule protein partitioning and reduces neurodegeneration. *Embo J* 40, e105001 (2021).

Shin, C. H. *et al.* Regulation of PLK1 through competition between hnRNPK, miR-149-3p and miR-193b-5p. *Cell Death Differ* 24, 1861–1871 (2017).

Vella, M. C., Choi, E.-Y., Lin, S.-Y., Reinert, K. & Slack, F. J. The *C. elegans* microRNA let-7 binds to imperfect let-7 complementary sites from the lin-41 3′UTR. *Gene Dev* 18, 132–137 (2004).

Vieux, K.-F. *et al.* Screening by deep sequencing reveals mediators of microRNA tailing in C. elegans. *Nucleic Acids Res* 49, gkab840- (2021).

Villarroya-Beltri, C. *et al.* Sumoylated hnRNPA2B1 controls the sorting of miRNAs into exosomes through binding to specific motifs. *Nat Commun* 4, 2980 (2013).

Zhang, L. *et al.* Systematic Identification of C. elegans miRISC Proteins, miRNAs, and mRNA Targets by Their Interactions with GW182 Proteins AIN-1 and AIN-2. *Mol Cell* 28, 598–613 (2007).

Zhang, L., Ward, J. D., Cheng, Z. & Dernburg, A. F. The auxin-inducible degradation (AID) system enables versatile conditional protein depletion in C. elegans. *Dev Camb Engl* 142, 4374–4384 (2015).

Zinovyeva, A. Y., Bouasker, S., Simard, M. J., Hammell, C. M. & Ambros, V. Mutations in Conserved Residues of the *C. elegans* microRNA Argonaute ALG-1 Identify Separable Functions in ALG-1 miRISC Loading and Target Repression. *Plos Genet* 10, e1004286 (2014).

Zinovyeva, A. Y., Veksler-Lublinsky, I., Vashisht, A. A., Wohlschlegel, J. A. & Ambros, V. R. Caenorhabditis elegans ALG-1 antimorphic mutations uncover functions for Argonaute in microRNA guide strand selection and passenger strand disposal. *Proc National Acad Sci* 112, E5271–E5280 (2015).

Chapter 4 - Discussion

miRNA and miRISC interactions with distinct auxiliary factors greatly influence the outcome of miRNA mediated gene regulatory processes. Characterizing miRNA binding partners is hence a promising approach to address some of the critical outstanding questions pertaining to miRNA regulatory mechanisms. Previously, studies in mammalian and human cell culture systems as well as *in vivo* models have adopted this approach to identify interactors of AGO and miRNA machinery components (Landthaler *et al*. 2008; Frohn *et al.* 2012; Zinovyeva *et al*. 2015; Wu *et al*. 2017). In this dissertation, I took a miRNA-centered approach by performing pulldowns to capture miRNA associated factors, which also enabled comparative profiling of interactions of three *C. elegans* miRNAs with distinct functions and spatiotemporal expression patterns. This study identified putative miRNA interactors that are general miRNA machinery co-factors, commonly associated with two or more miRNAs and with the key miRNA pathway component, Argonaute ALG-1. This study also identified miRNA specific co-factors, revealing potential sequence or context specific complexes.

Putative miRNA interactors identified in our study could be impacting miRNA biogenesis and miRNA-gene regulatory activity on multiple levels. Thus, a functional assessment of these newly identified factors is critical. Interactions identified in previous proteomic characterizations of mammalian miRNA/Argonaute bound complexes have rarely been followed up for their functional roles, in part because tissue culture systems offer a limited scope of functional analyses. At the same time, assessment of interactor impacts on vertebrate developmental programs *in vivo* is challenging. In our study, we were able to determine the functional requirement of a subset of proteins captured by our proteomics analysis. By taking advantage of well-established miRNA sensitized backgrounds in *C. elegans*, I identified miRNA co-factors functionally important for

several developmental processes including developmental timing and neuronal cell fate specification. In addition to identifying whether these proteins positively or negatively affect miRNA function, I also determined their context specificities by performing functional assays in three different miRNA sensitized backgrounds.

This study identified translational regulators, splicing proteins, and more surprisingly, metabolic factors as functional miRNA cofactors. Characterizing the mechanisms through which these diverse proteins coordinate with miRNAs can help identify previously unexplored mode of interplay between gene regulatory processes. A major interest in the field has been deciphering the extent and mechanism of interplay between splicing and miRNA machinery (Schorr and Mangone, 2021). Splicing factors could coordinate at the level of miRNA biogenesis, especially in case of intragenic miRNAs. They could also indirectly affect gene regulation by miRNAs by generating miRNA target transcript isoforms that either harbor or are devoid of miRNA recognition elements in their 3' UTRs. These mechanisms can significantly influence both miRNA expression profiles and the transcript landscape being targeted by miRNAs. In this study, GRLD-1 and RNP-7 were among the splicing factors that modified miRNA mutant phenotypes (Chapter 2), indicating a functional requirement. Splicing factors could also coordinate with miRNAs independent of their splicing activity to process miRNA intermediates. Future work could focus on depleting these factors to investigate the effects on miRNA biogenesis as well as target expression landscape to reveal possible modes of interplay.

An intriguing category of proteins identified to be important for miRNA function in this study are the intermediatory metabolic enzymes. Although some metabolic enzymes have been previously identified to bind RNA, prior studies have mostly focused on exploring the effects of such RNA binding activity on cellular metabolism (Castello *et al.* 2015; Ceijla. 2006; Lv *et al.*

2019). How metabolic enzyme-RNA partnering affect RNA metabolism is not well understood. Some studies show that glycolytic and other metabolic enzymes can promote translation by bridging RNA to translational machinery components (Lv *et al.* 2019; Simsek *et al.* 2017). The metabolic enzymes identified in this study could be interacting with the miRNAs or their targets and functioning through direct or indirect mechanisms to affect miRNA-mediated developmental processes. Thus, to begin to understand the possible mode of interplay, we must first confirm interaction of these metabolic enzymes with miRNAs/miRNA targets. Exploration of the underlying mechanism can reveal novel functions of metabolic enzymes in gene regulation.

Several RNA binding proteins were captured by our pulldowns and shown to functionally support miRNAs through functional assays. Some of the RBPs may differentially associate with individual members of the *let-7* family and support their functions through distinct mechanisms. Variations in functions of individual miRNA family members are believed to be due to differences in their spatio-temporal expression profiles and target base-pairing outside of the seed. Differential association with RBPs identified in our study may confer further functional specificities. Thus, further investigation on the mode of interplay between these RBPS and individual miRNA family member might help better understand how individual miRNA family members diverge in their functional roles.

I chose one RNA binding protein HRPA-1, for detailed investigation (Chapter 3). Although there is some evidence for structural and biochemical basis of miRNA regulation by human homologs of HRPA-1 (hnRNPA1 and hnRNPA2B1), hnRNP functional requirments have not been exhaustively studied. In addition, hnRNPA1 impact on miRNA biogenesis has been described for only two miRNAs, leaving the extent and applicability of hnRNPA1 miRNA-related activity unclear. In addition, changes in *in vitro* miRNA processing do not always correlate with

function; in other words, more miRNAs do not equal more miRNA activity. By utilizing the well-established *C. elegans* genetic tools, I uncovered HRPA-1 functional role in facilitating diverse miRNA-mediated developmental processes, suggesting that the HRPA-1 role in miRNA-related gene regulation may be broad. While a resolution of mechanisms underlying the potential modes of interplay between HRPA-1 and miRNAs is still needed, I propose several models for HRPA-1 activity based on our identification of mRNA and miRNAs targets of HRPA-1 and their roles in development.

How does HRPA-1 regulate the miRNAs whose functions it appears to support? The multifunctionality of RNA binding proteins posse a challenge in dissecting the mechanisms through which they interplay with miRNAs and miRNA-independent gene regulatory processes. Future investigation should focus on identifying RNA targets (mRNA or miRNA) that RBPs directly bind through cross-linking and immunoprecipitation (CLIP) experiments which could identify their binding motifs and inform future experiments. For example, if HRPA-1-CLIP captures miRNA intermediates, or mature miRNA, a direct role for HRPA-1 in miRNA biogenesis could be inferred. If HRPA-1 is involved in facilitating miRISC activity, (as described in Fig 3.7A), HRPA-1-CLIP would not only capture miRNA targets such as *lin-41, hbl-1*, and *cog-1*, but also identify HRPA-1 binding sites which would be valuable in dissecting whether HRPA-1 binding affects miRISC activity.

Interplay between miRNAs and RNA binding proteins has been studied with great interest, as these two classes of post-transcriptional gene expression regulators must directly and indirectly coordinate to fine-tune developmental expression programs. While many excellent studies have described global interactions of these gene regulators (Kim *et al.* 2021; Cottrell *et al.* 2018), they lack the mechanistic, functional resolution of the miRNA/RBP interactions and their impacts on

gene expression. The gene regulatory outcomes of these interactions are likely diverse and context dependent, necessitating studies that delve into the specific developmental, miRNA, RBP, and target contexts. Thus, *in vivo* mechanistic characterizations of individual miRNA/RBP regulatory relationships in various developmental contexts are critical for understanding how these two classes of post-transcriptional gene regulators ultimately set up robust developmental gene expression programs.

References

- Castello, A., Hentze, M. W. & Preiss, T. Metabolic Enzymes Enjoying New Partnerships as RNA-Binding Proteins. *Trends Endocrin Met* 26, 746–757 (2015).
- Cieśla, J. Metabolic enzymes that bind RNA: yet another level of cellular regulatory network?. *Acta Biochimica Polonica* 53, 11-32 (2006).
- Cottrell, K. A., Chaudhari, H. G., Cohen, B. A. & Djuranovic, S. PTRE-seq reveals mechanism and interactions of RNA binding proteins and miRNAs. *Nat Commun* 9, 301 (2018).
- Frohn, A. *et al.* Dicer-dependent and -independent Argonaute2 Protein Interaction Networks in Mammalian Cells*. *Mol Cell Proteomics* 11, 1442–1456 (2012).
- Kim, S. *et al.* The regulatory impact of RNA-binding proteins on microRNA targeting. *Nat Commun* 12, 5057 (2021).
- Landthaler, M. *et al.* Molecular characterization of human Argonaute-containing ribonucleoprotein complexes and their bound target mRNAs. *Rna* 14, 2580–2596 (2008).

- Lv, Y., Tariq, M., Guo, X., Kanwal, S. & Esteban, M. A. Intricacies in the cross talk between metabolic enzymes, RNA, and protein translation. *J Mol Cell Biol* 11, 813–815 (2019).
- Schorr, A. L. & Mangone, M. miRNA-Based Regulation of Alternative RNA Splicing in Metazoans. *Int J Mol Sci* 22, 11618 (2021).
- Simsek, D. *et al.* The Mammalian Ribo-interactome Reveals Ribosome Functional Diversity and Heterogeneity. *Cell* 169, 1051-1065.e18 (2017).
- Wu, E. *et al.* A continuum of mRNP complexes in embryonic microRNA-mediated silencing. *Nucleic Acids Res* 45, 2081–2098 (2017).
- Zinovyeva, A. Y., Veksler-Lublinsky, I., Vashisht, A. A., Wohlschlegel, J. A. & Ambros, V. R. Caenorhabditis elegans ALG-1 antimorphic mutations uncover functions for Argonaute in microRNA guide strand selection and passenger strand disposal. *Proc National Acad Sci* 112, E5271–E5280 (2015).

Appendix A - Chapter 2 Supplemental Material

Supplementary Tables for Chapter 2 are included as separate csv files.

Table A.1

Complete list of proteins identified by MudPIT in let-7(wt), miR-58(wt), miR-2(wt) and *let-7(mir-48 mir-241(nDf51); mir-84(n4037))* pulldowns.

Table A.2

Overlap observed among factors identified in let-7, miR-58, miR-2 pulldowns and ALG-1 IP and previously identified proteomics studies and genetic screens.

Table A.3

GO enrichment analysis of the proteins identified by MUDPIT in let-7(wt), miR-58 (wt), miR-2(wt) and *let-7(mir-48 mir-241(nDf51); mir-84(n4037))* co-immunoprecipitates.

Table A.4

Effects of miRNA and ALG-1 interacting protein gene knockdown on miRNA mutant phenotypes.

Table A.5

Top hits from functional assays modified miRNA target expression in reporter assays.

Appendix B - Chapter 3 Supplemental Material

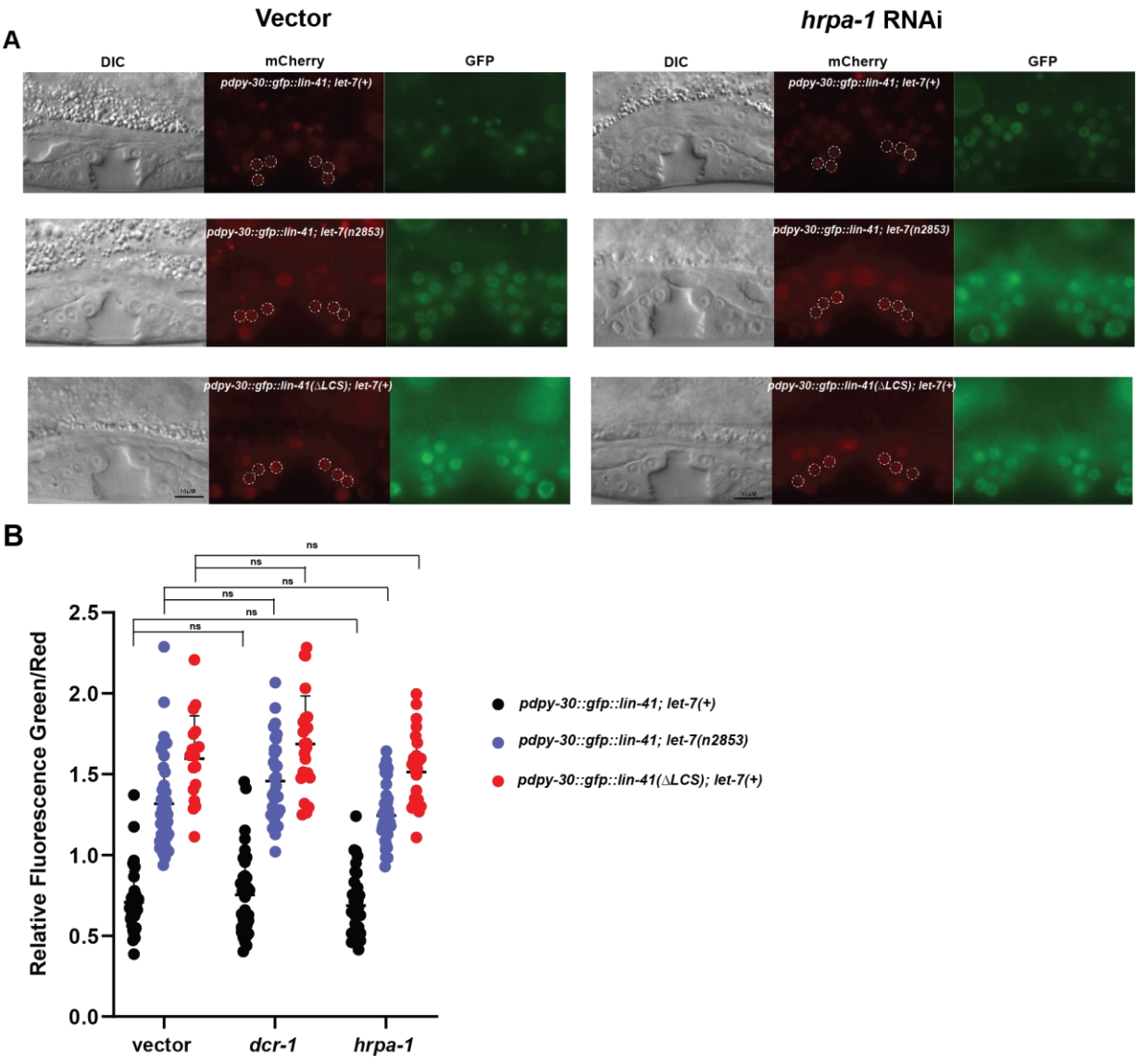

Figure B.4.1 Effects of *hrpa-1* RNAi on *pdpy-30::gfp::lin-41 3'UTR* reporter expression in the vulval cells of wild type and *let-7(n2853)* L4 larvae at 20ºC.

Compromised let-7 activity in *let-7(n2853)* mutant and deletion of let-7 complementary sites (LCS) in lin-41 3' UTR leads to de-repression of *pdpy-30::gfp::lin-41 3' UTR* reporter expression levels which was unchanged upon knockdown of *hrpa-1* (quantified in B). (B) Effects of empty

vector (negative control), *dcr-1* RNAi (positive control), and *hrpa-1* RNAi on *pdpy-30::gfp::lin-41 3'UTR* reporter expression levels in L4 animals. Each dot represents the relative intensity in an individual worm. Vulval precursor cells used for fluorescence quantification are highlighted with dashed circles. T-test was used to determine the statistical significance.

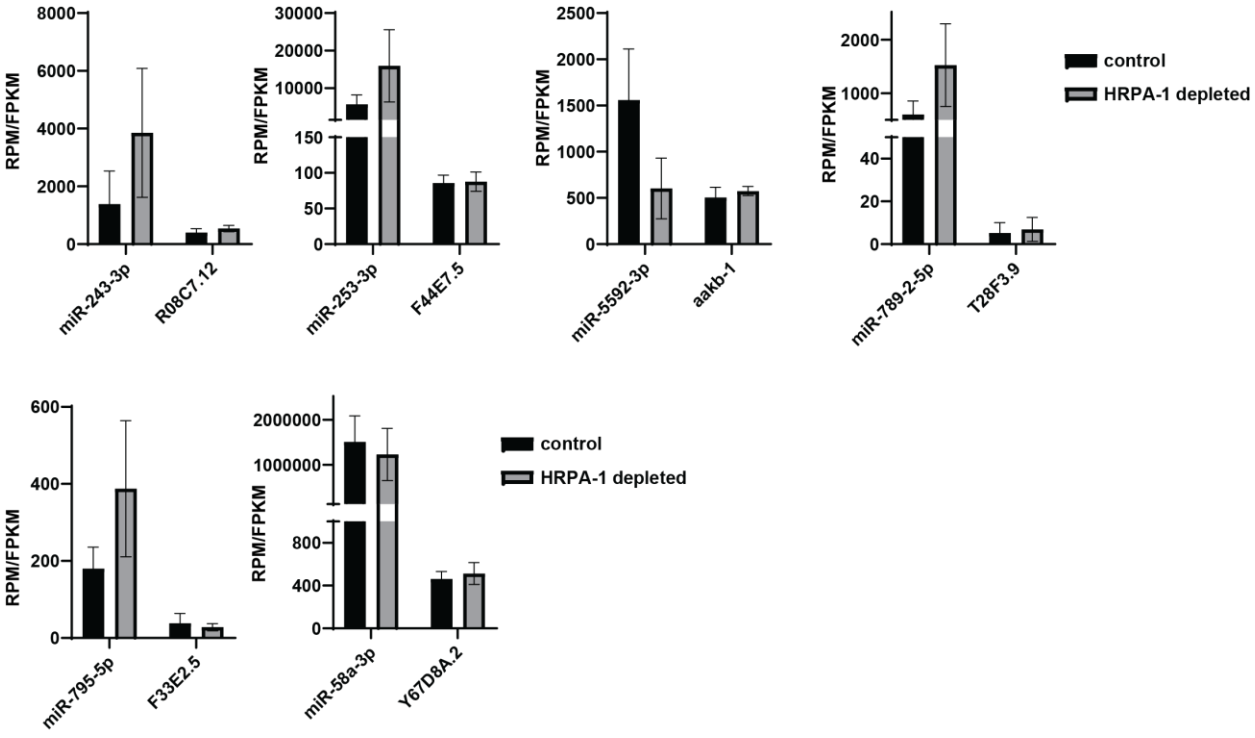

Figure B.2 Expression levels of differentially expressed intronic miRNAs and miR-58a as well as their host genes upon HRPA-1 depletion.

Y-axis shows RPM values of miRNA expression and FPKM values of host gene expression.

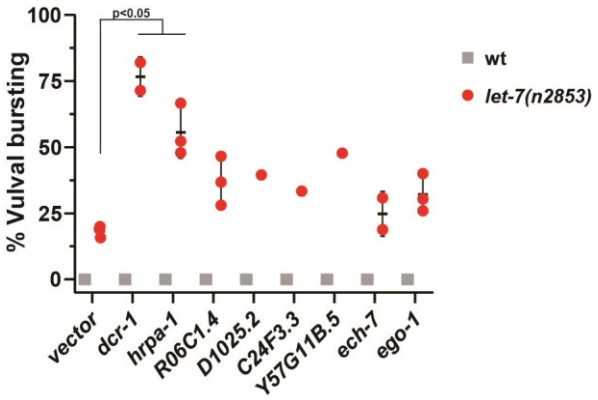

Figure B.3 Functional assay in *let-7(n2853)* background using genes downregulated by depletion of HRPA-1. Effects of RNAi knockdown of top non-collagen genes downregulated by loss of HRPA-1 on vulval bursting in wild type and *let-7(n2853)* backgrounds at 15ºC. T-test was used to determine the statistical significance.

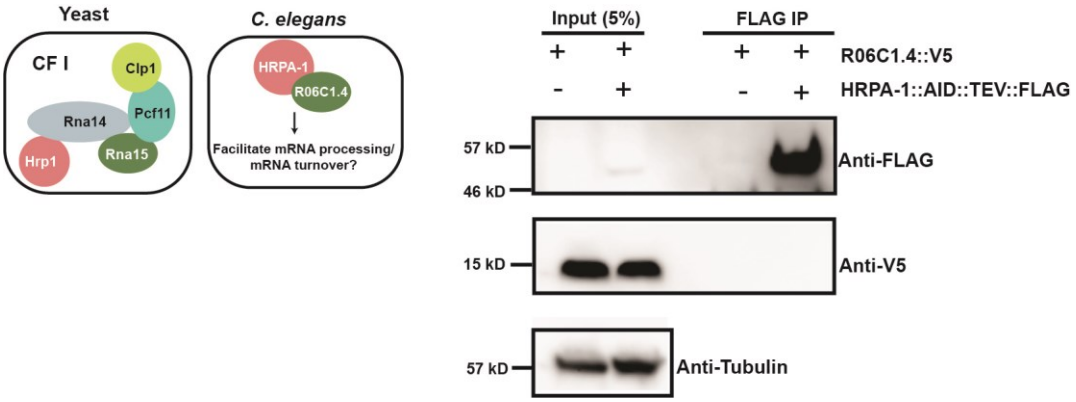

Figure B.4 Alternative model for gene regulation by HRPA-1 and R06C1.4.

(A) R06C1.4 is a homolog of Rna15, a component of yeast cleavage and polyadenylation complex. Model for HRPA-1 and R06C1.4 based gene regulatory mechanism in *C. elegans*. (B) Anti-FLAG based HRPA-1 IP did not capture R06C1.4::V5.

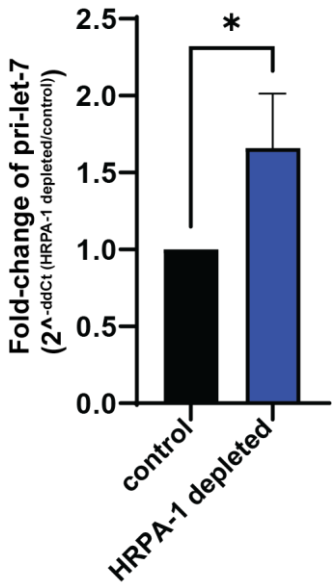

Figure B.5 Pri-let-7 level marginally increased by depletion of HRPA-1. Fold change in pri-let-7 level as quantified by RT-qPCR in HRPA-1 depleted RNA compared to the control.

Oligonucleotide	**Sequence**
dpy-10 crRNA	5'-GCUACCAUAGGCACCACGAG-3'
hrpa-1 crRNA	5'-CAGTGGGCTCATGCTCAAGG-3'
R06C1.4 crRNA1	5'-TAATCGATTTTTTTCTAGT-3'
R06C1.4 crRNA2	5'-CGCAACAGTCAAATGAACA-3'
R06C1.4::V5 donor (IDT Ultramer)	5'- CCTTCAATGGACGCAACCTTCGTGTCAACTACGCCAACAAGGGAGGTTCCG GTGGTTCTGGTGGATCCGGTAAGCCTATCCCAAATCCTTTGTTGGGTCTGG ACTCCACGTAAACTGACAACGCCGCCGAGTGACTCAAAGAGATTGCACTTG -3'
R06C1.4 genotyping primers	F: 5'-GGCCAAAACCTACTATTACC -3' R: 5'-ACAAGTGCAATCTCTTTGAGTC-3'
2'-OMe miR-58 oligo	5′: CAUCAUUGCCGUACUGAACGAUCUCAAGUC-3′
2'-OMe let-7 oligo	5′: UCUUCACUAUACAACCUACUACCUCAACCUU-3′
2'-OMe scrambled oligo	5′: CAUCACGUACGCGGAAUACUUCGAAAUGUC-3′
qPCR pri-let-7 primers	F: 5'-AAGCAGGCGATTGGTGGAC-3' R-5'GTTGTGAGAGCAAGACGACG-3'
qPCR pri-miR-58 primers	F: 5'-TTACTATCCCGGCTTCAGTG-3' R: 5'-CCATACCTTCCGTTCCGTAT-3'
qPCR *R06C1.4* primers	F: 5′-CTCCGTCTACGTTGGAAACG-3′ R: 5'-GTTGGCGTAGTTGACACG-3'

Table 4.1 List of Oligonucleotides Used in This Study

miRNA mutant	*let-7(n2853)*	*mir-48 mir-241(nDf51)*		*gfp::lin-41*[a]		*gfp::lin-41(ΔLCS)*[b]	*cog-1::gfp*[c]	
				wt	***let-7(n2853)***		**wt**	**lsy-6**
Phenotype / RNAi	**% Animals burst through vulva (n[d])**	**% Abnormal hypodermal *col-19::gfp* (n)**	**Seam cell # (n)**					
Vector	18.3±2.2 (78)	14.3±4 (72)	14±0.1 (72)	0.70±0.1	1.31±0.2	1.59	1.59	48.3±5.7
dcr-1	**63.9±17.2 (122)**	**66.1±26.8 (80)**	**14.87±0.4 (80)**	0.71±0.2	1.45±0.1	1.68	1.68	n.d
hrpa-1	**55.6±9.7[e] (113)**	**85±7.1 (94)**	**16.7±0.5 (94)**	0.66±0.1	1.23±0.1	1.51	1.51	**62.3±3.4**
R06C1.4	37.1±9.3 (86)	**44.2±4.4 (107)**	**14.5±0.5 (107)**	n.d		n.d	n.d	
C24F3.3	33.3 (52)	6.7±1.0 (48)	13.6±0.1 (48)	n.d		n.d	n.d	
gcsh-1	39.5 (54)	21±4.4 (63)	14.3±0.3 (63)	n.d		n.d	n.d	
T10H9.5	n.d	6.9±3.1	13.6±0.2	n.d		n.d	n.d	
Y57G11B.5	47.7 (43)	9.3±1.8 (68)	13.5±0.1 (68)	n.d		n.d	n.d	
ego-1	28.2±3.2 (60)	**46.2±11.9 (55)**	**14.5±0.7 (55)**	n.d		n.d	n.d	
ech-7	24.8±8.5 (37)	25.9±21.1 (39)	14.2±0.9 (39)	n.d		n.d	n.d	

Table B.2 Summary of RNAi based phenotypic and reporter assays performed in this study.

[a,b] Relative fluorescence (Green/Red) intensites for each RNAi are shown here*; n* ranges from 20 to 54

[c] Percentages of animals expressing uterine *cog-1::gfp*; *n* ranges from 88 to 110

[d] Total number of worms scored across replicates

[e] Highlighted in bold is the statistically significant value (p-value<0.05) as determined by a T-test (See Methods for details)

Phenotype / Genotype	% Abnormal hypodermal *col-19::gfp* (n)	Seam cell # (n)	Alae (n)			% Animals with defective ASEL cell fate (n)
			Complete	gapped	no alae	
wt	0 (62)	12.8 (62)	100 (45)	0 (0)	0 (0)	0 (68)
mir-48 mir-241(nDf51)	**15 (55)[a]**	**14.0 (55)**	**50 (16)**	**37.5 (12)**	**12.5 (13)**	**n.d**
hrpa-1(ok963)	0 (45)	12.6 45)	**54 (22)**	**37.5 (15)**	**8.5 (3)**	0 (86)
hrpa-1(ok963); mir-48 mir-241(nDf51)	**100 (65)**	**16.8 (65)**	**0 (0)**	**10 (4)**	**90 (34)**	n.d
R06C1.4(zen214); mir-48 mir-241(nDf51)	**42.3 (59)**	**14.7 (59)**	n.d	n.d	n.d	n.d
hrpa-1(ok963); lsy-6(ot150)	n.d[b]	n.d	n.d	n.d	n.d	**51.4 (67)**

Table B.3 Effects of loss of *hrpa-1* and *R06C1.4* on miRNA mutant phenotypes.

[a] Statistically significant values are highlighted in bold as determined using Chi-Square test.
[b] not determined

Supplemental tables B.4 and B.5 are included as separate csv files.

Table B.4
Effects of depletion of HRPA-1 on miRNA population.

Table B.5
Effects of depletion of HRPA-1 on global gene expression.

Appendix C -

An engineered, orthogonal auxin analog/AtTIR1(F79G) pairing improves both specificity and efficacy of the auxin degradation system in *Caenorhabditis elegans*

Portion of this chapter is a part of published article.

Hills-Muckey, K., Martinez, M. A., Stec, N., Hebbar, S., *et al*., (2021). An engineered, orthogonal auxin analog/AtTIR1 (F79G) pairing improves both specificity and efficacy of the auxin degradation system in *Caenorhabditis elegans*. *Genetics*.

I performed experiments and contributed to generation of Figure 7. Described below is the expanded version of my contribution to this publication.

Introduction

Uncovering mechanisms underlying developmental processes require precise spatio-temporal manipulation of gene expression. Assessing the functions of proteins that are crucial for developmental processes *in vivo* is challenging as depleting them often leads to severe developmental defects. Thus, the techniques aimed at achieving such manipulations need to be robust, specific, and most importantly, conditional, and reversible. Several techniques that are currently in use in *C. elegans* achieve protein depletion to a varying degree of efficacy. LoxP/Cre recombinase (Hubbard, 2014) or the FRP/FLP recombinase system (Davis *et al.* 2008), for instance are being utilized to tissue specifically knockout genes. A major limitation of these approaches apart from being irreversible is that stable mRNA and proteins that persist longer mask the null phenotypes of target genes (Elbashir *et al.* 2001; Zhang *et al*. 2015).

Auxin-inducible degron system (CeAIDv.1) overcomes these limitations by directly targeting proteins for depletion (Zhang *et al.* 2015). The technique entails fusion of protein of interest with a minimal degron tag referred to as Auxin-inducible degron (AID*) which is a signal peptide that directs proteasomal degradation of the protein only in the presence of plant hormone IAA (Zhang *et al.* 2015). The system requires TIR-1, a plant F-box protein to bind to degron fused protein, thus creating an avenue for directing spatial specificity as tissue-specific promoters allow for tissue-specific expression of TIR-1 (Gray *et al*. 1999; Ruegger *et al*. 1998). In addition, protein degradation is reversible making it an attractive feature for studying essential developmental proteins under desired developmental stage.

While this technique might help overcome limitations of other methods, the system is far from being perfect. For one thing, robust depletion of protein requires very high concentrations of IAA and lengthy treatment times which has been reported to trigger undesirable stress response

(Bhoi et al. 2021; Loose and Ghazi 2021). Especially when the protein-of interest is highly abundant, the efficiency of AIDv.1 has been particularly low. For instance, complete depletion of a highly abundant and ubiquitously expressed RNA binding protein, HRPA-1, was not achieved at 1mM IAA treatment for 3 hours (described in Chapter 3). Thus, for robust depletion, a combinatorial approach that depletes both *hrpa-1* mRNA and protein using RNAi and IAA treatment respectively had to be utilized. In addition, TIR-1 binding to degron fused protein could be leaky, resulting in loss-of-function phenotypes for certain crucial proteins in a TIR-1-dependent/auxin-independent manner. Thus, there is a need to improve this system to utilize its benefits to the best extent possible.

The limitations of the current system either stems from week binding of TIR-1 to degron in the absence of auxin or non-specific binding by chemicals analogous to auxin. Thus, a new and improved *C. elegans* AID version 2 was developed to facilitate more effective and specific conditional degradation. The improved system switches from auxin/$_{At}$TIR-1 pairing to auxin-derivative (5-Ph-IAA)/ mutant $_{At}$TIR-1 pair with altered and improved ligand binding specificity. The CeAIDv.2 entails 5-Ph-IAA/TIR-1(F79G) and the CeAIDv.1 refers to IAA/TIR-1(WT). Below I describe the details of how I tested the efficiencies of CeAIDv.1 and CeAIDv.2 in depleting HRPA-1.

Methods

CRISPR/Cas9 based gene editing

Endogenously tagged *hrpa-1::linker::AID::TEV::FLAG* was generated by inserting coding sequences of respective tags into the C-terminus of *hrpa-1* locus just before the stop codon through CRISPR/Cas9 mediated homologous recombination. The donor was ordered through IDT as

gBlock Gene Fragment and modified donor was generated using PCR as described previously (Ghanta & Mello, 2020) using primers with 5'Sp9 modification (Table C.1). Synonymous mutations in the guide binding region in the donor were incorporated to block Cas9 from re-editing.

To generate *hrpa-1::linker::AID::TEV::FLAG* strain, N2 worms were injected with the CRISPR-Cas9 RNA-protein complex (Paix *et al.* 2015). The injection mix consisted of Alt-R Cas9 (IDT, cat# 1081058) along with *hrpa-1* crRNA (Table), *dpy-10* crRNA (5'-GCUACCAUAGGCACCACGAG-3' (Arribere *et al.* 2014), tracer RNA (IDT, cat# 1072532) (AGCAUAGCAAGUUAAAAUAAGGCUAGUCCGUUAUCAACUUGAAAAAGUGGCACC GAGUCGGUGCUUU) and *hrpa-1::linker::AID::TEV::FLAG* donor (Table). Four independent lines of the *hrpa-1::linker::AID::TEV::FLAG* strain were obtained and the tagged endogenous loci were sequenced. Two lines were chosen and outcrossed two times.

***hrpa-1* crRNA**	5'-CAGTGGGCTCATGCTCAAGG-3'
hrpa-1::linker::AID::TEV::FLAG **donor**	CAAGGCCAGCAGCAAGGCGGCTGGGGAGGTCA ATCCGGTGCTCAGCAATGGGCCCACGCCCAGGG AGGAAACAGAAACTATGGATCCGGAGGTGGCG GGCCTAAAGATCCAGCCAAACCTCCGGCCAAGG CACAAGTTGTGGGATGGCCACCGGTGAGATCAT ACCGGAAGAACGTGATGGTTTCCTGCCAAAAAT CAAGCGGTGGCCCGGAGGCGGCGGCGTTCGTGA AGGAGAATCTGTACTTTCAATCCGGAAAGGACT ACAAAGACCATGACGGTGATTATAAAGATCATG ATATCGATTACAAGGATGACGATGACAAGTAAA TTAATTCCTTAAGCCCCTCTAAGTGTCCAACGTG TCTGAGCTTCCCGTGCTCTCTCCTCTGTATCGAT CTTCTCAACCATTTTTGCTCTGCTATC
Sp9 primers	Forward: /5Sp9/CAAGGCCAGCAGCAAGG Reverse: /5Sp9/GATAGCAGAGCAAAAATGGTTGAGAAG

Screening primers	Forward: 5'-GGAGGTAGTTGGATTCTGGC-3' Reverse: 5'-GTTGAATGGATGTCAACTGTGC-3'

Table C.1 List of oligonucleotides used to generate AID tagged strain

Western Blot

~ 40 worms were picked directly into the 2x Laemmli protein loading buffer and boiled at 95℃ for 5 min. HRPA-1 was detected using the Monoclonal ANTI-FLAG M2-Peroxidase (HRP) antibody (A8592-2MG) from Sigma-Aldrich at a 1: 500 dilution. Mouse anti-tubulin antibody (Sigma-Aldrich) was used to detect tubulin as a loading control.

Auxin treatment

IAA, 5-Ph-IAA and ethanol infused NGM plates were made as previously described. Embryos obtained through bleaching were transferred on to IAA or 5-Ph-IAA or ethanol control plates and were grown until the worms reached the young adult stage. For western blot analysis, 50-60 young adult worms were directly picked into Lamelli buffer and boiled for 5 min at 95C. HRPA-1 was detected using the Monoclonal ANTI-FLAG M2-Peroxidase (HRP) antibody (A8592-2MG) from Sigma-Aldrich at a 1: 500 dilutions. Mouse anti-tubulin antibody (Sigma-Aldrich) was used to detect tubulin as a loading control.

Phenotypic assays

For brood analysis, embryonic lethality and larval arrest assessment, embryos were hatched on auxin or control plates and maintained until they reached L4. Worms were then singled on

respective drug treatment plates and their full broods were scored. Worms were considered sterile if they had no progeny.

Statistics and image processing

All graphs were made on Graph Pad Prism v9. Statistical significance was determined using a two-tailed unpaired Student's t-test. Images were acquired using the Leica DM6 upright microscopes and images were captured using Leica DM6B camera. Images were processed on Adobe Illustrator.

Results

HRPA-1 is a ubiquitous RNA binding protein, essential for normal worm development as the deletion mutant shows severe developmental defects (Ryan and Hart, 2021; Ryan *et al.* 2021). Thus, in order to investigate its role in gene regulation, CRISPR/Cas9 was used to C-terminally tag the HRPA-1 with AID* which would enable modulation of HRPA-1 levels using auxin. We compared the efficiencies of *C. elegans* AID version 2 and version 1 for their relative efficiencies in depleting HRPA-1. We first determined the TIR-1 dependent/auxin independent degradation of HRPA-1::AID::TEV::FLAG in strains expressing TIR-1(WT) or TIR-1(F79G). As reported earlier for some of the other AID* fused proteins, we observed reduced expression levels of the target protein in TIR-1(WT) lysates in the absence of auxin treatment (Fig C.1A, B). No such reduction was observed in TIR-1(F79G) lysates. We then determined the efficiency of HRPA-1 depletion by C.e.AIDv2 system compared to that of C.e.AIDv1 system using two different concentrations of auxin analogs (100uM and 1uM) (Fig C.1A). While both C.e.AIDv1 and C.e.AIDv2 systems depleted HRPA-1::AID*, the fold change in target expression level in C.e.AIDv2 system was

higher (Fig C.1A,C). Interestingly, at a 100-times lower auxin analog concentration, we again observed C.e.AIDv2 to more efficiently deplete HRPA-1 than C.e.AIDv2 (Fig C.1A,C).

Treatments with both analogs of IAA led to developmental phenotypes comparable to the *hrpa-1(ok963)* mutant (Fig C.1D). We quantified brood size and F1 larval arrest following both auxin analog treatments (Fig C.1E, F). While both systems significantly reduced brood size, consistent with the higher fold depletion of HRPA-1 in C.e.AIDv2 system (Fig C.1E), we observed completely penetrant F1 progeny developmental arrest with *At*TIR-1(F79G)/5Ph-IAA system (Fig C.1F). Overall, C.e.AIDv2 depleted HRPA-1::AID* with a higher efficiency and more closely phenocopied *hrpa-1(null)* mutant phenotypes.

Figure C.1 Ce.AIDv2 is more effective in depleting HRPA-1 than Ce.AIDv1 and closely phenocopies *hrpa-1(null).*

(A) Representative western blot depicting the extent of HRPA-1::AID::TEV::FLAG depletion in animals expressing either TIR-1(WT) or TIR-1(F79G) following indicated concentrations of IAA or 5-Ph-IAA. (B) Quantification of HRPA-1 depletion in an TIR-1-dependent, auxin-independent manner. (C) Quantification of HRPA-1 depletion following exposure to two different auxin analogs. (D) Representative images of young adult *hrpa-1(ok963)* animal and *hrpa-*

1::AID::TEV::FLAG animal with or without 5-Ph-IAA treatment. (E-F) Brood sizes (E) and % broods with arrested F1 (F) associated with *hrpa-1::AID::TEV::FLAG* animals exposed to IAA or 5-Ph-IAA and *hrpa-1(ok963).*

References

- Arribere, J. A. et al. Efficient Marker-Free Recovery of Custom Genetic Modifications with CRISPR/Cas9 in Caenorhabditis elegans. Genetics 198, 837–846 (2014).
- Bhoi, A., Palladino, F. & Fabrizio, P. Auxin confers protection against ER stress in *Caenorhabditis elegans*. *Biol Open* **10**, bio057992 (2021).
- Davis, M. W., Morton, J. J., Carroll, D. & Jorgensen, E. M. Gene Activation Using FLP Recombinase in C. elegans. *Plos Genet* **4**, e1000028 (2008).
- Elbashir, S. M. *et al.* Duplexes of 21-nucleotide RNAs mediate RNA interference in cultured mammalian cells. *Nature* **411**, 494–498 (2001).
- Ghanta, K. S. & Mello, C. C. Melting dsDNA Donor Molecules Greatly Improves Precision Genome Editing in *Caenorhabditis elegans*. *Genetics* **216**, 643–650 (2020).
- Gray, W. M. *et al.* Identification of an SCF ubiquitin–ligase complex required for auxin response in Arabidopsis thaliana. *Gene Dev* **13**, 1678–1691 (1999).
- Hubbard, E. J. A. FLP/FRT and Cre/lox recombination technology in *C. elegans*. *Methods* **68**, 417–424 (2014).
- Loose, J. A. & Ghazi, A. Auxin treatment increases lifespan in *Caenorhabditis elegans. Biol Open* **10**, bio058703 (2021).

- Paix, A., Folkmann, A., Rasoloson, D. & Seydoux, G. High Efficiency, Homology-Directed Genome Editing in *Caenorhabditis elegans* Using CRISPR-Cas9 Ribonucleoprotein Complexes. *Genetics* **201**, 47–54 (2015).
- Ruegger, M. *et al.* The TIR1 protein of Arabidopsis functions in auxin response and is related to human SKP2 and yeast Grr1p. *Gene Dev* **12**, 198–207 (1998).
- Ryan, V. H. & Hart, A. C. sym-2 loss-of-function causes glutamatergic neurodegeneration after oxidative stress. *Micropublication Biology* **2021**, 10.17912/micropub.biology.000363 (2021).
- Zhang, L., Ward, J. D., Cheng, Z. & Dernburg, A. F. The auxin-inducible degradation (AID) system enables versatile conditional protein depletion in *C. elegans*. Dev Camb Engl 142, 4374–4384 (2015).

Appendix D - Copy right Permissions

This appendix includes copyright permissions for all the published work included in this thesis.

Chapter 2- Hebbar *et al*, 2022

This Scientific Reports article is distributed under the terms of the Creative Commons CC BY license, which permits unrestricted use, distribution, and reproduction in any medium, provided the original work is properly cited.

Chapter 3-Hebbar *et al*, 2022 (*bioRxiv*)

The author has obtained permission from all the other authors to reuse the preprint as a chapter in this thesis.

Appendix Chapter C- Hills-Muckey *et al*, 2021

Figure C.1 was used with permission from Oxford University Press

Licensee:	Ms. Shilpa Hebbar
Order Date:	Jul 17, 2022
Order Number:	5351440417297
Publication:	Genetics
Title:	An engineered, orthogonal auxin analog/$_{At}$TIR1(F79G) pairing improves both specificity and efficacy of the auxin degradation system in *Caenorhabditis elegans*
Type of Use:	Thesis/Dissertation
Order Total:	0.00 USD